
Theses and Dissertations

Spring 2011

Microbial ecology of a managed aquifer near the Iowa Army Ammunition Plant (Middletown, Ia)

Joshua Adam Livermore
University of Iowa

Follow this and additional works at: <https://ir.uiowa.edu/etd>



Part of the [Civil and Environmental Engineering Commons](#)

Copyright 2011 Joshua A. Livermore

This dissertation is available at Iowa Research Online: <https://ir.uiowa.edu/etd/2932>

Recommended Citation

Livermore, Joshua Adam. "Microbial ecology of a managed aquifer near the Iowa Army Ammunition Plant (Middletown, Ia)." PhD (Doctor of Philosophy) thesis, University of Iowa, 2011.

<https://doi.org/10.17077/etd.esm2cyxu>

Follow this and additional works at: <https://ir.uiowa.edu/etd>



Part of the [Civil and Environmental Engineering Commons](#)

MICROBIAL ECOLOGY OF A MANAGED AQUIFER NEAR THE IOWA ARMY
AMMUNITION PLANT (MIDDLETOWN, IA)

by
Joshua Adam Livermore

An Abstract

Of a thesis submitted in partial fulfillment
of the requirements for the Doctor of
Philosophy degree in Civil and Environmental Engineering
in the Graduate College of
The University of Iowa

May 2012

Thesis Supervisor: Associate Professor Timothy E. Mattes

ABSTRACT

With increasing global scarcity of freshwater, groundwater aquifers are an increasingly valuable reserve. However, anthropogenic activities endanger the integrity of groundwater resources through excessive withdrawal, insufficient recharge due to landscape changes, and contamination with foreign substances. Bioremediation to degrade contaminants in situ using native or augmented microbial communities is an increasingly popular strategy. While bioremediation is frequently economically favorable, the mechanisms and agents of compound degradation and long term ecological consequences are scarcely comprehended. This thesis is an investigation of microbial community structure and dynamics during a bioremediation event to attenuate an aquifer plume of the explosive compound RDX (Hexahydro-1,3,5-Trinitro-1,3,5-Triazine) originating from the Iowa Army Ammunition Plant in southeast Iowa .

Structure and dynamics of the native and altered aquifer microbial community were examined using culture-independent DNA based profiling methods in addition to state of the art high throughput sequencing of whole community rRNA genes. A variety of statistical approaches were used to resolve temporal and spatial sample relationships and novel organisms were differentiated from known taxa using phylogenetic reconstructions from collected DNA sequences.

Interrogation of the community dynamics of Eubacteria during the bioremediation revealed a unique Geobacteraceae-dominated community coincident with RDX degradation and metabolite accumulation. Census of the 18s rRNA gene sequences collected from deep sediment cores and wells exposed a surprisingly diverse subsurface eukaryotic community dominated by previously unobserved groups within the Fungi and Platyhelminthes (flatworms) Finally, a unique assemblage of the recently discovered group known as the Cryptomycota was present in the aquifer.

This work yielded two primary innovations. The first was providing evidence linking RDX degradation to specific microorganisms at the field scale. The second and most significant contribution was the revelation and characterization of a subsurface eukaryotic community. Current groundwater management practices fail to account for these ecosystem participants who likely contribute to predation, nutrient recycling, and possible contaminant degradation.

Abstract Approved: _____
Thesis Supervisor

Title and Department

Date

MICROBIAL ECOLOGY OF A MANAGED AQUIFER NEAR THE IOWA ARMY
AMMUNITION PLANT (MIDDLETOWN, IA)

by

Joshua Adam Livermore

A thesis submitted in partial fulfillment
of the requirements for the Doctor of
Philosophy degree in Civil and Environmental Engineering
in the Graduate College of
The University of Iowa

May 2012

Thesis Supervisor: Associate Professor Timothy E. Mattes

Copyright by
JOSHUA ADAM LIVERMORE
2012
All Rights Reserved

Graduate College
The University of Iowa
Iowa City, Iowa

CERTIFICATE OF APPROVAL

PH.D. THESIS

This is to certify that the Ph.D. thesis of

Joshua Adam Livermore

has been approved by the Examining Committee
for the thesis requirement for the Doctor of Philosophy
degree in Civil and Environmental Engineering at the May 2012
graduation.

Thesis Committee: _____
Timothy E. Mattes, Thesis Supervisor

Nandita Basu

Richard Valentine

John Logsdon

Stephen Hendrix

ACKNOWLEDGMENTS

I extend thanks to my wife, Sara Comstock, and my children, Abram and Stella Livermore, for tolerating my absence during the past year. I also thank my advisor Tim Mattes and the research group present and past especially Adina Chuang, Yang Oh Jin, Carmen Owens, Anne Alexander, Yi Liang, Meredith Dobson, and Meng Chen Lee.

I gratefully acknowledge Tonya Gibbs of Tetrattech Inc. for collecting many of the samples, providing logistic support, and responding to numerous site related queries. and to Collin Just of the University of Iowa for laboratory support.

ABSTRACT

With increasing global scarcity of freshwater, groundwater aquifers are an increasingly valuable reserve. However, anthropogenic activities endanger the integrity of groundwater resources through excessive withdrawal, insufficient recharge due to landscape changes, and contamination with foreign substances. Bioremediation to degrade contaminants in situ using native or augmented microbial communities is an increasingly popular strategy. While bioremediation is frequently economically favorable, the mechanisms and agents of compound degradation and long term ecological consequences are scarcely comprehended. This thesis is an investigation of microbial community structure and dynamics during a bioremediation event to attenuate an aquifer plume of the explosive compound RDX (Hexahydro-1,3,5-Trinitro-1,3,5-Triazine) originating from the Iowa Army Ammunition Plant in southeast Iowa .

Structure and dynamics of the native and altered aquifer microbial community were examined using culture-independent DNA based profiling methods in addition to state of the art high throughput sequencing of whole community rRNA genes. A variety of statistical approaches were used to resolve temporal and spatial sample relationships and novel organisms were differentiated from known taxa using phylogenetic reconstructions from collected DNA sequences.

Interrogation of the community dynamics of Eubacteria during the bioremediation revealed a unique Geobacteraceae-dominated community coincident with RDX degradation and metabolite accumulation. Census of the 18s rRNA gene sequences collected from deep sediment cores and wells exposed a surprisingly diverse subsurface eukaryotic community dominated by previously unobserved groups within the Fungi and Platyhelminthes (flatworms) Finally, a unique assemblage of the recently discovered group known as the Cryptomycota was present in the aquifer.

This work yielded two primary innovations. The first was providing evidence linking RDX degradation to specific microorganisms at the field scale. The second and most significant contribution was the revelation and characterization of a subsurface eukaryotic community. Current groundwater management practices fail to account for these ecosystem participants who likely contribute to predation, nutrient recycling, and possible contaminant degradation.

TABLE OF CONTENTS

ACKNOWLEDGMENTS	ii
ABSTRACT.....	iii
TABLE OF CONTENTS.....	v
LIST OF TABLES	vii
LIST OF FIGURES	viii
CHAPTER I: INTRODUCTION.....	12
Overview.....	12
Site Characteristics and Background.....	13
DNA Methods of Studying Community Structure	16
CHAPTER II: FIELD EVIDENCE OF GEOBACTERACEAE ASSOCIATED AQUIFER RDX DEGRADATION	20
Introduction.....	20
Materials and Methods	21
Results.....	26
Discussion.....	30
Figures and Tables.....	34
CHAPTER III: USING NYCODENZ TO EXTRACT EUKARYOTES FROM AQUIFER SEDIMENTS FOR SCANNING ELECTRON MICROSCOPY	42
Introduction.....	42
Materials and Methods	43
Results.....	45
Discussion.....	46
Figures	48
CHAPTER IV: EUKARYOTE DIVERSITY AND ABUNDANCE DISTRIBUTION IN A SANDY ALLUVIAL IOWA AQUIFER SAMPLED FROM WELLS AND SEDIMENT CORES	53
Introduction.....	53
Materials and Methods	55
Results and Discussion	58
Conclusions.....	62
Tables and Figures.....	63
CHAPTER V: REVEALING CRYPTOMYCOTA DIVERSITY IN 454 PYROSEQUENCING SURVEYS.....	75
Introduction.....	75
Materials and Methods	76

Results.....	81
Discussion.....	84
Figures	86
CHAPTER VI ENGINEERING AND SCIENTIFIC SIGNIFICANCE	95
APPENDIX A: MULTIVARIATE RRNA GENE DATA AS INDICATORS OF AQUIFER GEOCHEMICAL STATE DURING CARBON AMENDMENT	100
Abstract.....	100
Introduction.....	100
Materials and Methods	102
Results.....	106
Discussion.....	108
Figures	112
APPENDIX B: SUPPLEMENTARY TABLES AND FIGURES FOR CHAPTER II.....	116
APPENDIX C: SUPPLEMENTARY TABLES AND FIGURES FOR CHAPTER V	123
APPENDIX D: ENVIRONMENTAL HEALTH IMPLICATIONS OF WATER CONTAMINATION WITH THE MUNITIONS CONSTITUENT RDX.....	134
Introduction.....	134
Typical U.S. contamination conditions and comparison to recommended limits.....	137
REFERENCES	141

LIST OF TABLES

Table 1 Summary of TRFs identified as affiliated with RDX degradation process.	39
Table 2: Oligonucleotide primers used in this study to amplify eukaryotic 18S rRNA genes.....	63
Table 3: 18S rRNA gene pyrosequencing studies interrogated for potential Cryptomycota sequences	88
Table 4: Primer sequences used in Chapter II and the amplification conditions for primer pairs	116
Table 5: Wells samples from an aquifer near the Iowa Army Ammunition Plant	117
Table 6: Reported Maximum RDX concentrations at some U.S. Military facilities	138

LIST OF FIGURES

Figure 1: Map of wells sampled near the Iowa Army Ammunition Plant in Des Moines County Iowa, USA.....	34
Figure 2: Geochemical measurements from IAAAP monitoring well MW309 during acetate amendment for RDX bioremediation	35
Figure 3. Distributions of taxa in MW309 samples from October 2008 to July 2009 based on 454 pyrosequencing reads of the 16S rRNA gene	36
Figure 4. Phylml Maximum likelihood phylogenies of 16S rRNA gene sequences constructed from representative pyrosequencing OTUs and Deltaproteobacteria reference sequences	37
Figure 5: Two dimensional representation of a three dimensional CLANS map modeling clustering of terminal restriction fragments (vertices) by attraction values (lines) based on the Pearson correlation coefficient computed from absolute TRF intensity values.	38
Figure 6: Non-metric dimensionally scaled ordinations (NMDS) and detrended correspondence analysis ordinations (DCA) illustrating sample similarities of TRFLP and DGGE derived OTUs.....	40
Figure 7: Structure software models derived from TRFLP and DGGE sample OTU distributions.....	41
Figure 8: SEM micrographs of organisms cultured from an Iowa Aquifer	48
Figure 9: SEM micrographs of organisms extracted from aquifer sediments	49
Figure 10: Backscatter images and elemental compositions determined by energy dispersive spectroscopy	50
Figure 11: Secondary electron micrographs from Nycodenz extracted organism from aquifer sediment preserved with paraformaldehyde.	51
Figure 12: Secondary electron micrographs of organisms from a sandy aquifer 50 ft below ground surface and comparison pictures.....	52
Figure 13: Proportional distribution of log ₁₀ abundance of phyla collected from filtered well water (A) and sediments (B).....	64
Figure 14: Distribution of fungal (A) and metazoan (B) classes collected from sediments (red bars) and filtered well water (blue bars).....	65
Figure 15: Taxa distributions in groundwater and sediment samples determined from 454 pyrosequencing.	66
Figure 16: A non-metric dimensionally scaled model (NMDS) of TRFLP data from an aquifer near the Iowa Army Ammunition plant.	67

Figure 17: Principle coordinate analyses based on the UniFrac distance measured from aquifer pyrosequencing data.	67
Figure 18: Hypertree of a maximum likelihood phylogeny of groundwater eukaryotic OTUs (90% sequence identity clustering threshold) with reference sequences added to delineate the Metazoa kingdom	68
Figure 19: Subtree of a FastTree maximum likelihood phylogeny showing the diversity of Platyhelminthes 18S rRNA gene OTU sequences collected from groundwater.....	69
Figure 20: Subtree of FastTree maximum likelihood 18S rRNA gene phylogeny showing pyrosequencing OTUs closely related to Entomobryidae sequences	71
Figure 21: Subtree of FastTree maximum likelihood 18S rRNA gene phylogeny showing pyrosequencing OTUs closely related to Paralamyctes sequences	72
Figure 22: Subtree of FastTree maximum likelihood 18S rRNA gene phylogeny showing pyrosequencing OTUs closely related to <i>Hydra vulgaris</i> sequences.	73
Figure 23: Subtree of FastTree maximum likelihood 18S rRNA gene phylogeny showing pyrosequencing OTUs closely related to Harpacticoida sequences.	74
Figure 24: Subtree of RAxML Maximum Likelihood phylogeny of reference Cryptomycota sequences with query sequences from and Iowa Aquifer.	86
Figure 25: Linear regressions based on Tamura Nei 1993 distances between hypervariable regions of the same Cryptomycota sequence.....	89
Figure 26: Maximum likelihood phylogeny built from partial 18S rRNA genes of reference fungal lineages and sequences collected from 454 environmental pyrosequencing surveys	90
Figure 27: FastTree summary phylogeny of reference Cryptomycota sequences from a previous study and candidate sequences from 13 pyrosequencing sets.....	91
Figure 28: Maximum likelihood phylogenies of the Cryptomycota from 18S rRNA gene pyrosequencing libraries of aquifer, lacustrine, and marine environments with reference database sequences.....	92
Figure 29: Proportional environmental representation of operational taxonomic units (OTUs) within defined groups of a Cryptomycota maximum likelihood phylogeny.	93
Figure 30: Phylogenetic distances between several aquatic environments sampled for Cryptomycota diversity using 454 pyrosequencing	94
Figure 31: Axes 2 and 3 of a detrended correspondence analysis for 16S TRFLP data from IAAAP wells.	112

Figure 32: Shannon diversity (Log_2) for samples from well samples	113
Figure 33: First two axes of a detrended correspondence analysis for eukaryote data from IAAAP wells.	114
Figure 34- OTUs from the Eukaryote DGGE data on the first two axes of a principle component analysis.....	115
Figure 35:Two dimensional representation of a three dimensional CLANS map modeling clustering of terminal restriction fragments (vertices) by attraction values (lines) based on the Pearson correlation coefficient computed from absolute log transformed TRF intensity values.....	118
Figure 36: Photograph of a denaturing gradient gel used to separate 16S rRNA gene PCR fragments in samples during RDX bioremediation.	119
Figure 37: 16S rRNA gene maximum likelihood phylogeny of Betaproteobacteria pyrosequencing OTU representatives (labeled “IAAAP_Eub_OTU”) and reference sequences with Aquificae outgroup.	120
Figure 38: 16S rRNA gene maximum likelihood phylogeny of Bacteroidetes pyrosequencing OTU representatives (labeled “IAAAP_Eub_OTU”) and reference sequences with Aquificae outgroup.	121
Figure 39. TRF profiles for five time points from well MW309 highlighting Deltaproteobacteria and Bacteroidetes TRFs enriched during RDX bioremediation.	122
Figure 40: PhyML maximum likelihood phylogeny of Cryptomycota reference sequences and pyrosequencing derived OTUs collected from Mount Hope Bay (11).....	123
Figure 41: PhyML maximum likelihood phylogeny of Cryptomycota reference sequences and pyrosequencing derived OTUs collected from an Antarctic ocean research cruise (11).....	124
Figure 42: PhyML maximum likelihood phylogeny of Cryptomycota reference sequences and pyrosequencing derived OTUs collected from deep sea ocean samples (22).	125
Figure 43: PhyML maximum likelihood phylogeny of Cryptomycota reference sequences and pyrosequencing derived OTUs collected from deep sea ocean samples (22).....	126
Figure 44: PhyML maximum likelihood phylogeny of Cryptomycota reference sequences and pyrosequencing derived OTUs collected from Sydney Harbor (37).....	127
Figure 45: PhyML maximum likelihood phylogeny of Cryptomycota reference sequences and pyrosequencing derived OTUs collected from Mirs Bay and Tolo harbor(39).	128

Figure 46: PhyML maximum likelihood phylogeny of Cryptomycota reference sequences and pyrosequencing derived OTUs collected from the Cariaco Basin near Venezuela (56).....	129
Figure 47: PhyML maximum likelihood phylogeny of Cryptomycota reference sequences and pyrosequencing derived OTUs collected from an Iowa Aquifer.	130
Figure 48: PhyML maximum likelihood phylogeny of Cryptomycota reference sequences and pyrosequencing derived OTUs collected from the Wimereux and La Rochelle Coast and Lakes Pavin and Aydat (122).....	131
Figure 49: PhyML maximum likelihood phylogeny of Cryptomycota reference sequences and pyrosequencing derived OTUs collected from Lake Fuschlee in Austria (129).....	132
Figure 50: PhyML maximum likelihood phylogeny of Cryptomycota reference sequences and pyrosequencing derived OTUs collected from the deep sea sediments(135).....	133

CHAPTER I: INTRODUCTION

Overview

Aquifers provide an important water resource that is endangered by interaction with humans. In the U.S., groundwater provides 33% of municipal water and 98% of private water (94). It is also habitat for invertebrates and microorganisms. It is critical that humanity understand the consequences of our actions on these subsurface ecosystems to responsibly preserve dwindling water resources.

Anthropogenic interactions with aquifers seem simple and straightforward to the general public. We drill a well and remove the clean water that appears in a seemingly inexhaustible supply. When our source becomes contaminated from an origin either natural or anthropogenic, we select from a suite of treatment technologies to clean the water (36). Despite this simplistic view, we are managing aquifers for sustainable harvest of a resource much like we manage forests to sustainably harvest timber. Yet, it is outside of our paradigm to consider an aquifer as an ecosystem like forests, cornfields, activated sludge reactors, or any other fragile system we monitor for integrity. Professionals who deal with aquifers are well aware of the microorganisms inhabiting this environment, but tend to think of these organisms and their dynamics only in how they immediately benefit or endanger the water as our resource. That is, some microorganisms transform contaminants into innocuous compounds thus protecting the resource, while others are pathogens and their presence indicates a threat.

Distinct from individual microorganisms and their implications, the community of life in an aquifer represents a unique system that is disrupted by our activities (72). In terrestrial ecosystems we can visibly identify the consequences of our management or mismanagement actions. For example, we know that an improperly managed forest set on fire can burn out of control (134) and the disruption to that system is obvious by loss of trees, erosion, and disappearance of creatures dependent on the status quo. In contrast,

there are no visible cues to illustrate the consequences of pollution or management actions on our aquifers. Consequently, most people do not even perceive that anthropogenic disturbance on aquifers could have long term consequences.

I believe that responsible aquifer management demands understanding of the repercussions from disturbances and to this end we have been studying the responses of an aquifer to a management strategy called bioremediation. When feasible, bioremediation is considered to be a cost effective best practice for the removal of contaminants in aquifers (41). This opinion prevails though the process effects intrinsic change to the aquifer environment that may prove deleterious to specific organisms or system function as a whole. The objective of this thesis was to examine the microbial ecology of an aquifer that is actively managed for pollutant mitigation. First, I explored microbial eubacterial dynamics during the bioremediation process in an attempt to link degradation to specific microorganisms (Chapter 2). Next, I examined the sparsely acknowledged eukaryotic community in the contaminated and uncontaminated portions of the aquifer. To this end I developed an extraction method to visualize aquifer microeukaryotes using scanning electron microscopy (Chapter 3), analyzed the general subsurface eukaryotic community characteristics using 454 pyrosequencing (Chapter 4), and investigated the DNA sequence diversity of a fungal group called “Cryptomycota” from the Iowa aquifer pyrosequencing data as well as pyrosequencing sets from freshwater and marine environments (Chapter 5). Preceding these chapters is a brief discussion of the molecular methods used to characterize microbial communities and dynamics, and description of the state of the knowledge regarding the aquifer from which our samples were derived.

Site Characteristics and Background

Located approximately two miles from the Southern boundary of the Iowa Army Ammunition Plant (IAAAP), the studied aquifer is contaminated with RDX (Hexahydro-

1,3,5-Trinitro-1,3,5-Triazine) at a maximum detected concentration of 150 $\mu\text{g/L}$. Contamination originates from the ammunition plant and is believed to enter the groundwater at least partially via infiltration from nearby Brush Creek which also has documented RDX detections (175).

The lifetime health advisory for RDX in drinking water is 2 $\mu\text{g/L}$, and remedial action was taken at the site to bring concentrations below this level. Primary characterization of aquifer hydrologic characteristics and preliminary strategies for mitigation are documented in a technical memorandum detailing a modeling study finished in 2004 (175). This report revealed that contaminated portions of the aquifer are typically about 50 feet below ground surface in a region composed of heterogeneous, medium grained, alluvial deposited sand. Slug tests to estimate hydraulic conductivity permitted calculations of linear flow velocity which range from 8 to 500 ft/yr throughout the area (2.5 to 150 meters/yr).

Remedial action was conducted thereafter by Tetrattech Inc. who adopted a strategy of reductively enhanced bioremediation by carbon addition via a network of injection wells (169). The bioremediation process, while effective, is poorly understood at the field scale and we tracked the microbial community during the process to identify a possible bacterial agent of compound degradation (Chapter 2).

In addition to the bacterial community, I am interested in the subsurface eukaryotic community as an ecosystem participant during bioremediation or other management activities. Fortuitously, a 1991 study (78) examining and modeling the movements of microorganisms in aquifers was performed in a site with characteristics very similar to our own (surficial aquifer, medium sand, linear flow velocity 120 meters/yr) thus providing an opportunity to predict the optimal size of organisms for maximum dispersal. Their filtration model (78) and a refinement (23) predicted maximum dispersal (estimated <5% capture efficiency) of particles at 2 to 3 μm diameter captured predominantly from the interception mechanism. Larger sizes yielded

a progressive increase in capture efficiency reaching nearly 99% capture by a diameter of 10 μm where the predominant mechanism was gravity settling.

Based on the predictions from filtration theory we would expect negative size selection for single celled eukaryotic organisms (*Cryptosporidium parvum* cells, for example, are 3 to 5 μm in diameter) if we assume that dispersal ability confers fitness. Therefore, eukaryotic organisms with diameters between 1 to 5 μm might feasibly repopulate an aquifer region perturbed by contamination or remediation. Given the high linear groundwater velocities in the aquifer we studied (approximately 6 to 40 ft/month) large perturbed aquifer regions could hypothetically be regenerated biologically in the span of months to years.

Conversely, we do not expect that larger metazoan organisms like crustaceans or worms (50 μm to millimeters) would be able to repopulate a perturbed aquifer through passive dispersal as they are large enough to be held in place by straining. Rather, to disperse these organisms would need to actively move or "burrow". In the absence of data on how fast these organisms migrate in aquifers we can only conjecture that repopulation of perturbed regions would be slow, as up-gradient organisms would have no obvious incentive to disperse to disturbed areas. Speculatively, repopulation would occur over time in a random walk due merely to chance colonizations from adjacent unperturbed aquifer regions. Therefore, detection of recent local perturbation might be apparent through surveys of aquifer metazoans.

It is unclear, though unlikely, that RDX contamination of the studied aquifer constitutes perturbation or disturbance. A review of RDX toxicology is included in Appendix D. In general, RDX is acutely toxic when the solid is swallowed though minimal toxicity is also observed in aqueous solution at the solubility level (approximately 35 mg/L). Concentrations observed in this aquifer never exceed 200 $\mu\text{g/L}$. Additionally, RDX is not bioaccumulative further attenuating possible status as an agent of relevant biological perturbation. In contrast, remediation methods for removal of RDX

might constitute a disturbance. Addition of a carbon source to an aquifer promotes biological activity thus inducing electron acceptor depletion and subsequent hypoxia (180). Aquifer metazoans may be intolerant of hypoxia which we would detect by comparing adjacent aquifer regions affected and non-affected by acetate additions as discussed in Chapter 4.

DNA Methods of Studying Community Structure

Analyzing biological communities begins with sampling its constituents. For ants, birds, fish, and most macrobiotic communities this means physically capturing members and assigning them to a species based on their morphology. For communities of organisms that are not visible to the naked eye, this approach is unfeasible because of difficulties in taxonomic assignment from morphological data. Additionally, communities of microscopic organisms have large populations requiring that a manual sample be prohibitively profuse to be representative.

One solution to this problem is to indiscriminately collect large numbers of small organisms and extract the DNA of the collective. A region of the 16S and 18S ribosomal RNA gene is found in prokaryotes and eukaryotes, respectively, and is used as the target of the polymerase chain reaction (PCR) (121, 181). A random sample from the pool of PCR products serves as proxy for sampling organisms. Cloning and sequencing large numbers of amplicons is an effective but highly laborious and expensive process (181). A variety of other methods have been perfected to rapidly separate and enumerate unique PCR products including denaturing gradient gel electrophoresis (DGGE), terminal restriction fragment length polymorphism (TRFLP), single strand conformational polymorphism and others (128). In our laboratory we have used DGGE and TRFLP.

DGGE was invented by Leonard Lerman while working at SUNY in Albany (62). Standard electrophoresis separates fragments of DNA by their molecular weight with smaller pieces of DNA traveling through a gel at a faster rate than larger ones. In

contrast, DGGE is designed to separate fragments of DNA that have identical length but different sequences. This is accomplished by exploiting the melting characteristics of DNA. A Guanine-Cytosine (G:C) pair has three hydrogen bonds while an Adenine-Thymine (A:T) bond has only two. Therefore, any mutation that changes a G or a C to an A or a T will yield a molecule that has a lower melting temperature. This property is harnessed by casting gels that are highly denaturing at the bottom, non-denaturing at the top, and a linear denaturing gradient between the two extremes.

After products are loaded onto gels they are electrophoresed. As the sequences with the lowest melting temperature denature, effective surface area increases resulting in a complete retardation of electrophoretic mobility. To ensure a fragment never fully melts, a 40 nucleotide base pair “GC” clamp composed of guanines and cytosines is added to one end.

After electrophoresis is complete the gels are stained with a high sensitivity dye and photographed. Bands of interest are excised from the gel for amplification or cloning. Photographs are digitized by defining bands based upon their migration distance and determining relative abundance based upon intensity. The final result is a matrix with bands in rows, samples in columns, and relative or absolute intensities as the entries. This matrix is used in subsequent analysis.

While useful in some cases, DGGE is plagued with problems resulting in its demise as a mainstream technique. The polyacrylamide gels used are extremely difficult to cast and impossible to cast reproducibly. Reproducibility is further hindered by spontaneous degradation of denaturants. A gel left in the refrigerator for one day will suffer complete loss of denaturing capacity meaning that gels can never be made ahead or precast for sale. Handling procedures following a run are also extremely challenging owing to the fragility of the gels. Finally, the presence of single stranded incomplete PCR products can lead to observable bands that do not represent unique organisms in a sample and results in an overestimation of diversity.

TRFLP (116) is another method that is used to separate PCR products of identical length into distinguishable units by unique sequence. This is accomplished by exploiting the sequence-specific cutting behavior of restriction enzymes. PCR is conducted using primers labeled with a fluorophore, a molecule that will fluoresce when exposed to light of a certain wavelength. Whole PCR products are restricted and a portion electrophoresed on an automated capillary DNA sequencer (University of Iowa DNA facility uses the ABI 3730). As the fragments pass through a fluorescence detector, the labeled terminal fragments fluoresce with intensity relative to their abundance. An internal size standard correlates retention time with size of the fragment in base-pairs. As in DGGE, TRFLP profiles are converted into a matrix with fragments in rows and samples in columns with entries containing relative or absolute intensities.

The automated nature of the process is favorable and has led to widespread adoption of this technique for characterization of microbial communities. There are also fewer problems with reproducibility than DGGE because there is no gel to handle. An obvious problem is the potential to have two organisms in a sample with the same terminal restriction fragment. There are also reported problems associated with single stranded DNA resulting in false fragments (128). Both DGGE and TRFLP have advantages and biases (43, 128), but TRFLP has emerged as our preferred method because it is highly sensitive, cost effective, largely automated, and minimizes the steps from sampling to analysis.

An emergent technology to quantify unique sequences in a PCR reaction is pyrosequencing (147). This method permits the independent sequencing of up to 1 million to millions of PCR products from a single sample. Pyrosequencing is a method of “sequencing by synthesis” whereby a strand of DNA is replicated and the incorporation of a nucleotide during polymerization produces a burst of light that is detected and recorded. Sequential addition and removal of the four nucleotides A,C,T, and G provides a means of differentiating the next nucleotide in a strand. 454 pyrosequencing reproduces

the process in 1,000,000 wells on a plate the size of a credit card resulting in the same number of sequences in parallel. Consequently, 454 sequencing a 16S or 18S rRNA gene PCR product would be the equivalent of sampling 1,000,000 random organisms from the environment thus providing a sufficiently large sequence sample to characterize environments economically.

CHAPTER II: FIELD EVIDENCE OF GEOBACTERACEAE ASSOCIATED AQUIFER RDX DEGRADATION

Introduction

Clean and fresh water under the earth's surface is an important resource as groundwater aquifers comprise 33% of municipal and 98% of private fresh water resources in the U.S. (94). Despite great public interest in aquifer protection, groundwater pollution has been reported in every U.S. state comprising an estimated minimum total of one quadrillion gallons of contaminated water (142). Sources of some of this contamination are hundreds of military sites fouled with toxic munitions (102), many of which have been shown to migrate readily in aquifers (158, 174). One of these munitions constituents is RDX (Hexahydro-1,3,5-trinitro-1,3,5-triazine) which is toxic and a suspected carcinogen.

Bioremediation is being used at the Iowa Army Ammunition Plant (IAAAP) in Middletown, Iowa to remove an aquifer RDX plume that has migrated off-site. This proven effective process consists of adding acetate to the groundwater as an electron donor to induce aquifer hypoxia favorable for reductive transformation of RDX by a number of possible pathways including sequential denitration (120), direct enzymatic cleavage (79), reduction by biogenic Fe(II) (183) and others (42, 180). While we understand that adding carbon to an aquifer will likely result in biologically mediated RDX decomposition (180), the microorganisms responsible in subsurface environments remain unknown. Previous attempts to identify anaerobic RDX degraders included enrichment culture strategies (16, 171, 187) and stable isotope probing (45, 148) both of which are designed to elucidate organisms who utilize a given contaminant as a nutrient or energy source. The sole field based study examined the prevailing in situ microbial community during an RDX bioremediation by cheese whey addition in one aquifer and a mulch biowall in another (65), though useful inference from that investigation is severely

constricted as only a single time point was assessed in each aquifer. The totality of all the above studies renders conflicting conclusions regarding probable microbial participants, as each implicated different organisms or consortia as possible agents of RDX degradation (For example, *Geobacter*, *Acetobacteria*, *Clostridia* (16); *Gordonia*, *Williamsia* (171), *Desulfovibrio* (187), *Sphingobacteria* (45); *Enterobacter* and *Pseudomonas* (148))

To identify potential RDX degrading organisms at the field scale during an active bioremediation we collected samples from the RDX contaminated aquifer near IAAAP before, during, and after acetate injections from injection sites and wells up-gradient and down-gradient from injections. Using data from the DNA based microbial community characterization techniques terminal restriction fragment length polymorphisms (TRFLP), denaturing gradient gel electrophoresis (DGGE), clone libraries, and 454 pyrosequencing we statistically delineated and phylogenetically characterized consortia associated with RDX degradation and metabolite production.

Materials and Methods

Site Characterization

The Iowa Army Ammunition Plant located near Burlington, IA (40° 48' N, 91° 15' W) is the origination point of RDX groundwater contamination. Located within the Mississippi River valley, the contaminated aquifer is of alluvial origin and composed of medium to coarse grain sized sands. Groundwater flow velocities in the immediate area of interest range approximately between 24 and 40 ft/yr based on slug tests, measurements of hydraulic gradient, and porosity (176). Our investigation focused on wells in this aquifer within a one mile radius (Fig. 1). The wells designated SMW04-SMW08 and SMW10 are injection wells while MW309, EMW02, and EMW04-EMW07 are monitoring wells located down-gradient of the injection site and are thus subject to

impact by acetate injections. MW505 and MW502 are background wells located up-gradient of the injection wells. Samples were taken before, during, and after injections which occurred in October 2007, January-March 2008, and the largest mass during April 2009 (1300 kg).

Sample collection, Analytical Measurements, and DNA extraction

Groundwater wells were low-flow (<400 ml/min) purged with a peristaltic pump while monitoring dissolved oxygen, pH, conductivity and ORP using a YSI model 556 field probe with flow cell. After readings stabilized, one liter of water was passed through 0.22 μm PES filters (Sterivex filters, Millipore, Billerica, MA, USA). Filters were immediately shipped to the University of Iowa on ice and frozen at -20°C until further processing. Ferrous iron and sulfide were measured using a Hach DR2020 and water samples were delivered to Accutest Laboratories for measurement of nitrate, total organic carbon, hexahydro-1,3,5-trinitro-1,3,5-triazine (RDX), and its nitroso-metabolites MNX, DNX, and TNX. Sterivex filters were opened with a tubing cutter and filter aseptically removed from housing using a sterile scalpel. Filter material was cut into 24 to 36 pieces before DNA was extracted using the MO-BIO ultraclean soil DNA isolation kit with the cell lysis step performed on a Biospec mini-beadbeater 8 for two minutes.

DNA amplification and microbial community profiling

To characterize and differentiate the microbial community during the phases of bio-stimulation we amplified the 16S rRNA gene and differentiated unique taxa by TRFLP coupled with a clone library, DGGE, and 454 pyrosequencing. Primers targeted the V1-V3 regions of the 16S rRNA gene (all primer sequences and reaction conditions in Appendix B, Table 4). Amplification was performed using the universal 16S primer

pair 8fm and 1492r (181) with the Qiagen Taq PCR master mix kit, 0.5 μ M of each primer, and 2 μ l of DNA extract (0.4 to 2 ng) as the PCR template. Concentrations of all PCR products were measured using the DS DNA broad range kit for the Qubit fluorometer (Invitrogen, Carlsbad, CA, USA).

For TRFLP the forward primer was tagged with a 5' 6-FAM fluorophore and following amplification exactly one μ g of purified PCR product (measured using fluorometer) was digested with MspI (New England Biolabs, Ipswich, MA, USA) at 37 $^{\circ}$ C for four hours then desalted by glycogen precipitation. Seventy ng of digested PCR product was sent to the University of Iowa DNA facility for electrophoresis on an Applied Biosystems 3730 DNA analyzer (Life Technologies Corporation, Carlsbad, CA, USA) with the GeneScan 500 LIZ size standard. Output was analyzed using the Applied Biosystems Peak Scanner software followed by T-REX (44) yielding a table with each terminal restriction fragment (TRF) treated as an operational taxonomic unit (OTU) with abundance defined by measured peak area. To phylogenetically identify terminal restriction fragments (TRFs), we produced clone libraries from two representative TRFLP amplifications using the Topo TA 2.1 cloning kit (Invitrogen, Carlsbad, CA, USA). Clones were sequenced at the University of Iowa DNA facility, and classified using the RDP classifier (178). Clones were also digested and fragment analyzed as above, and TRF length predictions produced from sequences using TRiFLE (92)

For DGGE, approximately 400 ng of each PCR product was processed using the Dcode universal mutation detection system (Life Science Research, Hercules, CA, USA) employing an 8% polyacrylamide gel with 30%-60% urea/formamide gradient where 100% is 7M urea and 40% v/v formamide. Gels were run at 60V for 15.5 hrs at 60 $^{\circ}$ C then immediately stained with Sybr Gold nucleic acid stain (Invitrogen, Carlsbad, CA, USA). Stained gels were photographed and lane profiles digitized using Carestream Health Molecular imaging software version 5.0 (Carestream Health Inc, Rochester, NY, USA).

454 Pyrosequencing

A subset of the samples were re-amplified for the multiplexed 454 amplicon pyrosequencing reaction (161) using primers from a previous study targeting the V1-V3 region (21). We sent gel purified re-amplifications to the University of Iowa DNA facility for quality control testing on an Agilent Bioanalyzer (Santa Clara, CA, USA) and subsequent sequencing on the 454 GS FLX instrument (Branford, CT, USA). Quality filtered sequence reads were processed using Quantitative insights into microbial ecology (Qiime)(29). Samples were filtered to retain sequences between 200 and 1000 bases with quality scores greater than 25 units and no more than three primer base mismatches. Operational taxonomic units were selected using Uclust (55) at a 97% sequence similarity threshold and thereafter were represented by the most abundant sequence in each cluster. Chimeric OTUs were identified using ChimeraSlayer (74) and non-chimeric OTUs were retained and phylogenetically identified using the RDP classifier with the Greengenes core set as the source database (50).

Statistical analysis of TRFLP and DGGE profiles

To identify TRFs associated with RDX degradation and metabolite production we used random forest classification (26, 101) and CLANS clustering (63, 64). The TRF intensity matrix was standardized by resampling to a uniform intensity level (i.e. rarefaction (80)) using `single_rarefaction.py` in Qiime). Samples were manually classified as RDX degrading/RDX non-degrading and metabolite producing/metabolite non-producing based on the direction of concentration change at time of sampling. The RDX and MNX sample classifications were used independently to train the random forest classifier implemented through the `supervised_learning.py` script in Qiime. TRFs most associated with a given classification were identified based on maximum values of Gini variable importance (69) and the relative confidence in the RDX and MNX classifications assessed by the values of estimated generalization error.

An unsupervised clustering was implemented using CLANS which is a program for grouping of variables in vector space based on attraction values of the user's choosing for which we selected Pearson's R. We used the "cor" function in the R statistical environment to compute Pearson correlations between peak areas of each TRF pair and also between the TRF peak areas, dissolved oxygen (DO), DO concentrations amended with a negative sign to infer inverse correlation, and MNX concentrations. Computations were repeated using \log_{10} values of TRF intensities. Pearson correlations were imported into CLANS in which variables are represented by points placed randomly into a confined three dimensional space. Clustering is modeled by permitting variables to co-migrate in space with direction and force dictated by computed attractions thus resulting in spatial grouping of co-correlated variables. When migration ceases (after at least 10,000 iterations in our analysis), we assume steady state has been reached and assess the resultant clusters. In addition to the random forest classification and CLANS clustering, we used ordinations and a Bayesian clustering approach to support inferences regarding distinctiveness of microbial communities. First, raw TRFLP and DGGE intensity matrices were converted to relative intensity matrices and presence absence matrix where any peak with area greater than 5% of the total area of all peaks in a sample assigned a value of "2", any peak present below 5% of all area assigned a "1", and any peak absent from a sample assigned a "0". To obtain a consensus of samples that group together we used both the TRFLP and DGGE area matrices analyzed in parallel with three different multivariate statistical tests. Using the relative abundance matrix we performed non-metric dimensional scaling and detrended correspondence analysis with the Vegan package in R (132) while the presence-absence matrix was analyzed using Structure 2.31 (140) which uses a Bayesian method originally designed to analyze multi-locus genotype data, but will reveal clusters in any multi-parameter data set. We performed the Structure analysis assuming 2, 3, 4, and 5 clusters all with optimized parameters of $\lambda=0.67$ under the "admixture" model with correlated character frequencies.

Phylogenetic analysis of DNA sequences

Clone and OTU sequences were aligned using the SINA aligner on the SILVA website (141) then imported into ARB (118) along with the SILVA v106 non-redundant reference database. Within ARB we added sequences we collected into the provided guide tree by maximum parsimony. To reassess phylogenetic positioning, a representative sequence subset was extracted, imported into the Seaview alignment editor (70), trimmed to eliminate outlying sequences and positions, and phylogeny computed using PhyML(73) with optimal parameters determined by the ModelGenerator software and assessed confidence using 500 bootstrap replicates

Data Deposition

Novel DNA sequences collected in this study have been deposited in Genbank (Accession Nos. JQ350561-JQ350696)

Results

Geochemical results from groundwater wells during acetate addition

The two wells of greatest interest were EMW02 and MW309 both of which are immediately down-gradient of the injection wells (~30 meters) but responded differently to acetate injections. EMW02 remained aerobic with dissolved oxygen typically greater than 4 mg/L, nitrate concentrations typically greater than 15 mg/L, and other electron acceptor markers consistent with aerobic conditions RDX concentrations in EMW02 varied, but changes were not necessarily coincident with acetate addition and no appreciable RDX metabolites were observed. In contrast, well MW309 experienced decreases in dissolved oxygen and nitrate and increases in Fe(II) and Mn(II)(Fig. 2) consistent with iron reducing conditions. The observed changes in electron acceptor regime were accompanied by a decrease in RDX concentrations and during some time periods accumulation of the metabolites MNX, DNX, and TNX. Values of MNX had

strong correlation to DNX and TNX supporting our use of MNX in all subsequent analyses as the sole indicator of metabolite production ($R=0.94$ and 0.84 respectively, $n=21$). The injection wells (SMW04-SMW08) and other monitoring wells (EMW04-EMW06) all appeared to remain aerobic ($DO >2$ mg/L) with no appreciable decrease in nitrate concentrations. The up-gradient background wells are partially located in a different geologic unit and were hypoxic during the course of testing with all but one sample having DO concentrations below 0.5 mg/L, nitrate concentrations below the detection limit, Fe(II) concentrations greater than 1 mg/L, and no detectable RDX.

High throughput pyrosequencing of samples from MW309

Having identified several samples from MW309 as being the most likely candidates for a degrading community based on terminal electron acceptor and DNA profile results (following), we pyrosequenced five MW309 samples taken from 10/9/2008 through 7/20/2009 thus covering conditions before, during, and after RDX degradation and metabolite production. From 45,775 sequences we differentiated 4099 OTUs. Samples before and after the degradation period were dominated by Betaproteobacteria (94% (10/9/2008)-, 99% (12/9/2008)-, 75%, (7/20/2009); Fig. 3) identified by the RDP classifier as being taxa within the Rhodocyclales and Burkholderiales classes. The samples we identified as a probable degrading community were marked by a drastic shift to dominance by Deltaproteobacteria (54% (4/22/2009)-, 63% (5/5/2009)-) and Bacteroidetes (25% in each) with Betaproteobacteria relative abundance falling below 3% in each sample (Fig. 3).

Phylogenetic analysis of representative OTUs

To evaluate phylogenetic placements of pyrosequencing OTUs, we built maximum likelihood phylogenies resulting in recovery of some previously known Deltaproteobacteria clades, thus placing pyrosequencing OTUs at positions we presume to be more accurate (85) (Fig 4). In May and July of 2009, most Deltaproteobacteria

sequences were affiliated with the Geobacteraceae (72% and 71% respectively, Fig. 4) while the most abundant in April 2009 belonged to a previously unclassified clade (91%) The closest ancestor in this reconstruction is *Peredibacter starrii*, which is in the Bdellevibrionales, but the clade is not topologically distinct from the rest of the Bdellovibrionales references which are monophyletic

Dominant Betaproteobacteria OTUs on 10/9/2008 and 12/9/2008 (before period of RDX degradation and metabolite accumulation) resolved into the Rhodocyclales and Burkholderiales classes as in the maximum parsimony phylogeny (~20% and ~30% respectively of total Betaproteobacteria sequences on the two dates) but were joined by sequences in the Hydrogenophilales on 7/20/2009 (after RDX degradation and metabolite accumulation). The three most abundant Betaproteobacteria OTUs grouped in the Ferritrophicum genus (class Hydrogenophiles) and Rhodocyclales class (~20% and ~10% respectively of 7/2/2009 Betaproteobacteria sequences) (Fig. 37).

Finally, the majority of Bacteroidetes sequences were represented by OTUs in unique Flavobacteriales groups (>70% of all Bacteroidetes sequences from all samples based on three most abundant OTUs). Other OTUs were placed in the Chitinophagaceae and Saprospiraceae (both class Sphingobacteriales), clade WchB1-32, and sequences in a unified clade containing sequences from clades WchB1-69 and KD1-131 (Fig. 38)

CLANS clustering and Random forest classification of TRFLP Profiles

To support inferences based upon the five samples from MW309 we used a large number of TRFLP samples in conjunction with multivariate statistics. After removing under-sampled TRFLP profiles (samples with sum peak area two orders of magnitude less than the mean or lower) we analyzed 60 TRFLP samples from 13 wells (Appendix B, Table 5). The CLANS map used to delineate TRFs affiliated with anaerobic measurements and metabolite production reveals a continuum of TRF clusters at one extreme positively correlated with DO concentration and the other negatively correlated.

(Fig 5). The densest, and thus most highly inter-correlated cluster, is tightly affiliated with negative DO correlation as well as positively correlated with MNX concentration. Based on observed estimated generalization errors calculated in the Random Forest simulation, we infer that MNX producing/non-producing state was a slightly more robust supervised classification scheme than RDX degrading/non-degrading state (MNX error = 0.13, RDX error = 0.22). Gini Importance values were used to deduce the most important TRFs in the random forest, and the majority of the most highly Gini-rated TRFs were also in the low DO cluster in the CLANS analysis (8 of 10 highest ranked TRFs in MNX classification, and 6 of 10 highest ranked in RDX classification). Based on this concurrence, we used a combination of both analyses to rank TRFs by excluding all those that did not appear in the low DO cluster of at least one of the two CLANS maps (Absolute intensity based map; Fig. 5, Log₁₀ intensity based map; Appendix B, Fig. 35), and those with Gini Importance value less than 0.001 in both random forest classifications. The important TRFs were then ranked based on their MNX classification based Gini Importance (Table 1). After this filtering procedure 16 TRFs remained and were assigned phylogeny based on clones with correspondent observed TRF (Genbank Accs. JQ350561- JQ350647). Based on phylogenetic assignments obtained from clone DNA sequences, out of 16 highest ranked TRFs, seven were classified as Deltaproteobacteria, six as Bacteroidetes, one as Clostridia, and one ambiguous TRF (clones consistent with both Deltaproteobacteria and Bacteroidetes).

Analysis of a subset of TRFLP and DGGE samples with multivariate statistics.

We used a Bayesian classification method and ordinations to delineate samples that epitomize the RDX degrading community. Due to constraint of only 14 available lanes on a DGGE gel, we restricted our analysis to a subset of samples from MW309, EMW02, MW502, and MW505. Visualization of the denaturing gradient gel reveals the distribution of OTUs to be highly heterogeneous across samples (Appendix B, Fig. 36).

The general trend observed in NMDS and DCA ordinations was samples grouping together according to well of origin (Fig 6). The notable exception to this trend is the close association of two samples from MW309 taken on 4/22/2009 and 5/5/2009. In all ordinations these two samples aligned closer to each other than to any other sample, and in three of the four ordinations they were not closely associated with other samples from MW309. During this time period MW309 was anaerobic based on measured electron acceptors (Fig 2) and was accumulating the metabolites MNX, DNX, and TNX at the fastest rate observed during the course of sampling (Fig. 2).

The model generated using the software Structure further supports that the samples from MW309 on 4/22/2009 and 5/5/2009 deviate significantly from a baseline community (Fig. 7). Based on the model selected (admixture), we interpret output from Structure as the probability that a sample belongs to a given community type. For both DGGE and TRFLP, independent runs of the model assuming two, three, and four communities revealed MW309 samples on 4/22/2009 and 5/5/2009 most likely belong to a different dominant community type than every other sample which was always supported by greater than 80% probability when assuming three or four total communities, and somewhat supported when assuming two communities (probability approximately 50% and 60% for TRFLP and DGGE respectively).

Discussion

This is the first report linking field scale RDX degradation to dynamics of specific microorganisms. Our evidence indicates a dominance of Deltaproteobacteria including *Geobacter spp.* during an RDX degradation and metabolite production phase in one monitoring well. This inference is supported pyrosequencing, CLANS analysis, random forest classification, and ordination of TRFLP and DGGE profiles,. Each of these analyses provides evidence that Geobacteraceae-like sequences are predominant in the community when RDX is degrading and RDX reduction products (MNX, DNX, and

TNX) are accumulating. It is well established that *Geobacter spp.* are ubiquitous in subsurface environments under iron-reducing conditions (83). Additionally, genomic evidence reveals members are adapted to competitive assimilation of acetate (146) supported by empirical observations (13, 35, 86). While certain *Geobacter spp.* are known to degrade RDX (103-106), this is the first evidence linking presence of Geobacteraceae to RDX transformation in the field..

Many laboratory studies designed to identify possible RDX assimilators failed to identify *Geobacter spp.* as potential degraders (45, 148, 170, 187) which may be plausible given the mechanism of degradation by Fe(III)-reducing organisms does not necessarily imply assimilation. *Geobacter metallireducens* is capable of directly reducing RDX (106) by an unknown mechanism and the same phenomena has been observed in other unrelated Fe(III) reducing genera as well (104). Additionally, RDX can be reduced by biogenic Fe(II) resultant from respiration by *Geobacter metallireducens*.(105, 183). We hypothesize the latter mechanism is more likely given the observations that RDX degradation frequently coincides with iron reduction (103, 107) and that surface bound Fe(II) catalyzes the reduction of RDX (71, 183) with the production of the nitroso reduction products as intermediates much like we observed in this study. Indeed, in situ and laboratory microcosm studies in which acetate is added as an electron donor to microcosms or when Fe(II) is the RDX reducing agent both consistently show the production of these same reduced nitroso intermediates (48, 71, 103, 105, 107, 180, 183). Production of these metabolites is rarely attributed to direct enzymatic transformation and no organisms known to directly utilize this pathway (42) were prevalent in our samples.

While *Geobacter*-like sequences are well defined and exert some dominance in our samples, a large number of the sequences collected grouped in a unique Deltaproteobacteria clade possibly representing a novel class. This clade was positioned outside other Deltaproteobacteria precluding inference about the metabolic nature of its

members though we might surmise it may have metabolism similar to the Geobacteraceae given their close dynamic association in our samples.

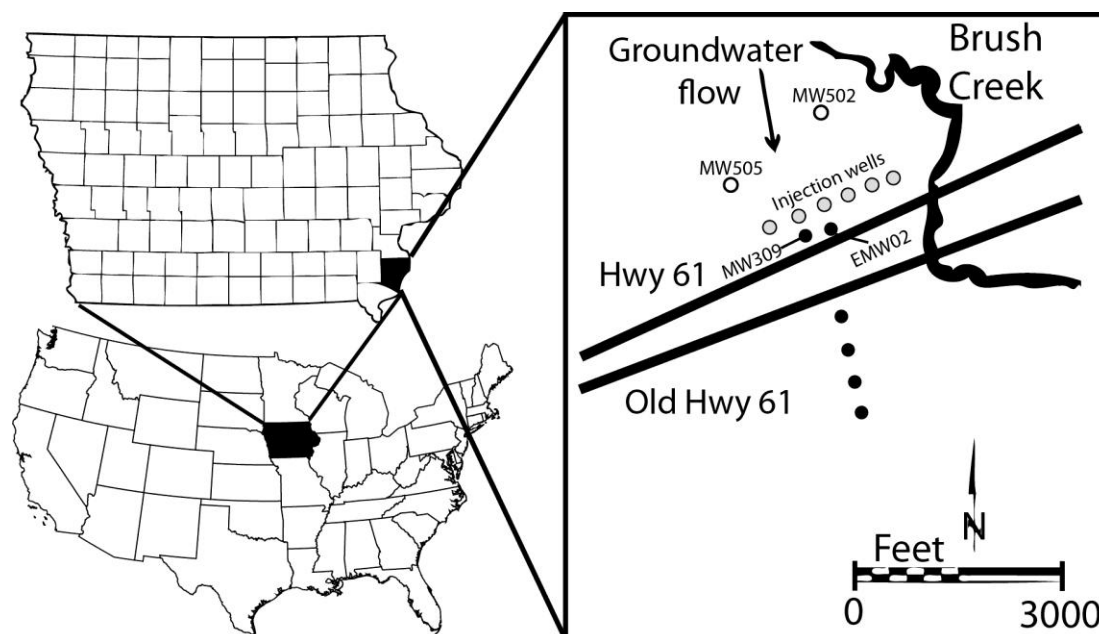
The other phylum we found closely associated with RDX degradation was Bacteroidetes. Therein we identified Sphingobacteriales sequences that positioned phylogenetically with the Chitinophagaceae. Sequences closely related to this family were previously identified as affiliated with RDX degradation based on a study using stable isotope probing to interrogate anaerobic microcosms inoculated with $^{15}\text{-N}$ and $^{13}\text{-C}$ ring labeled RDX (45). Additionally, we found sequences grouping with the WchB1-69 Bacteroidetes clade which has members identified from other Fe(II) reducing environments (113, 179). Despite these two finds, the dominant Bacteroidetes we found grouped phylogenetically with the Flavobacteriaceae which is typically regarded as an aerobic family (20). Within Flavobacteriaceae, one group of OTUs clustered near *Maritimimonas* (Fig 38) which is a gut symbiont of the veined rapa whelk (a marine mollusk) (133), while the remaining *Flavobacteria* OTUs clustered outside of known genera. The significance of the *Flavobacteria* in our samples is not clear, but their status as opportunistic heterotrophs (99) might indicate a fermentative or microaerophilic role in the degradation of high molecular weight organic materials from biomass produced concurrent with biostimulation.

Many of the observed Betaproteobacteria sequences dominating before and after the period of RDX degradation were Fe(II) oxidizers(81) in the *Ferritrophicum* genus, or Fe-oxidizers closely related to *Dechloromonas* and *Ferribacterium* genera indicating sufficient oxygen during these periods for iron oxidation.

In conclusion, this work supports the hypothesis that *Geobacter* species are associated with RDX degradation during acetate amendment of subsurface environments. Substantial additional evidence is necessary to determine if and how the associated *Geobacter spp.* are catalyzing the RDX degradation and if other iron reducers such as those in the Sphingobacteriales may be catalyzing in situ degradation as well. Finally, we

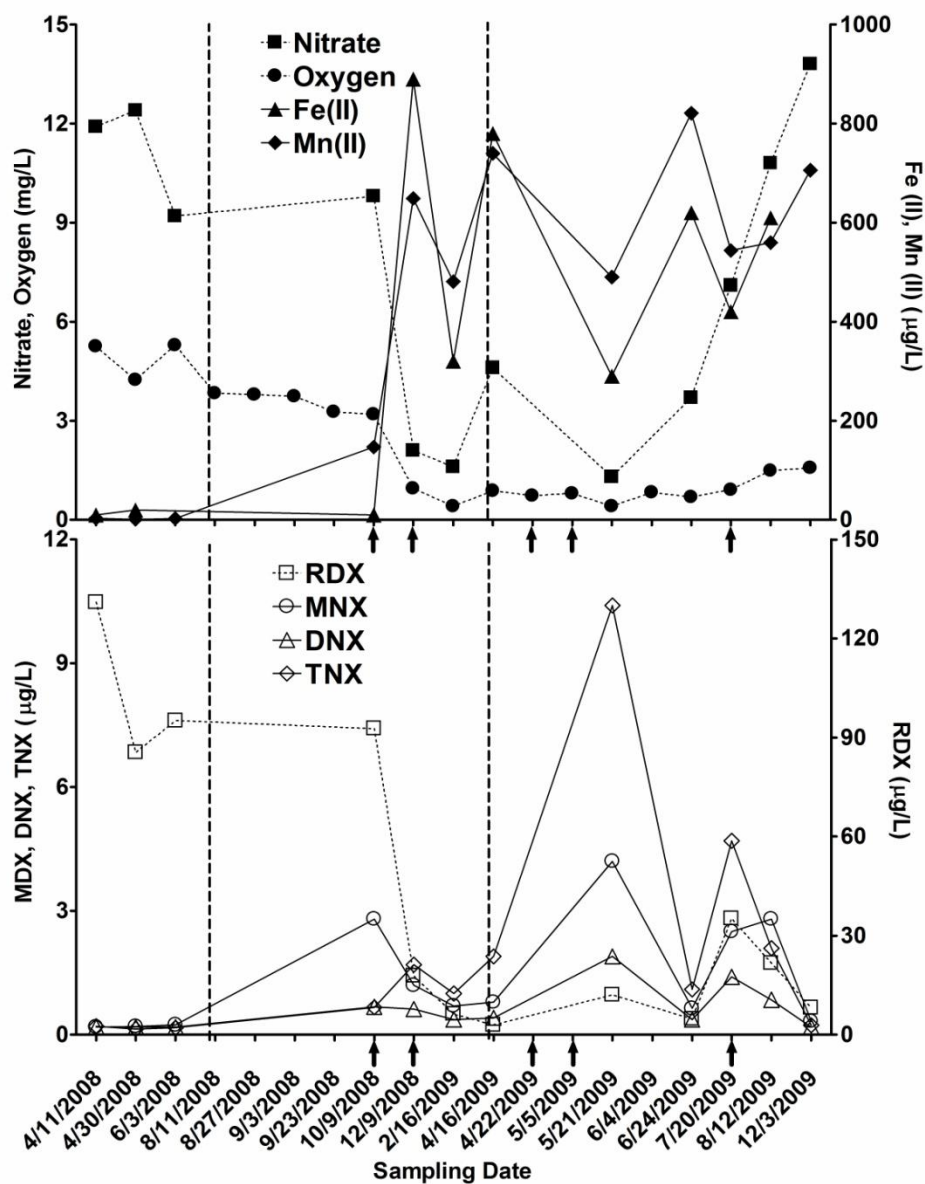
identified novel groups of organisms in the Deltaproteobacteria and Bacteroidetes affiliated with RDX degradation, and these may represent either unknown participants or potential biomarkers for bioremediation performance evaluation.

Figures and Tables



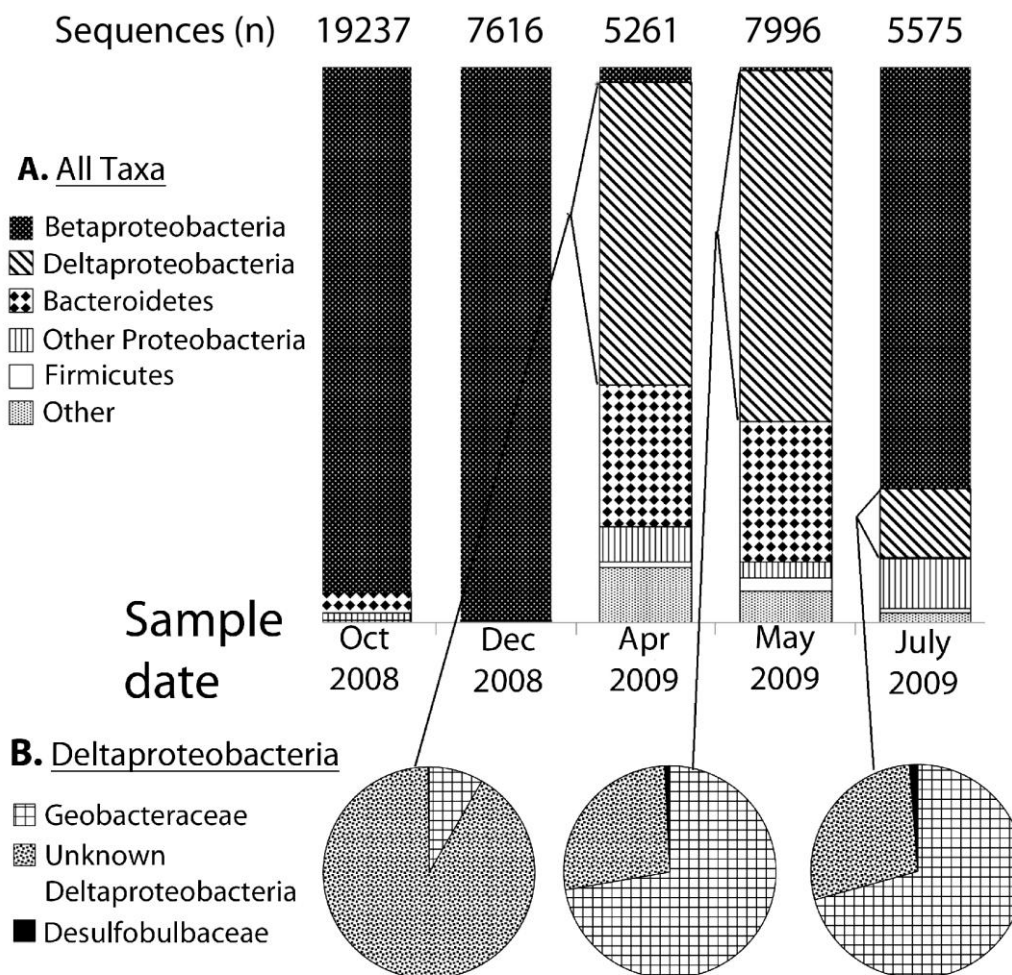
Notes- The location is three kilometers southeast of the plant boundary. Open circles mark wells unaffected by remediation activities, gray circles mark acetate injection wells, and black circles mark down-gradient wells affected by injections.

Figure 1: Map of wells sampled near the Iowa Army Ammunition Plant in Des Moines County Iowa, USA.



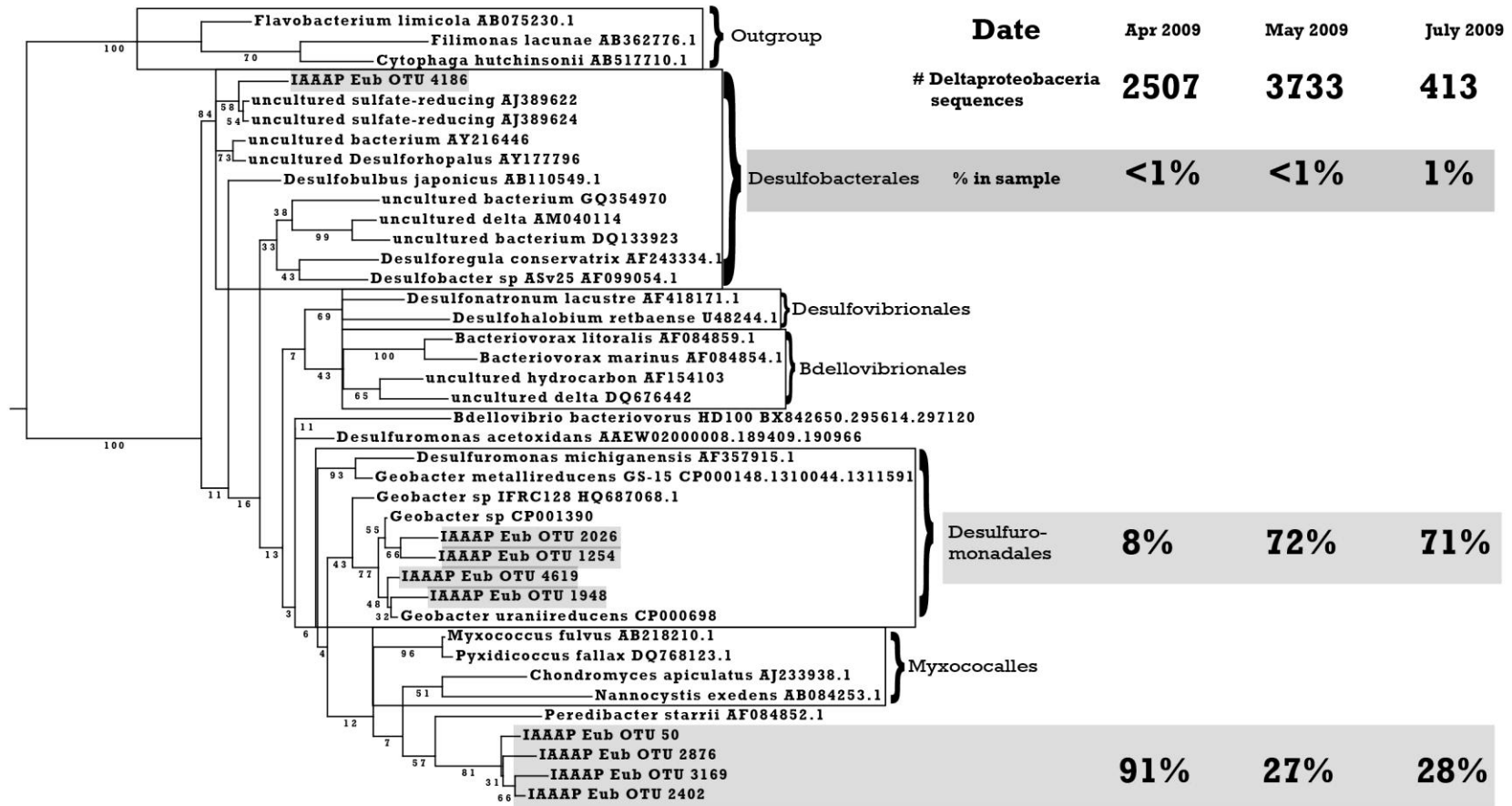
Notes- Closed symbols indicate terminal electron acceptor concentrations including oxygen (circle), nitrate (square), Fe(II) (triangle), and Mn(II) (diamond) while closed symbols indicate RDX (square), MNX (circle), DNX (triangle) and TNX (diamond) concentrations. Vertical lines indicate dates of acetate injection and arrows denote sample dates for 454 pyrosequencing.

Figure 2: Geochemical measurements from IAAAP monitoring well MW309 during acetate amendment for RDX bioremediation



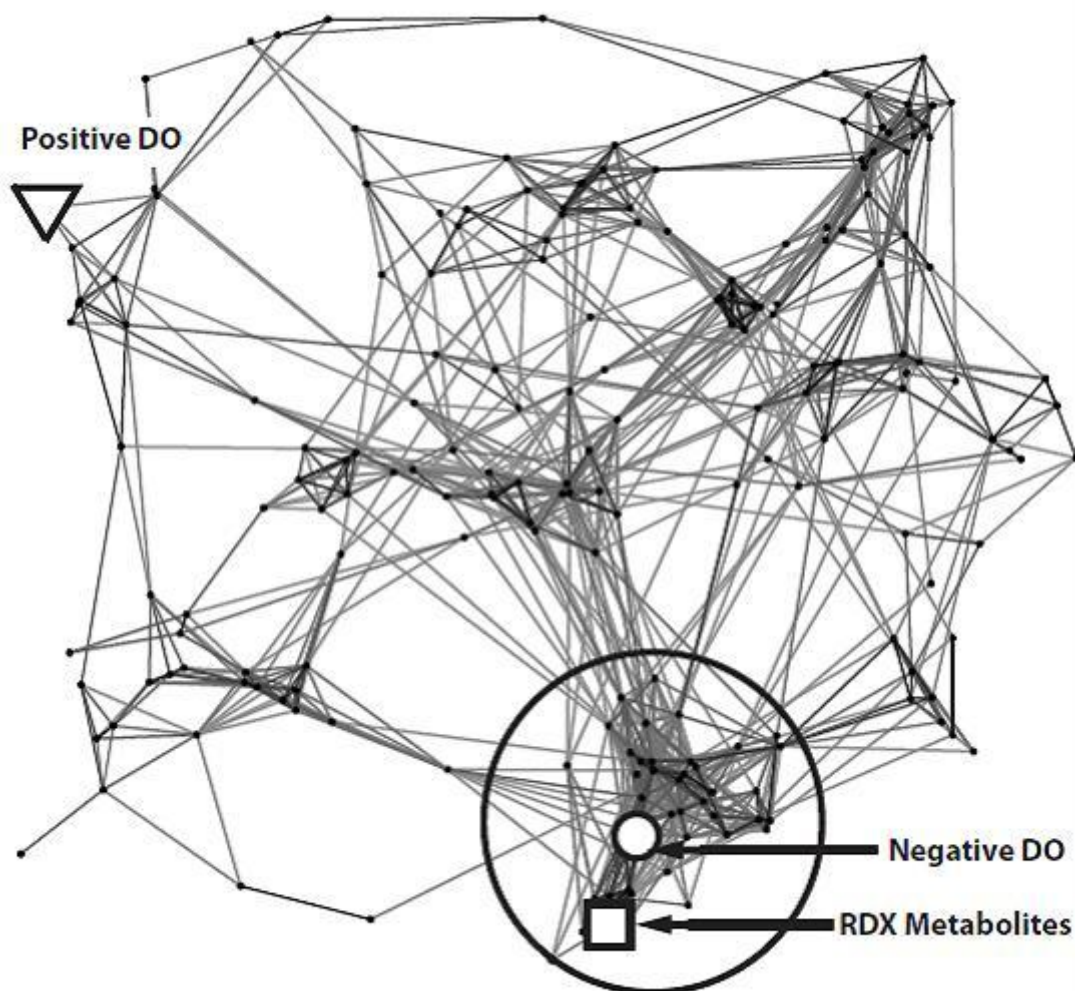
Notes- A- distribution of all major phyla or Proteobacteria subphyla. B- Distributions of families in the Deltaproteobacteria from 4/22/2009, 5/5/2009, and 7/20/2009

Figure 3. Distributions of taxa in MW309 samples from October 2008 to July 2009 based on 454 pyrosequencing reads of the 16S rRNA gene



Notes- 491 nt alignment, TN93+G+I model, SPR moves, 500 bootstraps, bootstrap values are on the branches. Percentages indicate proportion of total Deltaproteobacteria sequences in the indicated sample.

Figure 4. Phyml Maximum likelihood phylogenies of 16S rRNA gene sequences constructed from representative pyrosequencing OTUs and Deltaproteobacteria reference sequences



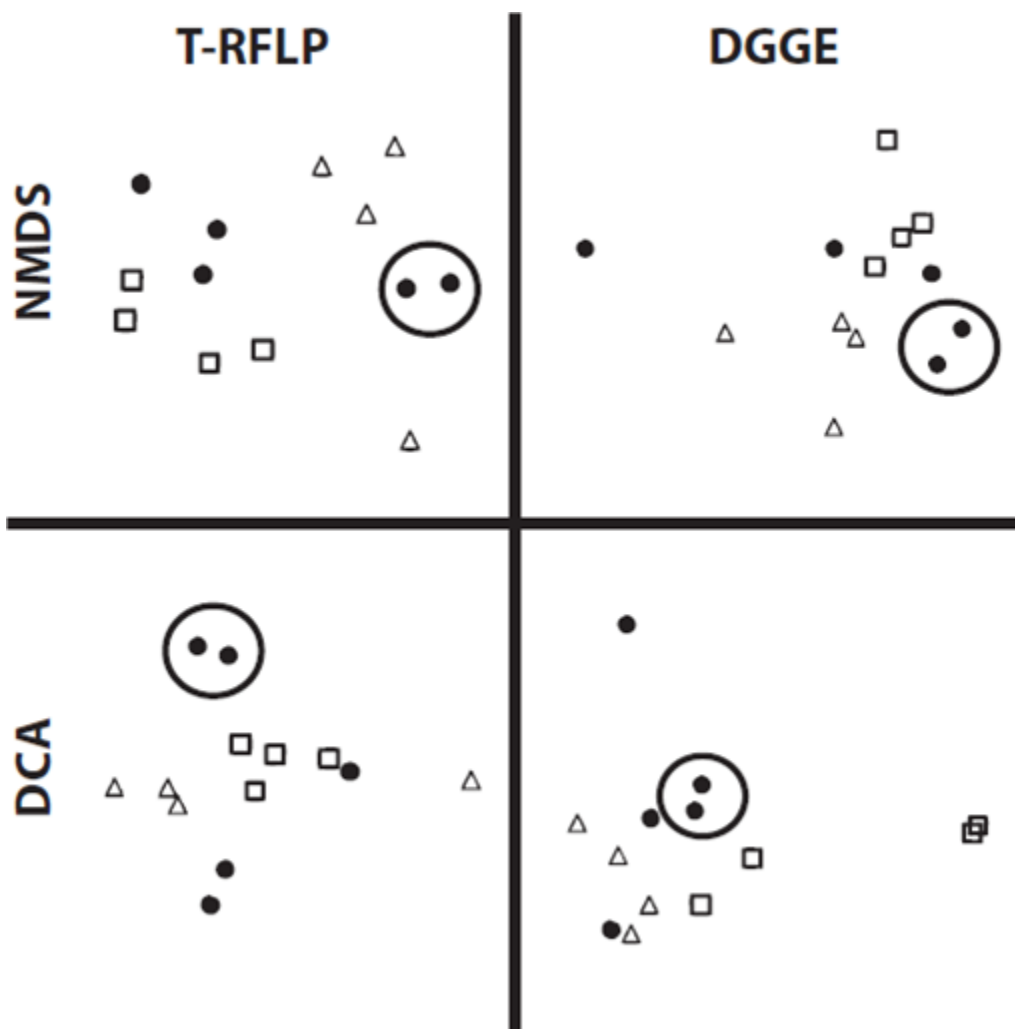
Notes- ∇ =point of maximum correlation to dissolved oxygen concentration, \circ = point of maximum negative correlation to dissolved oxygen, \square = point of maximum positive correlation to MNX concentration. The cluster encompassing TRFs presumed affiliated with RDX degradation is circled

Figure 5: Two dimensional representation of a three dimensional CLANS map modeling clustering of terminal restriction fragments (vertices) by attraction values (lines) based on the Pearson correlation coefficient computed from absolute TRF intensity values.

Table 1 Summary of TRFs identified as affiliated with RDX degradation process.

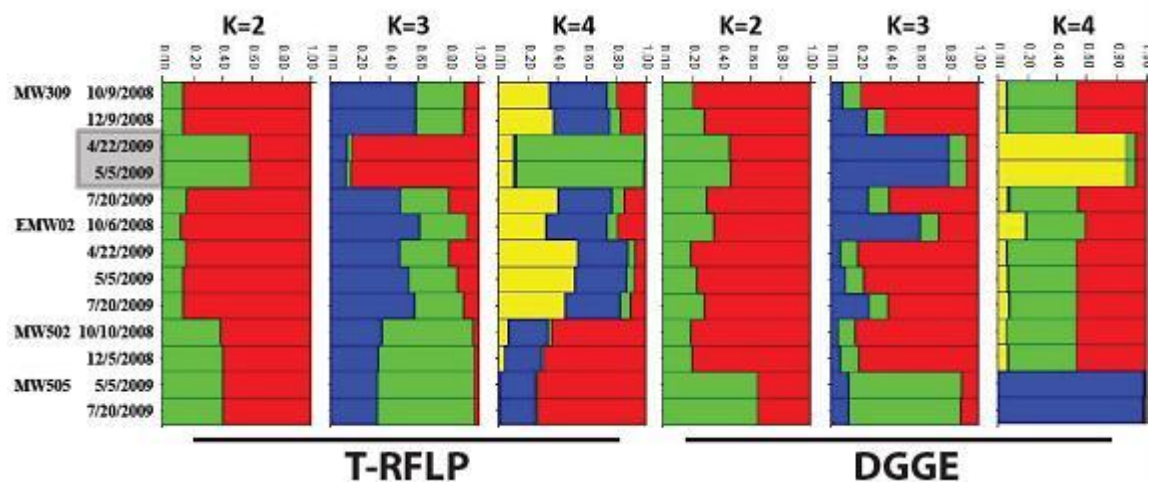
TRF size	Abs CLANS	Log CLANS	MNX rank	MNX importance	RDX rank	RDX importance	Identity from clones	Clone Source
201	X	X	1	1.62	8	2.18	Bacteroidetes	A9, A3, A10, A17, A24, A26, A28, A31, A33, A43, A44, A46, A47, B24
182		X	2	1.69	51	3.66	Deltaproteobacteria	A11, A15, A20, A42, A45, B5
84	X	X	3	1.88	1	1.87	Bacteroidetes	A2, A5, A8, A21
160	X	X	4	2.12	2	1.94	Deltaproteobacteria	A18, A37, A39
88	X	X	5	2.18	16	2.81	Bacteroidetes	A2, A30
159	X	X	6	2.24			Deltaproteobacteria	A9, A42, A45
538	X	X	8	2.38	3	1.99	Bacteroidetes	Firmicutes, Clostridia A4
286	X	X	9	2.44	6	2.11		A5, A8, A35, A41, A48
162	X	X	11	2.55	7	2.16	Deltaproteobacteria	Same as 182
499	X	X	12	2.58	NA	NA	Deltaproteobacteria	A18, A34, A37, A39
205	X	X	13	2.58	31	3.28	Bacteroidetes	Deltaproteobacteria, Bacteroidetes
298	X	X	16	2.84	23	3.15		A16, A32
507	X	X	24	3.21	15	2.80	Deltaproteobacteria	A5
344	X	X	91	4.38	20	2.98	Unknown	NA
505	X	X	102	4.45	12	2.62	Deltaproteobacteria	A21, A48
481	X		112	5.01	11	2.43	Bacteroidetes	A11, A42

Notes- “Abs CLANS,” and “Log CLANS,” indicate the TRF appeared in the Low DO/ MNX affiliated cluster in one of the two CLANS maps while MNX and RDX rank indicate rank of Gini importance in each of the Random Forest classifications. The list is ordered by MNX rank. Importance values are shown as $-\log_{10}$ (Gini importance) so that lower value indicates greater importance. Phylogenetic classifications are based on RDP classifier assignments of clones with the same size TRF (Genbank accs. JQ350561- JQ350647, sequence identifiers from "clone source" column are included in genbank annotation). Two highly ranked TRFs from MNX random forest classification were not classified as important in RDX random forest classification (marked "NA"). TRF size 344 bp had no correspondent clone and was thus not classified.



Notes- Symbols: ●=MW309, □=EMW02, △=background wells MW502 and MW505. In each ordination a circle encloses samples taken from MW309 on 4/22/2009 and 5/5/2009.

Figure 6: Non-metric dimensionally scaled ordinations (NMDS) and detrended correspondence analysis ordinations (DCA) illustrating sample similarities of TRFLP and DGGE derived OTUs.



Notes- Colored bars indicate the probability a sample belongs to a given community type.
K values are the specified number of community types used to construct each model.

Figure 7: Structure software models derived from TRFLP and DGGE sample OTU distributions.

CHAPTER III: USING NYCODENZ TO EXTRACT EUKARYOTES FROM AQUIFER SEDIMENTS FOR SCANNING ELECTRON MICROSCOPY

Introduction

Aquifers tend to be stable and isolated environments, providing conditions which lead to the *in situ* evolution of a rich diversity of organisms that play a crucial role in the overall aquifer ecosystem (52, 72). A diverse microbial groundwater population likely harbors significant metabolic capabilities, a property that can facilitate natural or enhanced *in situ* bioremediation of contaminated aquifers. Microbial ecology approaches aimed at identifying, characterizing, and quantifying known pollutant-degrading microorganisms have provided useful information for developing optimized and/or novel *in situ* bioremediation schemes (160). However, because many pollutant-degraders are eubacteria, most ecological studies relevant to bioremediation focus solely on prokaryotic community members and ignore the eukaryotes.

We have been investigating community structure in an aquifer in southeastern Iowa contaminated with the explosive RDX as it is undergoing biostimulation with acetate as a means to effect RDX reduction. Our preliminary data suggests substantial changes in eukaryotic community composition during biostimulation events.

Problematically, molecular methods commonly used to study prokaryotic communities have limited utility for eukaryotes in groundwater environments because they have yet to be characterized. We do not even yet know what they might look like. This report describes a Nycodenz method used to successfully extract whole, minimally altered eukaryotes from groundwater sediments and subsequently image them using scanning electron microscopy.

Materials and Methods

Site characteristics

The Iowa Army Ammunition Plant located near Burlington, IA (40° 48' N, 91° 15' W) is a source of RDX (explosives) groundwater contamination. Located within the Mississippi River valley, the contaminated aquifer is of alluvial origin and composed of intermediate sands. Groundwater flow velocities range between 80 and 130 ft/yr (176). Acetate is being injected into the aquifer immediately up-gradient of the RDX plume near the well known as MW309.

Sample collection

Aquifer sediment was obtained through direct push method by PSA Environmental (Lee's Summit, MO). Cores 1.5 inches in diameter were aseptically collected down-gradient from the site of acetate injection (Fig 1) as well as from an unaffected region of the same aquifer. Samples were collected from 5 to 10 ft below ground surface (bgs), 10 to 15 ft bgs, and 50 to 55 ft bgs. Following collection, cores were immediately stored on ice before being transported to the University of Iowa where they were stored at -80° C until analysis.

Sediment sample preparation for scanning electron microscopy

Strategy 1: To suspend organisms, 5 grams of collected sediment were placed in a 50 ml falcon tube with 45 ml of 0.1% sterile pyrophosphate solution and agitated on a shaker at 200 rpm for 2 hours. Large particles were permitted to settle for one minute before decanting supernatant into a new tube. To attach organisms to a surface, poly-L-lysine coated silicon wafers were bathed in organism suspension for 30 minutes. Organisms adhering to the surface of the wafer were then fixed with glutaraldehyde and osmium tetroxide before dehydration with a graded ethanol series terminating with hexamethyldisilazane (HMDS) treatment.

Strategy 2: Approximately 2 grams of sediment were incubated overnight at 4⁰ C with either 8 ml 3% paraformaldehyde or glutaraldehyde. Following incubation, 7 ml of 0.1% pyrophosphate was added and samples were agitated on a shaker at 200 rpm for 2 hours. Five ml of supernatant was used to bath a silicon wafer and the remainder was filtered through an isopore filter (Millipore, Billerica, MA). Organisms on wafers and filters were dehydrated with a graded ethanol series and HMDS.

Strategy 3: Organisms were fixed in sediment and suspended as in strategy 2. Supernatant containing suspended organisms was carefully placed on a 60% Nycodenz blanket (density= 1.3 g/ml)(Axis-Shield, Oslo, Norway) of equal volume and centrifuged in a swing bucket rotor at 3000g for 30 minutes. Soil particles migrated to the bottom of the tube while organisms were retained at the Nycodenz-water interface. Organisms were collected from the interface and placed on silicon wafer or collected on an isopore filter. then dehydrated as in strategy 2.

Wafers and filters were fixed to aluminum stubs and either sputter coated for secondary electron scanning electron microscopy or left unsputtered for variable pressure SEM and electron dispersive spectroscopy.

Fungal pure culture isolation and preparation

Sediment samples were suspended in sterile water and shaken at 200 rpm for one hour. Approximately 100 µl was placed on yeast, peptone, and dextrose plates (YPD) amended with 75 µg/ml kanamycin to suppress bacterial growth. Colonies with fungal-like morphology were harvested and fixed with glutaraldehyde and osmium tetroxide before dehydration with a graded ethanol series terminating with HMDS treatment.

Scanning electron microscopy and spectroscopy

Secondary electron images were obtained from either a Hitachi 3400N or S4800 microscope. Variable pressure SEM was performed on a Hitachi S3400N microscope with a Bruker EDS system for energy dispersive spectroscopy.

Results

Pure culture

Pure cultures of fungi were produced to verify their presence in the aquifer and provide a positive control for the fixation and microscopy methods. Based on colony morphology and comparison of fungal SEMs to our own, we determined we successfully cultured Fungi of unknown identity from aquifer sediments (Fig 8) thus verifying the presence of eukaryotic organisms in this aquifer as well as demonstrating fixation and dehydration procedures were performed adequately. Additionally, a single fungal spore was imaged (Fig 8).

Sediment extractions

The first method with any success involved a sample fixed with paraformaldehyde, extracted with Nycodenz, and organisms subsequently fixed to a silicon wafer. Three images of aquifer organisms were obtained this way (Fig 9). Organisms were not readily identifiable. To verify what we were imaging was indeed the relics of living tissue and not inorganic material, an un-sputtered set of Nycodenz extracted samples on isopore filters was examined using variable pressure SEM and energy dispersive spectroscopy (EDS). Inorganic alumino-silicates were easily confirmed as such by EDS and could be identified by angular morphology (Fig 10). Organic material was differentiated by a high proportion of carbon and trace mineral content (Fig 10) and the non-angular structures we investigated proved organic. This confirms successful extraction of organisms from sediment.

Following EDS analysis, the same set of samples was sputter coated with gold and re-examined using secondary electron SEM. Three unique organism morphologies were observed in these samples (Fig 11). A number of filaments were present that greatly resembled those found in fungal pure cultures suggesting successful direct extraction of fungi from the aquifer sediments. The second were flattened cylinders and a third were

round unidentifiable amorphous globes. These globes probably represent a set of organisms that were not preserved well in formaldehyde as it is lost from soft tissues during buffer rinses or dehydration.

A final set of sediment samples were preserved with glutaraldehyde to investigate the effect on structural preservation of organisms. The predominant morphology observed in these was globular but regular and appeared to have superior preservation to that observed with formaldehyde fixation (Fig 12). While not identical to each other, each of the organisms in the four images obtained appear to be yeasts or fungal spores based on comparison to previously taken SEM micrographs of yeasts (Fig . 12).

Discussion

Based on searches of databases and literature archives, this work represents the first time Nycodenz has been used to extract whole organisms from sediments for the purpose of scanning electron imaging. The success of this method is significant because it provides a way to assess the morphology of uncultured aquifer eukaryotes. This method permits studying the morphology and ecology of a set of organisms that have been almost entirely ignored by those exploiting, polluting, remediating, and even those studying groundwater environments.

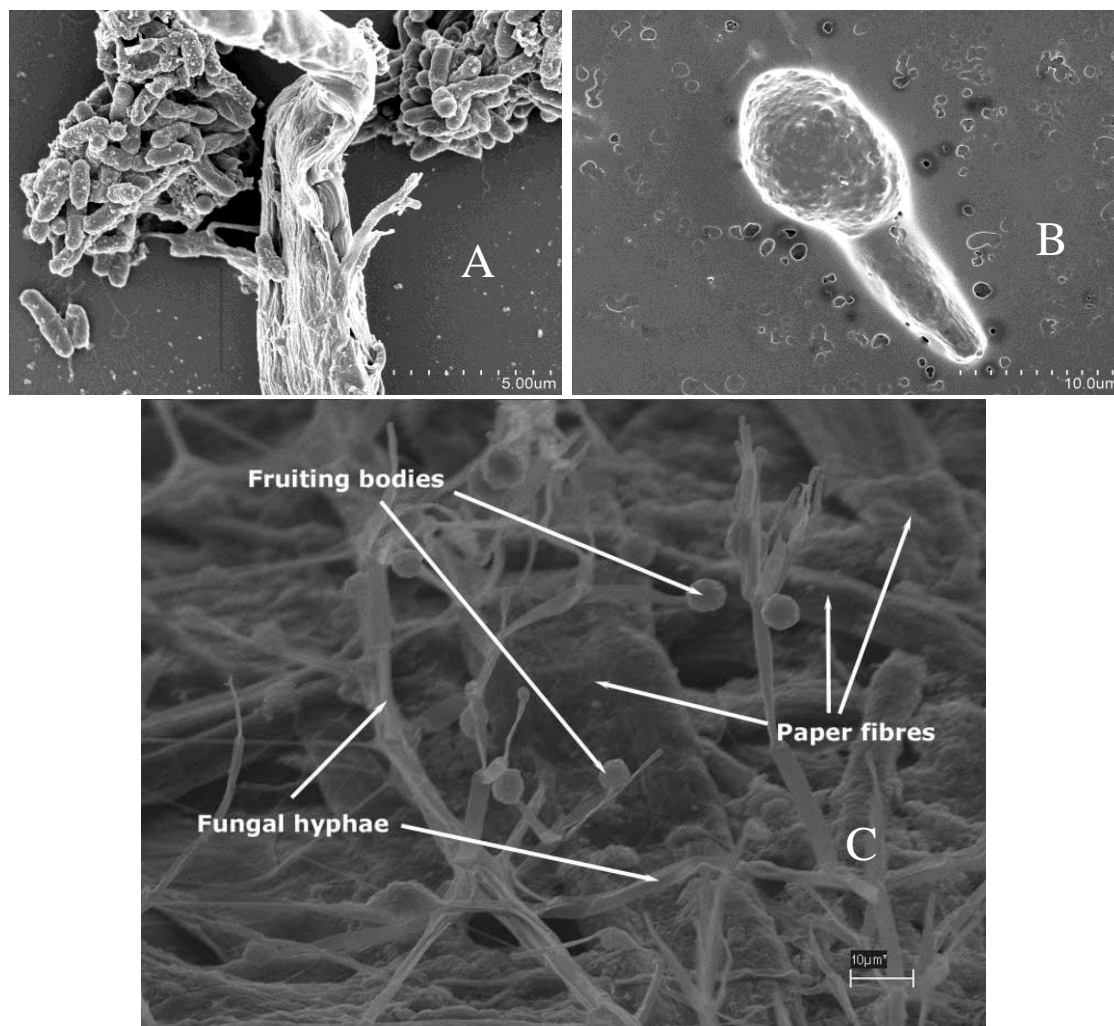
Of the three preparation strategies, the most satisfying results were obtained by fixing the cells in the sediment with glutaraldehyde followed by Nycodenz extraction and collection on isopore filters. Methods that did not employ Nycodenz yielded no detectable organisms from these samples. Collection on filters proved necessary because the concentration of eukaryotic organisms in groundwater is likely low because of low nutrient inputs.

The recovery of yeasts or fungal spores from an aquifer is also significant. Fungi have not been reported in any Iowa aquifer. Most groundwater studies never even addressed the possibility of eukaryotic organisms in aquifers. Only one recent study has

investigated eukaryotes in an organics contaminated aquifer (24). Their central finding was that eukaryotic diversity in an anaerobic aquifer contaminated with landfill leachate was dominated by single cell fungi (yeasts). Our work supports the presence and potential importance of these organisms in shallow, sandy, organically affected aquifers. However, we also recovered what appear to be fungal filaments. The importance these organisms may play in subterranean ecology has yet to be determined as this is the first report of their presence in an aerobic subsurface environment.

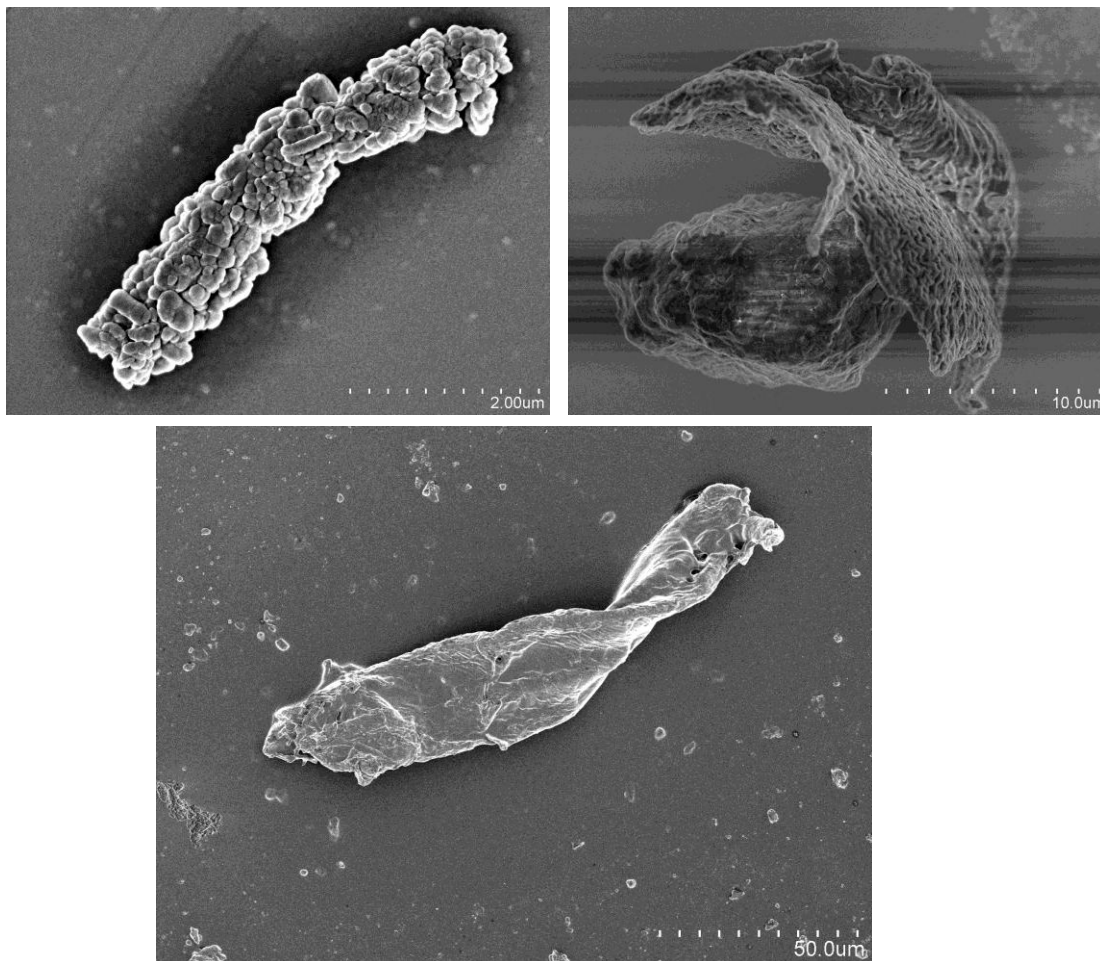
Moving forward, a comprehensive analysis of this aquifer will require examination of organism morphologies across a range of acetate affected and unaffected conditions so that we may explicitly address the hypothesis that acetate amendment affects the eukaryotic communities in aquifers.

Figures



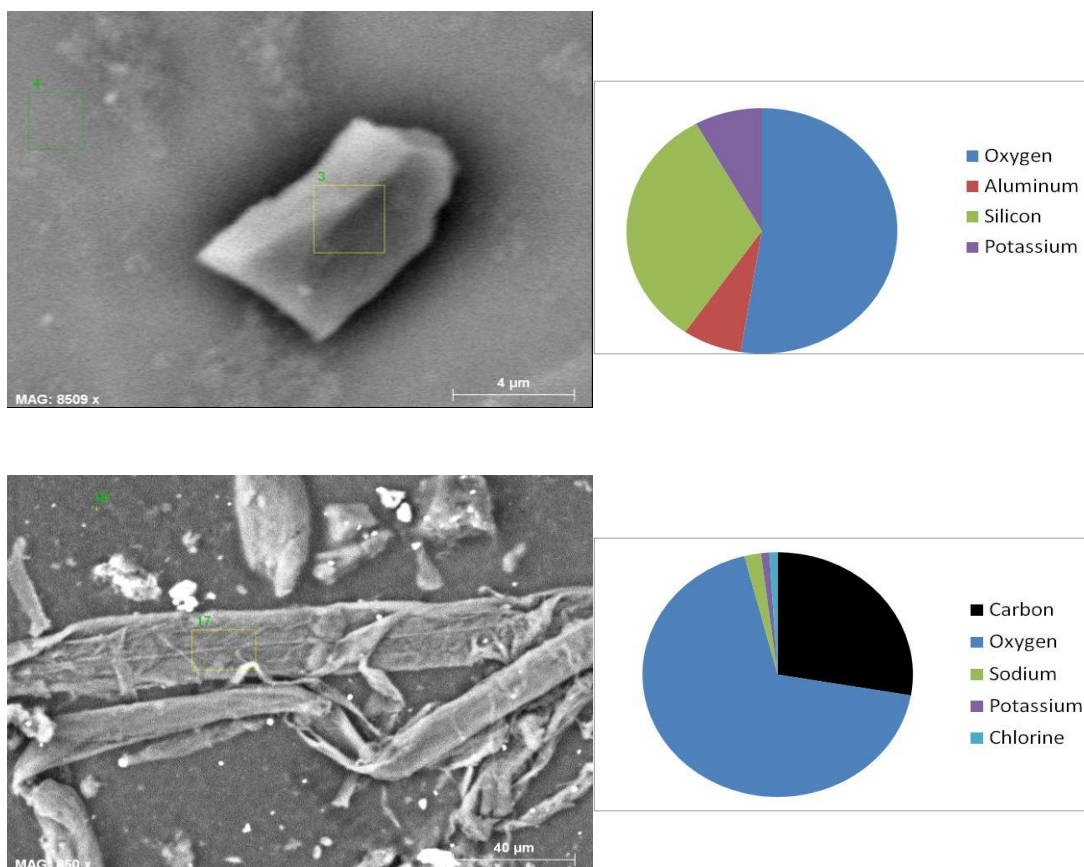
Notes- A- Fungal filament from an organism isolated from a shallow sandy aquifer flanked by bacteria. B- Fungal spore from the same isolate. C- Fungal hyphae and spores similar to those found in our isolate grown in a paper matrix for comparison (Photo: Neil Andrews, Canterbury University)

Figure 8: SEM micrographs of organisms cultured from an Iowa Aquifer



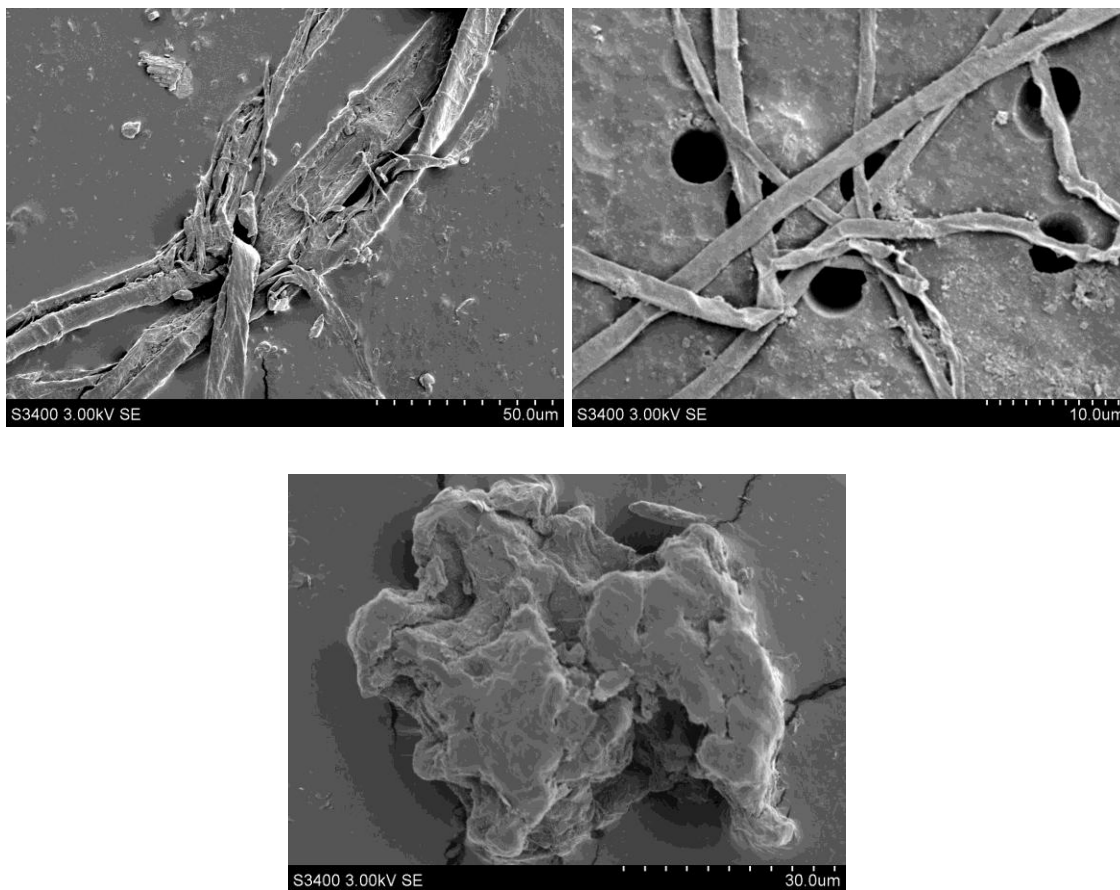
Notes- Unknown organisms extracted from a groundwater aquifer and preserved with paraformaldehyde

Figure 9: SEM micrographs of organisms extracted from aquifer sediments



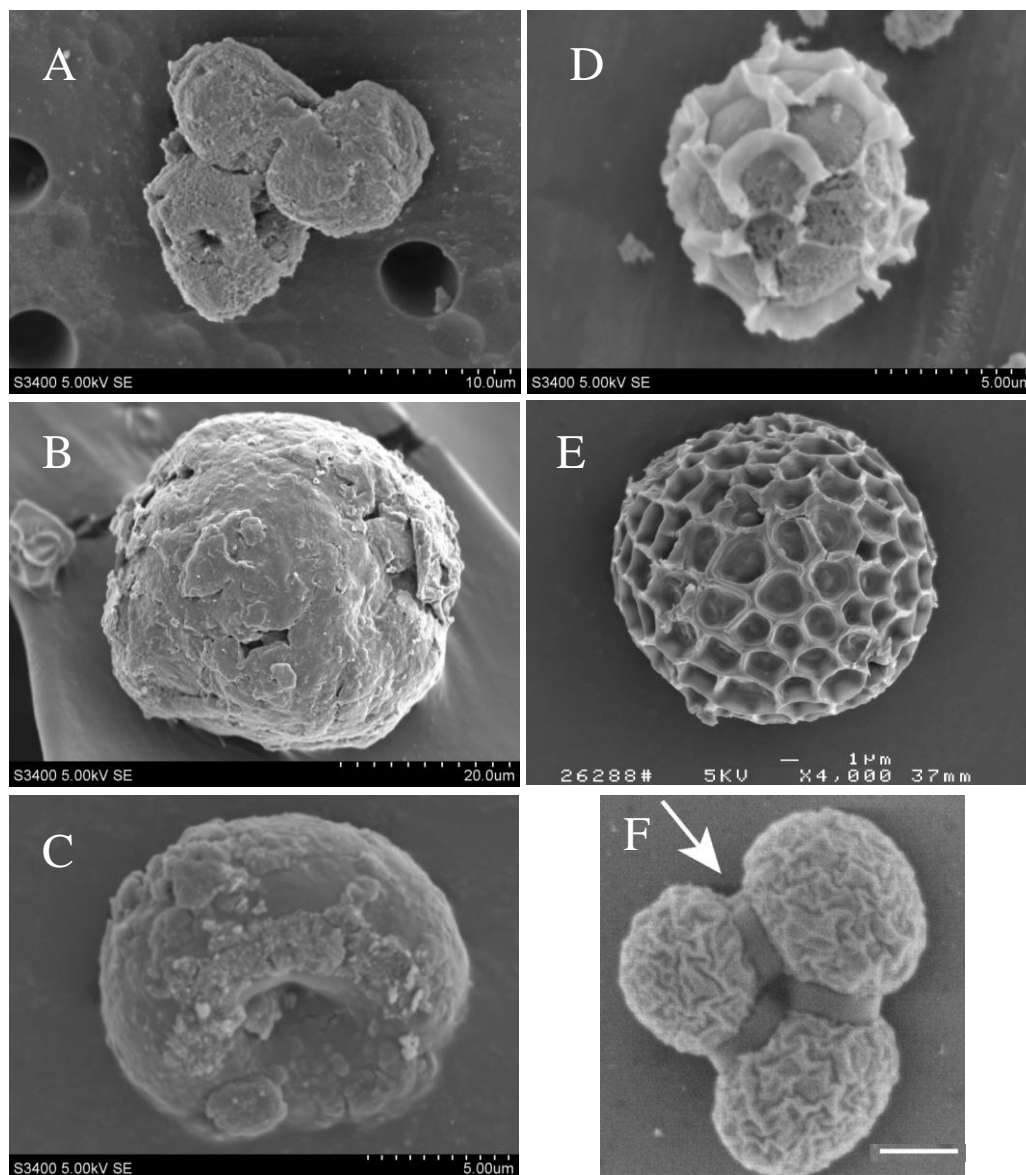
Notes- Top- an aluminosilicate particle easily differentiated from organic tissue by angular morphology and confirmed by EDS. Bottom- a strand confirmed as organic tissue due to high composition of carbon, oxygen and trace minerals.

Figure 10: Backscatter images and elemental compositions determined by energy dispersive spectroscopy



Notes- Top left-Similar to fungal filaments in pure culture.

Figure 11: Secondary electron micrographs from Nycodenz extracted organism from aquifer sediment preserved with paraformaldehyde.



Notes- A, B, C, D - These organisms were extracted using glutaraldehyde fixation, and Nycodenz extraction. E- *Tilletia Contraversa* spore (image from Pest and Disease image library <http://old.padil.gov.au>). F- Dividing *Saccharomyces cerevisiae* (143). Scales: A- 10 μm , B- 20 μm , C- 5 μm , D- 5 μm , E- 1 μm , F- 1 μm .

Figure 12: Secondary electron micrographs of organisms from a sandy aquifer 50 ft below ground surface and comparison pictures.

CHAPTER IV: EUKARYOTE DIVERSITY AND ABUNDANCE
DISTRIBUTION IN A SANDY ALLUVIAL IOWA AQUIFER
SAMPLED FROM WELLS AND SEDIMENT CORES

Introduction

Aquifers tend to be stable and isolated environments, providing conditions which lead to the in situ evolution of a rich diversity of microorganisms that play a crucial role in the overall aquifer ecosystem (52, 72). A diverse microbial groundwater population may harbor significant metabolic versatility, a property that could facilitate natural or enhanced in situ bioremediation of contaminated aquifers. Microbial ecology approaches aimed at identifying, characterizing, and quantifying known pollutant-degrading microorganisms can provide useful information for developing optimized and/or novel in situ bioremediation schemes. However, because many pollutant-degraders are eubacteria, most ecological studies relevant to bioremediation focus solely on prokaryotic microbial community members and ignore the eukaryotes.

We have been investigating microbial community structure in an aquifer in southeastern Iowa contaminated with the explosive RDX as it is undergoing biostimulation with acetate as a means to effect RDX reduction. Our preliminary data suggests substantial changes in eukaryotic community composition during biostimulation events. RDX, the primary contaminant of concern, is present at concentrations of 100 $\mu\text{g/L}$ or less, which is at least an order of magnitude below the no observed effect level for invertebrates (47, 117, 127, 137, 149, 164). This suggests that acetate, and not RDX, is and will remain the relevant agent of aquifer perturbation during the course of this study. Our hypothesis is that eukaryote dynamics in the RDX-contaminated aquifer, when perturbed by acetate injections will be governed by the ecological principles of competitive exclusion and secondary succession with endemic eukaryotes being replaced by globally pervasive generalist eukaryotes.

The few studies that address the roles of micro-eukaryotes in contaminated environments indicate that protists affect biodegradation processes consequent with bacterial grazing activities through selective predation, prevention of media clogging, and nutrient recycling (24, 60, 96-98, 130). The occurrence, diversity, and functional roles of macro-eukaryotes in contaminated aquifers are poorly understood. As they are comprised primarily of invertebrate species, the macro-eukaryotes are mostly if not entirely dependent on aerobic conditions. Depriving aerobic organisms of oxygen for extended periods leads to death. As most forms of organic pollution can induce hypoxia in aquatic systems it is expected that organic enrichment will lead to the loss of some fauna. Organically induced hypoxic conditions completely eliminate sediment associated invertebrates in contaminated marine environments (91). Brad and co-workers (24) examined the eukaryote composition of a landfill leachate-contaminated aquifer and identified many fungi and protozoa, but were unable to find macro-eukaryotes in the contaminated zone. Following disturbance by an oxygen depletion event, sediments affiliated with surface waters are rapidly re-colonized by invertebrates that filter back to the area through the water column. In aquifers, dispersal is slow as organisms must pass through sediment to invade new areas as they lack a strictly aqueous medium for rapid movement.

Very little is known globally about the ecology and evolution of subsurface macro-eukaryotes making predictions regarding response to perturbation difficult. However, the recent Protocols for the Assessment and Conservation of Aquatic Life In the Subsurface (PASCALIS) research project (68) significantly advanced our knowledge of the composition and distribution of macro-eukaryotes in uncontaminated, stable aquifers. The project identified 931 species unique to aquifers, with 43% being found only in a single aquifer (i.e. endemic) (49). Generalizations from the PASCALIS project were that groundwater diversity is low locally relative to regionally with larger differences in species composition between sampling sites compared to differences

between surface water sampling sites (68). Both of these generalizations are consistent with the notion that aquifers are stable ecosystems and have great limitations on organism dispersal. Macro-eukaryotic diversity in groundwater highlighted in the project includes oligochaete worms (38), small crustaceans (66), snails, flatworms, small arachnids (49), and others. These are very large organisms relative to the generalist protists and demonstration of the dominance of specialized organisms in pristine aquifers would further reinforce this idea.

We hypothesize that perturbing stable aquifer environments through intentional carbon amendment will serve as a disturbance and lead to destruction and displacement of the relatively large macro-eukaryotes leaving an environment to be colonized by generalist organisms like protists and some fungi.

Materials and Methods

Groundwater sampling

RDX-contaminated wells (MW309 and EMW02) and control wells (MW117, MW117s, and MW304s) were sampled in July and August 2010 (Fig. 1). Specific conductance, ORP, temperature, dissolved oxygen and pH was measured with a Hydrolab Quanta G (Hach Co., Loveland, CO). From each well approximately 25 L of water were purged before sampling 30 L of aquifer water from each well. Preliminary microscopic examination of mesh filters did not reveal obvious eukaryotes greater than 120 μm in the majority of wells precluding collection and sorting of organism by microscopy and tweezers. As an alternative strategy, groundwater was collected in graded filter series. All 30 liters of groundwater was filtered first through 120 μm mesh, then 2 liters of filtrate was passed through a 5 μm disc filter, and finally through a 0.22 μm Sterivex filter. Filters were stored on ice and transported to the University of Iowa within 6 hours where they were stored at -80°C until further processing.

Sediment sampling

On July 22, 2010 five aquifer sediment cores were collected by PSA Environmental (Lee's Summit, MO) using a direct push rig (Fig. 1). The five cores were located in a transect perpendicular to the direction of groundwater flow with samples taken at 5' to 10', 10' to 15' and 50' to 55' below ground surface (water table was less than 8' below ground surface at the time of sampling). Samples were immediately transported to University of Iowa on ice. At the lab, 100 g of each sample was frozen at -80°C while the remainder was split with half being stored at -20°C and the other half in a refrigerator.

DNA extraction, PCR, TRFLP, and Pyrosequencing

DNA was extracted from 2.5 grams of sediment and from all filtered groundwater samples using the MO Bio Ultraclean soil DNA isolation kit. DNA was also extracted from the five deepest groundwater core samples using an indirect protocol modified from Brad et al 2008 (24) in which 100 g of sediment was suspended in 100 ml of 0.1% pyrophosphate buffer and agitated at 200 rpm for two hours to force organisms into suspension. 60 ml of the liquid phase was then run through Sterivex filters and DNA extracted using the MO Bio ultraclean soil DNA kit. To target a gene for community composition analysis, 18S rRNA genes were amplified using primers EukA and EukB (All primers shown in Table 2).

To generate a profile of the microbial community from the 18S rRNA genes we used Terminal Restriction Fragment Length Polymorphism (TRFLP) and 454 pyrosequencing. For TRFLP, the 18S rRNA genes were reamplified using forward primer 3NDF tagged with a 6-FAM fluorophore and reverse primer V4_Euk_R2. Reactions were purified with Qiaquick PCR clean up kits (Qiagen inc, Valencia, CA, USA), concentration measured using the Qubit dsDNA broad range assay (Invitrogen, Carlsbad, CA, USA), and one μg of PCR product was digested with restriction enzyme

MspI. Digests were purified by glycogen precipitation, suspended in ultrapure water, and 70 ng sent to the University of Iowa DNA facility for electrophoretic fragment analysis on an ABI 3730 genetic analyzer. The final output of a TRFLP analysis is a table of relative abundances of characters (taxa) in each sample.

As a fingerprinting method, TRFLP provides a qualitative assessment of community structure and differences between samples, but does not immediately provide information about the phylogeny of organisms present. To directly assess changes in the phylogenetic composition of samples we used 454 pyrosequencing. The nearly full length 18S rRNA gene PCR's were amplified using primers 3NDF and V4_Euk_R2 with each primer tagged with the adapters specified in the Roche protocol for Lib-L preparation (6). The forward primers were also tagged with a 10 bp barcode (7) unique to the sample so that each sequence could be assigned to samples following sequencing. PCR products were gel-purified with the Qiaquick gel clean up kit or purified using Ampure beads (Beckman Coulter, Danver, MA, USA). Purified samples were sent to the University of Iowa DNA facility for a quality control check on an Agilent Bioanalyzer (Agilent technologies, Santa Clara, CA, USA) before sequencing using the Titanium chemistry on the 454 GS-FLX (Hoffman-La Roche, Grenzacherstrasse, Basel, Switzerland).

Sequences were analyzed using the Quantitative insights into microbial ecology (Qiime) pipeline (29). During this process, sequences were assigned to samples based on barcode sequence and those with a machine generated quality score lower than "25" were removed. Sequences were then clustered phylogenetically with Uclust at a clustering threshold of 97% sequence similarity (55) and clusters assigned a genotype by using a locally installed version of the Basic Local Alignment Search Tool (BLAST) (10) using the Non-redundant SILVA (v106) rRNA gene set (141) as the database. The top BLAST hit was used for preliminary taxonomic assignment. Clusters were assembled into an OTU table with samples in columns and assigned taxa in rows. The body of the table contained the number of each taxa found in each sample.

To compare samples based on a taxonomic measure we used Unifrac (100). OTUs from pyrosequencing were aligned using the ARB software (118) guided with eukaryotic sequences from the 106 reference release of the SILVA database (141). Aligned sequences were then inserted into the reference eukaryotic tree by maximum parsimony. The tree was uploaded to <http://bmf2.colorado.edu/fastunifrac> for computation of the weighted UniFrac distance and ordination by principal coordinate analysis.

To confidently assign phylogenetic identity and explore the extent of diversity of metazoan operational taxonomic units we used a Maximum Likelihood phylogeny approach. Sequences were clustered in Uclust at a 90% sequence similarity threshold, selecting the longest sequence as representative. Reference sequences were collected from the Silva 108 database (141) guided by a multigene phylogeny used to define major eukaryotic groups in a previous study (184). OTU and reference sequences were aligned and masked using SSU Align then alignments were manually inspected and trimmed in Seaview. Aligned sequences were used to construct a maximum likelihood phylogeny using PhyML (GTR model) implemented in Seaview. We collected OTUs that clustered with or near metazoan references and aligned them using the SINA online aligner. Aligned metazoan OTUs were combined with all metazoan reference alignments sequences from the Silva 106 non-redundant set in addition to sequences from the Hacrobia-Telonemia group an outgroup. Sequences were trimmed in Seaview and a Maximum Likelihood phylogeny constructed using FastTree with the GTR model.

Results and Discussion

General observations of eukaryotic sequences and distributions

From over 700,000 sequences we identified approximately 5000 unique OTUs of which approximately 1400 are fungi, 1500 are metazoans, 500 are alveolates or rhizaria, and 1200 were identifiable as eukaryotic but not classifiable. Most of the remaining

OTUs were either of plant origin which are not expected in this analysis and likely are results of field contamination by grass pollen.

To determine if sampling from well water and sediments are comparable processes, we examined the distribution of taxa recovered from both sample types. The two sample types share the same five most abundant phyla (Platyhelminthes, Annelida, Dikarya, Arthropoda, Cercozoa, Fig 13). In samples collected from wells, metazoans in the phyla Platyhelminthes and Annelida predominate whereas the most abundant taxa observed in sediments samples are fungi in the Dikarya. This observation may indicate an intrinsic sampling bias, or the two methods may be sampling different environments altogether (i.e. wells may be unrepresentative microenvironments).

To test the hypothesis that sample bias differentiates our samples rather than incomparable environmental conditions, we examined the distribution of fungal and metazoan classes. These kingdoms were selected because both received adequate sampling in wells and sediment samples. In the fungi, the rank of class distributions is nearly identical though samples from wells recovered two rare classes not observed in sediments (Fig 14). The distribution of metazoans is highly similar between sediments sharing four of the five most abundant taxa in each condition with analogous rank order (Fig 14).

The observed similarities in phyla distributions and class distributions of fungi and metazoans support the hypothesis that sediment collection and well water filtering sample the same environment. However, higher relative abundance and richness of metazoans indicate they are more efficiently sampled from wells than sediments indicating a bias when attempting to compare the samples based on abundance of these two kingdoms. Conversely, our data indicates that within kingdom variation is largely conserved between the methods providing for cross sample type comparison. Finally, greater fungal and metazoan recovery in samples from filtered well water compared to

sediments suggests this may be a preferable method for sampling eukaryote taxa from aquifers.

Comparison of acetate-affected and acetate-unaffected samples

Our central hypothesis is that acetate amendment will result in observable changes in eukaryote abundance and distribution likely marked by replacement of native metazoans with generalist fungi or protists. To test this hypothesis we examined taxa in all samples at the kingdom level. There are no apparent systematic differences between kingdom distributions observed in acetate-affected vs. acetate-unaffected samples (Fig. 15). However, differentiating between samples is obscured by high frequency of sequences that could not be assigned a taxonomic identity at the kingdom level using the BLAST approach. We used two methods to overcome this deficiency: TRFLP to examine organism distributions in the samples without explicitly addressing taxonomy, and UniFrac (100) to compare samples based on taxa membership in an inferred phylogeny.

The OTU table from the TRFLP profiles of all samples was used to generate a non-metric dimensionally scaled ordination which orients samples in space based on their similarities (Fig. 16). The ordination was constructed using the isoMDS function of the Vegan (132) package in the R statistical environment (168). NMDS reveals no apparent difference between acetate-affected and acetate-unaffected samples as both conditions have fully overlapping distributions in the ordination. The results from the Unifrac analysis of samples was much like the TRFLP analysis in that there are no apparent differences between acetate-affected and acetate-unaffected samples as both sample types are distributed in the whole ordination space (Fig. 17).

Phylogeny of Metazoan OTU sequences

Based on the phylogeny of all OTUs with reference sequences, metazoans constitute a relatively small proportion of total eukaryotic diversity in this aquifer (Fig 18). The phylogeny of probable metazoan sequences with all metazoan references from

SILVA 106 NR revealed many metazoan OTUS that clustered with the Platyhelminthes in addition to OTUs clustering with the Paralamyctes, Entomobryidae, Hydra, and Harpacticoida (Figs 19-23).

Most of the Metazoan OTUs clustered with the Platyhelminthes, the majority of which were most closely related to the Catenulidae representing what appear to be at least six families lacking sequence representation in the current database. This greatly expands the realm of known Platyhelminthes organisms. This phylum is widespread in the well samples and some sequences were found in sediment samples as well. The function of these flatworms in subterranean ecosystems is difficult to extrapolate given that members of the Catenulidae have lifestyle ranging from strictly predatory grazers in freshwater environments (154) to obligately marine fixed sessile forms gaining energy from chemoautotrophic symbionts (135). Phylogenetic position of the Catenulidae sequences from the Iowa aquifer are unresolved environmentally as they are closely related to both freshwater and marine representatives.

Another intriguing set of sequences clustered in the Harpacticoida order near the Nitocra genus. Studies of ancient European aquifers. indicates a large number of subsurface crustaceans and we expected to find more of them in our survey. If our sequences prove in future work to be most closely related to Nitocra, this would represent a potential morphology well suited to subsurface life based on body shape and manner of food collection.

Remaining sequences grouped closely to Hydra, Paralamyctes, and Entomobryidae. The hydra are cosmopolitan, and isolation of obligately sediment affiliated members could provide important insights about the evolution of cnidarians and potential ancestral states. Paralamyctes and Entomobryidae are insect creatures and may represent creatures that fell in the well during sampling. However, sequences from both groups were most closely related to sequences from species endemic to Gondwana which and should not appear in Iowa.

Conclusions

There are no obvious differences between acetate affected and unaffected portions of the aquifer and there are any number of explanations. The aquifer environment may be sufficiently heterogeneous to harbor aerobic refugia wherein obligately aerobic taxa could persist. It is equally possible that subterranean taxa are suited to tolerance of hypoxic or microaerophilic conditions through reduction of metabolic demands or dormancy (34). A final possibility is that the aquifer was repopulated with sufficient speed from up-gradient acetate unaffected regions. This seems plausible for motile taxa such as worms. The distance from the unaffected upgradient aquifer to sample wells (MW309, EMW02) is approximately 30 meters. For example, a two millimeter length flatworm traveling a modest 100 body lengths per day could repopulate our sample location 150 days following a disturbance event.

Regardless, this work demonstrates the presence of substantial unknown eukaryotic diversity in the subsurface. Introduction of carbon substrates is relatively benign in contrast to more invasive activities such as aquifer thermal remediation or contamination with highly toxic substances and future studies may indicate observable long term changes to subsurface eukaryotic communities given these kinds of disturbances.

Tables and Figures

Table 2: Oligonucleotide primers used in this study to amplify eukaryotic 18S rRNA genes

Name	Sequence	Reference
Full 18S rRNA gene		
EukA (forward)	AACCTGGTTGATCCTGCCAGT	(121)
EukB(reverse)	TGATCCTTCTGCAGGTTACCTAC	(121)
V4 region 18S rRNA gene pyrosequencing primers		
3NDF	GGCAAGTCTGGTGCCAG	(32)
V4_Euk_R2	ACGGTATCT(AG)ATC(AG)TCTTCG	(25)
Pyrosequencing Adapters		
PrimerA-key	CCATCTCATCCCTGCGTGTCTCCGACTCAG	(6)
PrimerB-key	CCTATCCCCTGTGTGCCTTGGCAGTCTCAG	(6)

Notes- Degenerate positions are indicated in parentheses within the sequence

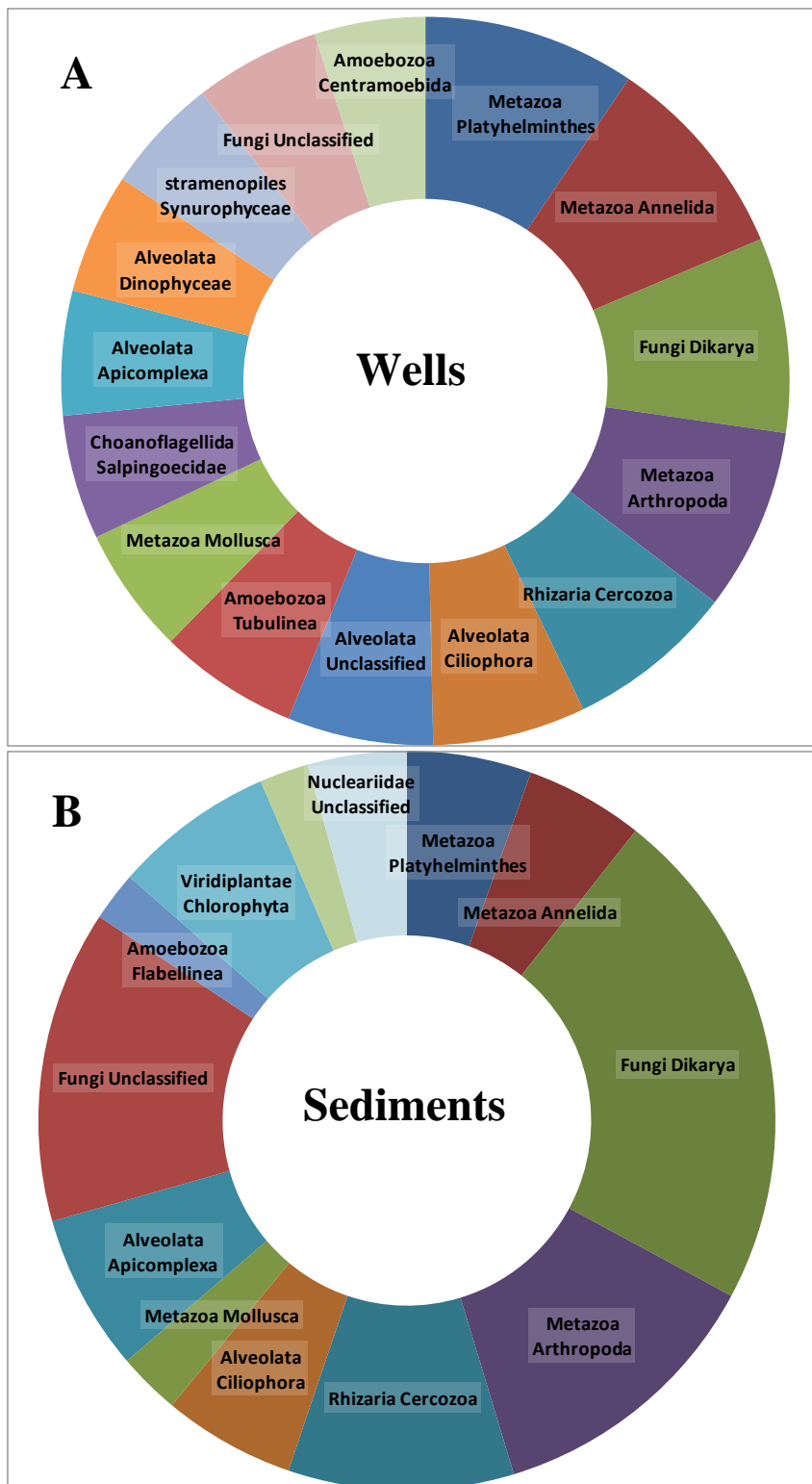
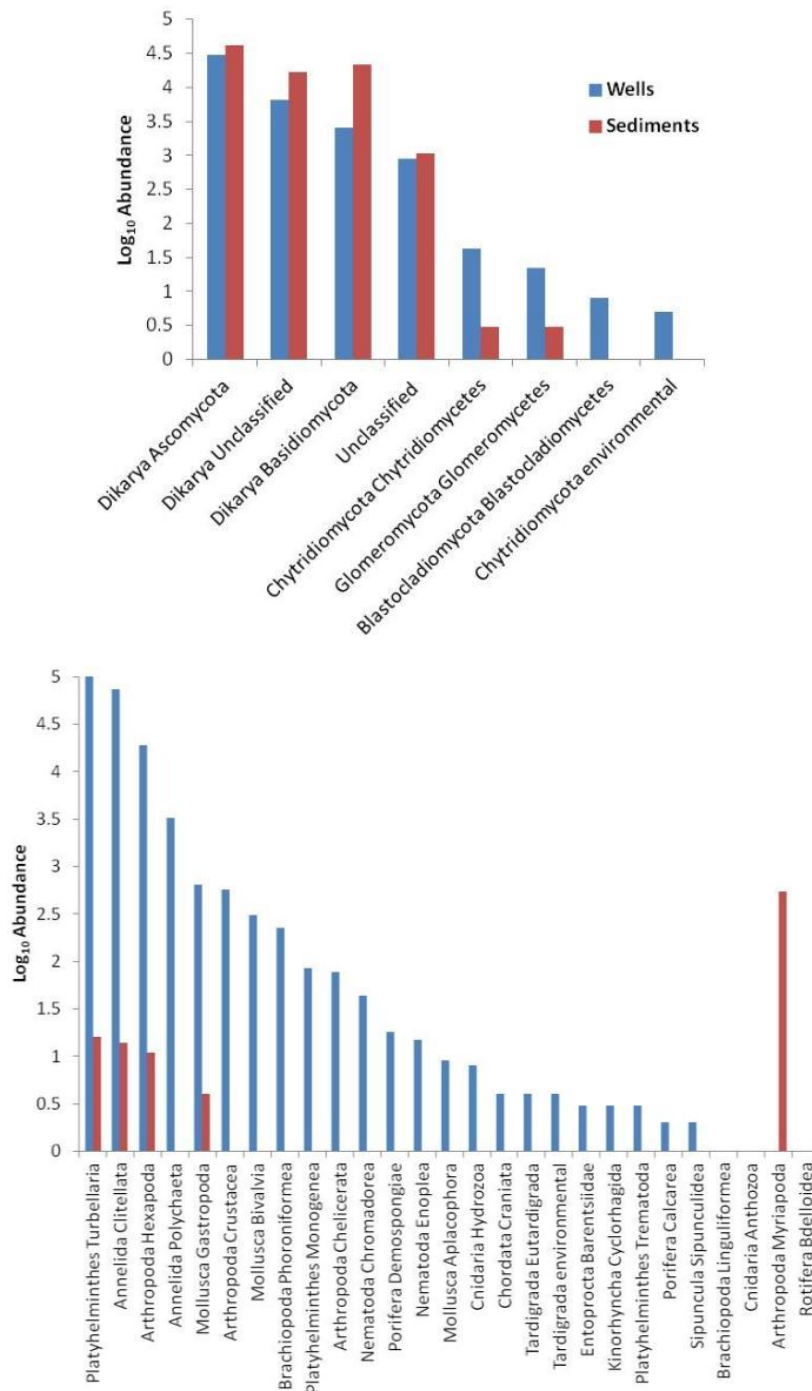
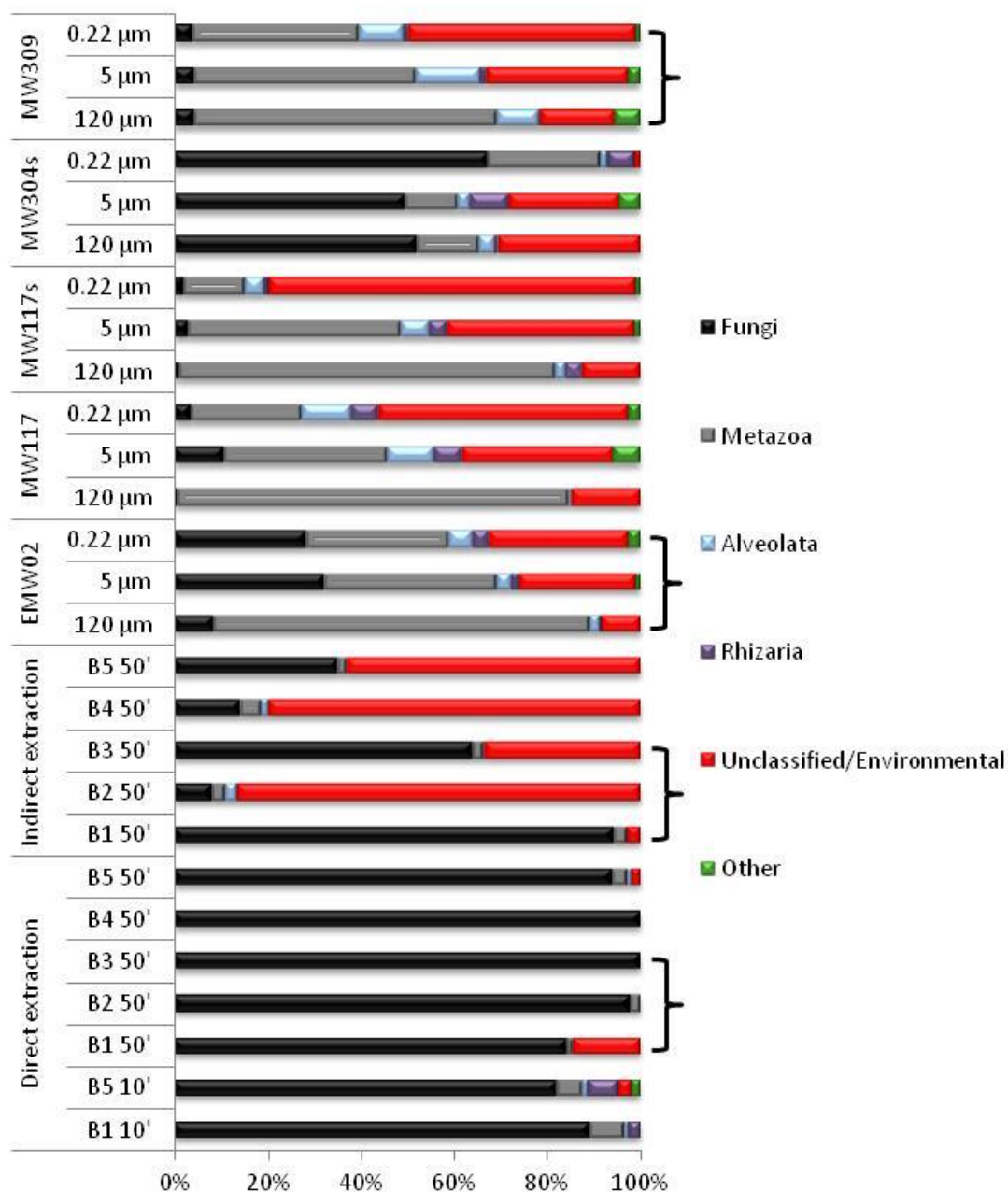


Figure 13: Proportional distribution of log₁₀ abundance of phyla collected from filtered well water (A) and sediments (B).



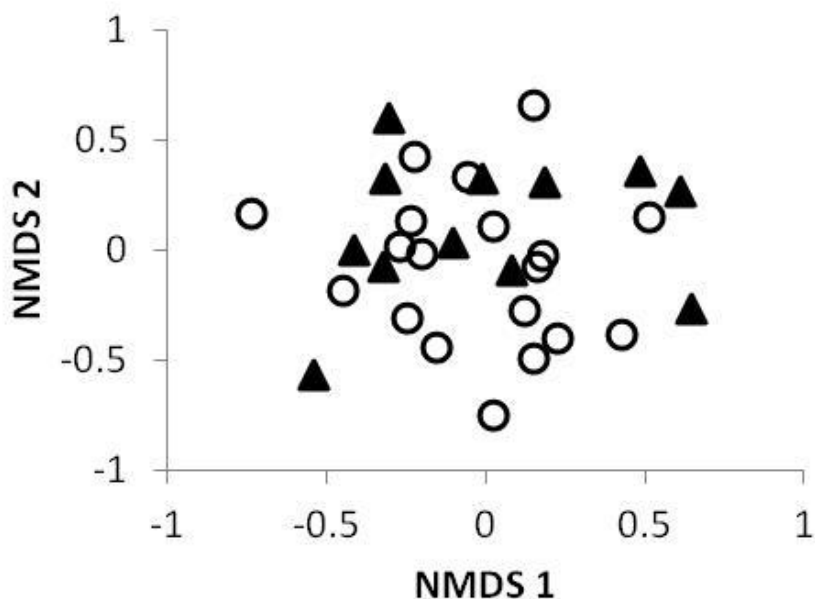
Notes: Top graph is distribution of Fungal classes and bottom graph is distribution of metazoan classes. Blue bars are log₁₀ sequence abundances from filtered well water and red bars are from sediment samples.

Figure 14: Distribution of fungal (A) and metazoan (B) classes collected from sediments (red bars) and filtered well water (blue bars)



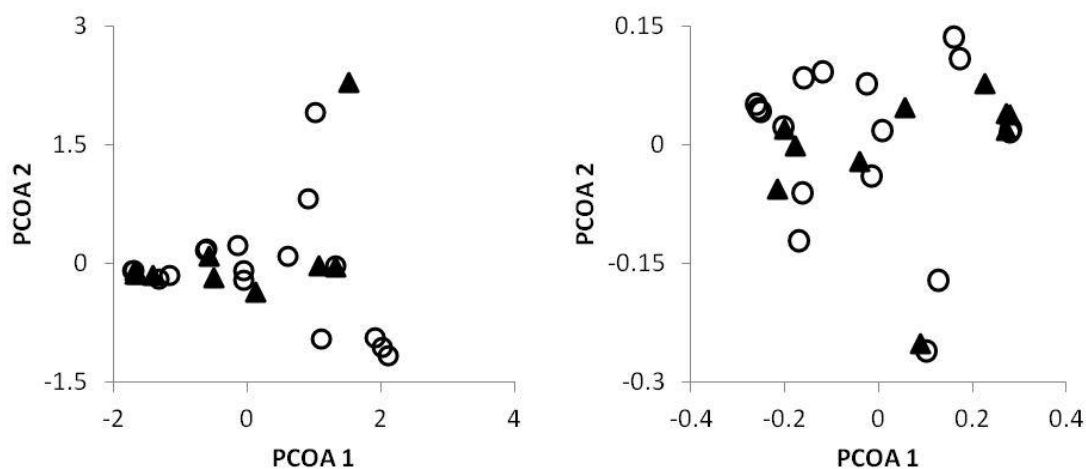
Notes- B1 through B5 were aquifer sediment cores sampled either with direct DNA extraction or indirect collection of organisms by agitation in buffer followed by filtration of buffer and DNA extraction from the filter. Acetate affected samples are indicated by brackets.

Figure 15: Taxa distributions in groundwater and sediment samples determined from 454 pyrosequencing.



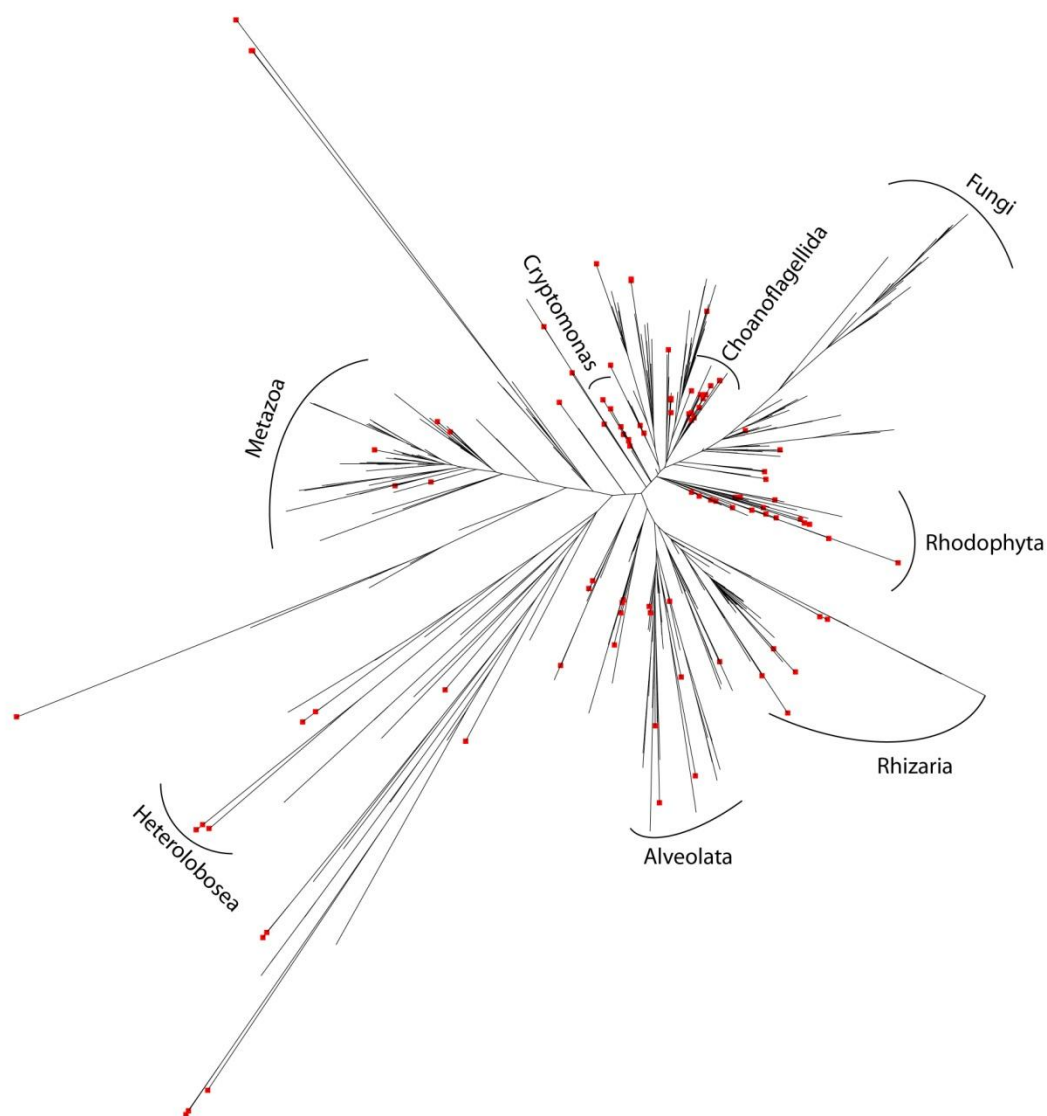
Notes- Closed triangles are from acetate-affected locations while the open circles are from acetate-unaffected locations

Figure 16: A non-metric dimensionally scaled model (NMDS) of TRFLP data from an aquifer near the Iowa Army Ammunition plant.



Notes- Closed triangles are from acetate-affected locations while the open circles are from acetate-unaffected locations. Left- weighted non-normalized UniFrac distance metric, Right- weighted normalized UniFrac metric

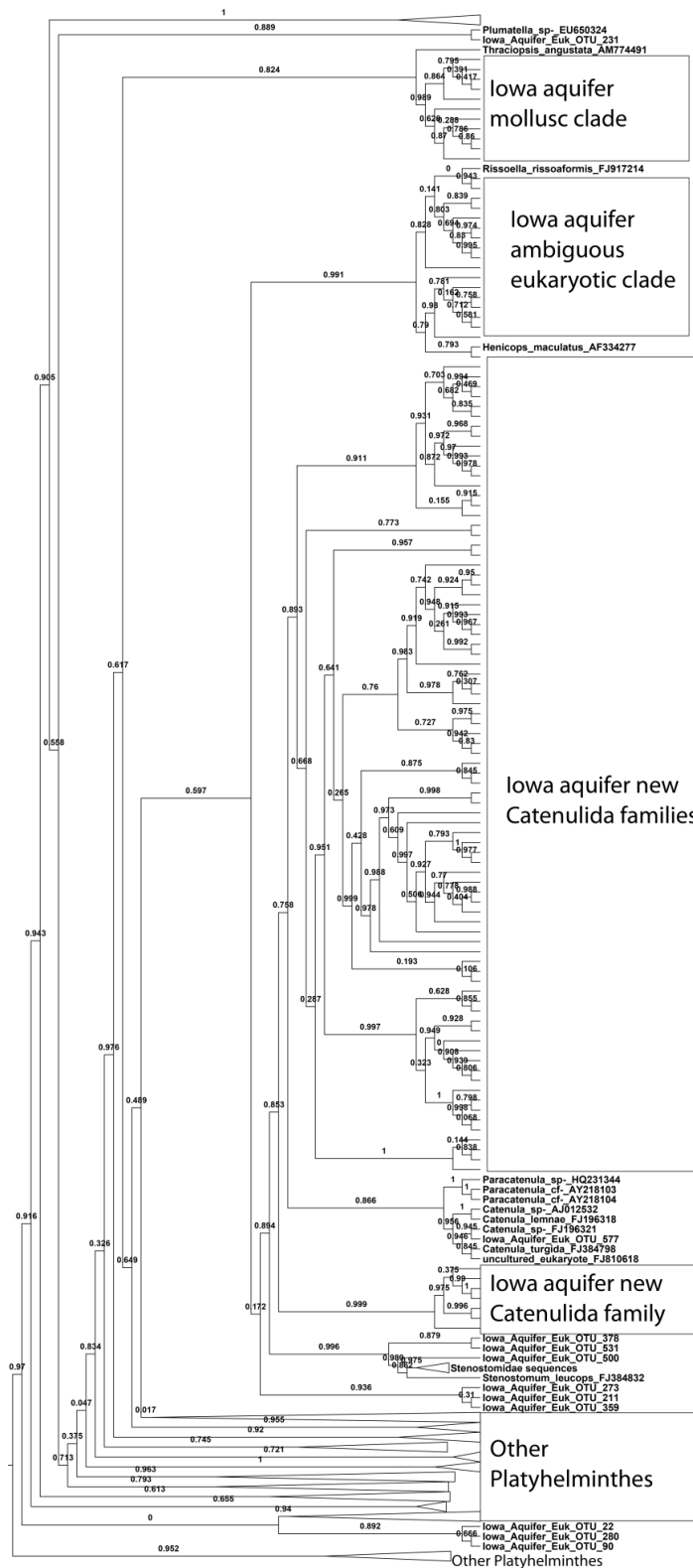
Figure 17: Principle coordinate analyses based on the UniFrac distance measured from aquifer pyrosequencing data.



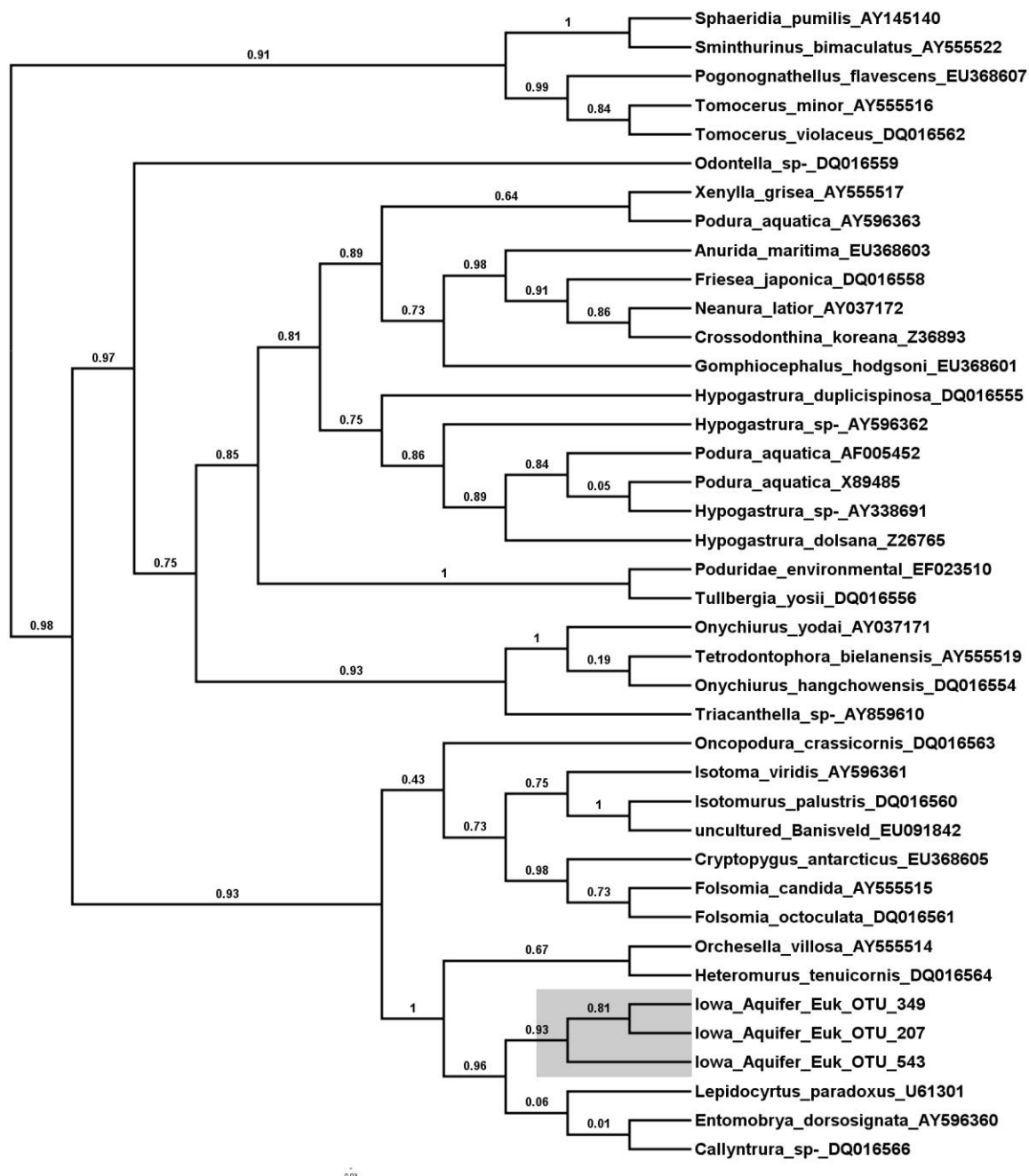
Notes- Phylogeny built from 101 reference sequences and 597 OTUs representing 520,688 high quality sequence reads. Red dots on termini indicate position of reference sequences. Resolved groups are marked at arches specifying extent of the group.

Figure 18: Hypertree of a maximum likelihood phylogeny of groundwater eukaryotic OTUs (90% sequence identity clustering threshold) with reference sequences added to delineate the Metazoa kingdom

Figure 19: Subtree of a FastTree maximum likelihood phylogeny showing the diversity of Platyhelminthes 18S rRNA gene OTU sequences collected from groundwater.

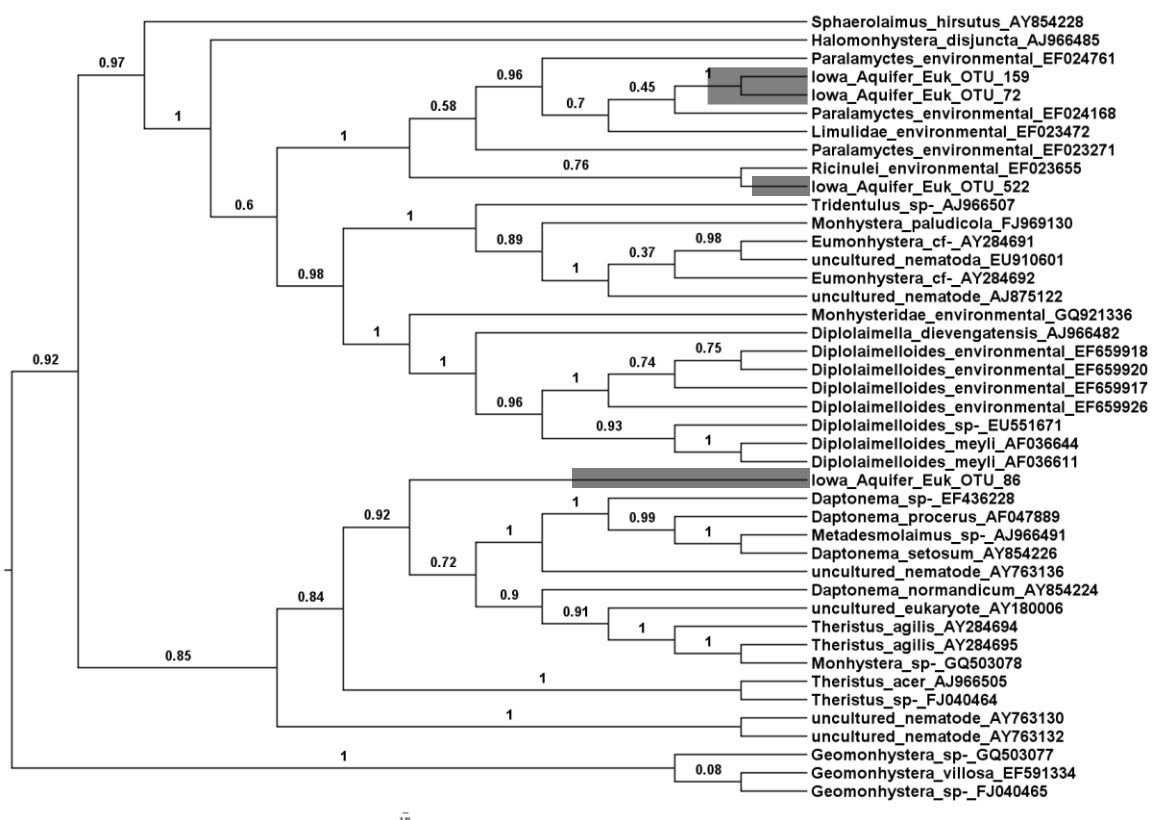


Notes- Iowa aquifer clade sequences names were deleted from most tips and phylogeny for clarity, but remaining names are denoted as "Iowa Aquifer Euk OTU" followed by the OTU number. Shown as a cladogram for clarity.



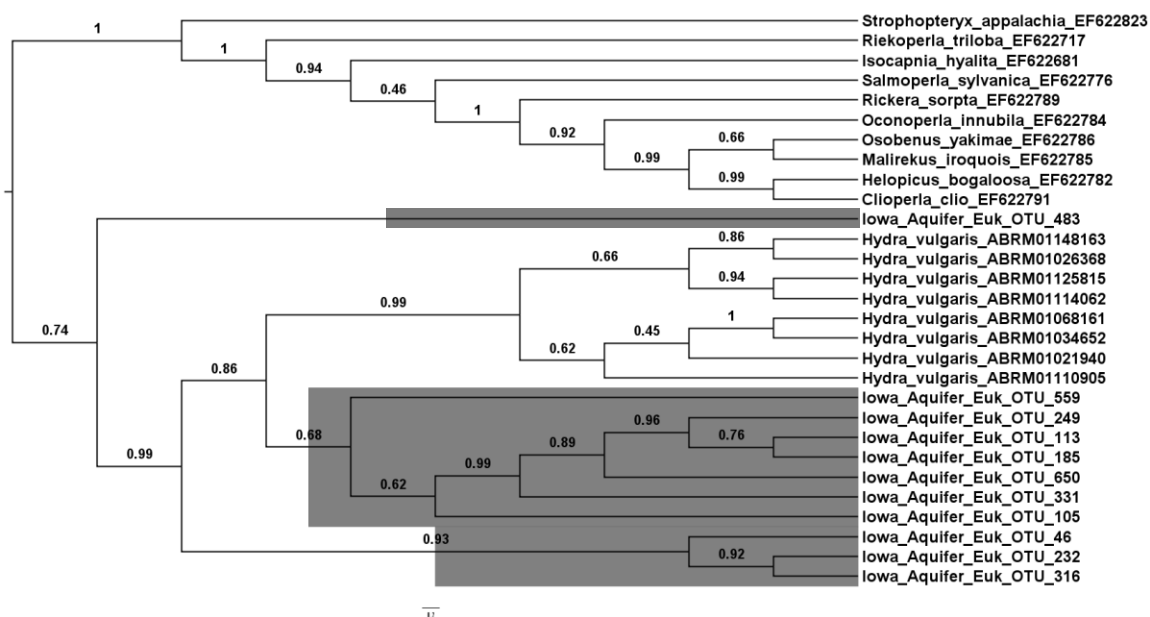
Notes- Branch support labels are Shimodaira-Hasegawa test clade probabilities.
Experimentally collected OTUs from the Iowa aquifer are branch highlighted.

Figure 20: Subtree of FastTree maximum likelihood 18S rRNA gene phylogeny showing pyrosequencing OTUs closely related to Entomobryidae sequences



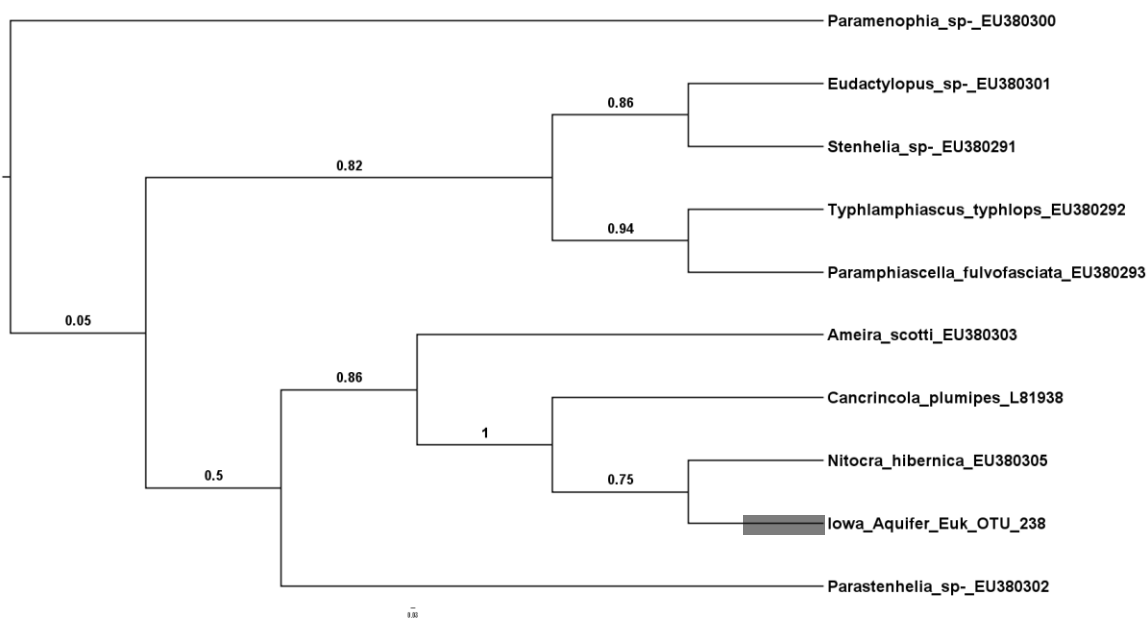
Notes- Branch support labels are Shimodaira-Hasegawa test clade probabilities.
Experimentally collected OTUs from the Iowa aquifer are branch highlighted.

Figure 21: Subtree of FastTree maximum likelihood 18S rRNA gene phylogeny showing pyrosequencing OTUs closely related to Paralamyctes sequences



Notes- Branch support labels are Shimodaira-Hasegawa test clade probabilities.
Experimentally collected OTUs from the Iowa aquifer are branch highlighted.

Figure 22: Subtree of FastTree maximum likelihood 18S rRNA gene phylogeny showing pyrosequencing OTUs closely related to *Hydra vulgaris* sequences.



Notes- Branch support labels are Shimodaira-Hasegawa test clade probabilities.
Experimentally collected OTUs from the Iowa aquifer are branch highlighted.

Figure 23: Subtree of FastTree maximum likelihood 18S rRNA gene phylogeny showing pyrosequencing OTUs closely related to Harpacticoida sequences.

CHAPTER V: REVEALING CRYPTOMYCOTA DIVERSITY IN 454 PYROSEQUENCING SURVEYS

Introduction

From the eyes of a human, fungi are everywhere: on our dinner plates, producing our fuel, colonizing our skin, and providing us with useful drugs like antibiotics. Yet somehow, one massive group representing perhaps half or more of all fungi has managed to escape our grasp until very recently. Recently named "Cryptomycota" (89) members have appeared in molecular surveys of soil (111, 123), lakes and rivers (12, 109, 110), oceans (166), groundwater (24, 119), and a drinking water treatment system (138), and are typically identified simply as an "unclassified fungus." Recent work has indicated that this group, which may be the earliest diverging fungal lineage (88, 108), is distinct from the remaining fungi (82, 87, 88, 108), primarily because members lack the typically defining fungal characteristic of chitinous cell walls (88).

While the Cryptomycota have been identified as a discrete and highly diverse lineage, we lack understanding of the extent of their diversity or the ecological characteristics of clades within the group. Additionally, their relation to the rest of the fungi and appropriate assignment of taxonomic level is irresolute due to limited sampling relative to their high probable evolutionary and ecological diversity. However, gene-targeted high-throughput sequencing approaches provide an opportunity to sample large numbers of taxa from representative environments (161). We hypothesize that interrogating previously collected 18S rRNA gene high-throughput sequencing sets for Cryptomycota sequences will permit assessment of the extent of their environmental diversity, reveal the distribution of diversity among environments, and increase our confidence in ancestral positioning relative to the classically defined fungi (189). Environments already represented in current databases include high throughput sequencing sets from freshwater lakes, marine sediments, and suspended marine

communities. We are especially interested in potential Cryptomycota diversity in the marine upper water column in which members of the group have not been identified.

Additionally, to add sequences from a novel environment not represented in previously collected sequencing sets we sampled sediments and groundwater 17 meters below the ground from an aquifer in south-east Iowa in the north-central United States. The exact location in Iowa was environmentally dynamic throughout geologic history being variously marine, marine coastal, glacio-fluvial, and currently terrestrial (14). Such dynamism makes the aquifer an attractive location to seek Cryptomycota diversity as numerous opportunities existed for lineages from the various environments to colonize the sediments.

Materials and Methods

Collection of groundwater samples and sediment

We collected groundwater and sediment samples from a surficial alluvial aquifer near Burlington, IA, USA. Five direct push sediment cores within a half mile radius were collected by PSA Environmental (Lee's Summit, Missouri, USA) to a depth of approximately 17 meters. Groundwater was collected from four wells within three kilometers of the sediment samples presumably drawing from the same alluvial aquifer. Approximately 30 L was pumped from each well by inertial pump to purge the local suspended microbial community before sampling 20 L. Organisms from each sample were size stratified by three stage filtration first through sterile polyester mesh, then an isopore membrane (Millipore, Billerica, MA, USA), and finally, a Millipore Sterivex filter with pore diameters of 120 μm , 5 μm , and 0.22 μm respectively. All samples were immediately transported to the University of Iowa on ice and frozen at -80°C .

DNA Extraction, PCR amplification, and 454 Pyrosequencing

To collect cells from sediments we transferred 50 g of soil to Erlenmeyer flasks containing 100 ml of 0.1% pyrophosphate buffer, agitated the samples on a platform shaker for one hour at 200 RPM, and passed 60 ml of the suspension through Sterivex filters for DNA extraction. To collect genetic material from the eukaryotic community we extracted DNA from the Sterivex filters using the Ultraclean Soil DNA kit (MO Bio Laboratories, Carlsbad, CA, USA). PCRs were performed using Phusion high fidelity polymerase (Thermo Fisher Scientific, Waltham, MA, USA) at a concentration of 0.02 Units/ μ l with 200 μ M of each of the four dNTPs. The 18S rRNA gene was amplified using primers EukA and EukB (121)(0.5 μ M each with 0.4 mg/ml bovine serum albumin in reaction mixture) under amplification conditions of 98° C for 1 minute, 35 cycles of 98° C for 10 seconds, 57° C for 30 seconds and 72° C for 45 seconds concluding at 72° C for 5 minutes. PCRs were then re-amplified using primers 3NDF(32) and V4_Euk_R2 (25) (0.2 μ M each) targeting the V4 region. Primers used for reamplification were amended with pyrosequencing adapters and 10 nucleotide barcodes recommended for Lib-L amplicon library preparation and optimized for the titanium chemistry of the 454 pyrosequencing reaction (Roche Diagnostics, Basel, Switzerland). Amplification parameters for the reamplification were 98° C for 1 minute, 5 cycles of 98° C for 10 seconds, 59° C for 30 seconds, and 72° C for 30 seconds followed by 30 cycles of 98° C for 10 seconds and 72° C for 30 seconds concluding at 72° C for 5 minutes. Tagged PCR products were purified using AMPure XP beads (Beckman-Coulter, Brea, CA, USA). The University of Iowa DNA facility performed quality assurance and control on reactions before subjecting samples to pyrosequencing.

Sequence filtering, alignment, and phylogenetics

Quality filtered sequence reads were processed using the Quantitative insights into microbial ecology (Qiime) environment (29). Samples were de-multiplexed and

filtered to retain median length sequences (130 bp in length to 350 bp in length depending on the study) with quality scores greater than 25 and no more than three primer base mismatches. Operational taxonomic units (OTUs) were selected using Uclust at the 97% sequence similarity threshold and all other settings at default (55). Representative sequences were chosen as the most abundant sequence represented by each OTU.

To identify possible OTUs belonging to the proposed Cryptomycota, we built a fungal phylogeny guided by sequences used in a previous study (88) wherein they verified the existence of the Cryptomycota group and its fungal classification. Representative sequences were collected from the Silva (v106) non-redundant, truncated, ribosomal small subunit database(141) and from Genbank. Reference sequences and OTUs from each study were aligned using SSU Align which uses the Infernal aligner (126) and a hidden Markov model (54) to align sequences according to a secondary structure model for small subunit rRNA. Sequences that did not conform to the secondary structure model were removed from the dataset for being potentially non-specific or chimeric. As recommended by the software, nucleotide positions with low posterior probability or insert states were removed by SSU Align following the alignment to maximize comparability of sequences in phylogenetic analysis. Alignments were also manually inspected using Seaview(67).

To establish the relationships between reference sequences and the OTUs collected, a maximum likelihood phylogeny was built with FastTree (139) using the generalized time reversible (GTR) nucleotide substitution model. Cryptomycota reference sequences appeared in a monophyletic group and query sequences clustering within or near the references were retained and realigned. The alignment of candidate Cryptomycota sequences and references was trimmed in Seaview before constructing a RAxML(163) maximum likelihood phylogeny with the GTR+I model using 500 rapid bootstraps.

Interrogating environmental datasets of 454-sequenced 18S rRNA gene amplicons

To detect novel sequence diversity in the Cryptomycota we interrogated ten previously published 18S rRNA gene 454 pyrosequencing sets from eight studies (Table 3) with sequences from freshwater suspended communities (122, 129), marine suspended communities (11, 22, 37, 39, 56, 122), and marine sedimentary community (135). While all studies sequenced portions of the 18S rRNA gene, the region was variable targeting either the V9 (11, 22, 37, 56, 135), V3 (122, 129), or V4 (22, 39) hypervariable regions. Sequences were processed as above except that a small subset of query sequences were chosen randomly from each clade of candidate Cryptomycota sequences identified in the FastTree phylogeny to form a truncated set of sequences representing each potential grouping. The truncated set of candidate sequences and references were used to construct a PhyML maximum likelihood phylogeny using the GTR model, subtree prune and re-graft (SPR) moves and 100 bootstraps

Building a summary phylogeny of all candidate Cryptomycota sequences.

To generate a summary phylogeny from all of the collected sequences and thus attempt a crude phylogenetic reconstruction of the Cryptomycota we utilized all of the candidate cryptomycota sequence sets from each study and from the Iowa aquifer. Sequences were aligned and masked with SSU align and manually inspected using Seaview. As the studies targeted different portions of the 18S rRNA gene, many of the candidate Cryptomycota sequences did not overlap presenting a problematic scenario for conventional molecular phylogenetics.

Ideally, we would trim sequences to a uniform length permitting nucleotide distance and probability computations based on a given substitution model, but this is impossible for any two sequences that do not overlap. To overcome this difficulty we utilized a capability of the FastTree (139) phylogenetic program which begins with a profile based neighbor joining procedure permitting estimation of nucleotide distance

between two non-overlapping sequences by comparing each to longer sequences spanning the entire length of the gene. Based on this property, we utilized the full length of the reference sequences as a scaffold for approximation of phylogenetic positions of fragmentary sequences we collected. Confidence values were approximated using the Shimodaira-Hasegawa test (157) as bootstrap character re-sampling would be non-meaningful given the large number of fragmentary sequences. Following the profile neighbor joining step we increased the number of Subtree pruning and re-grafting moves from the default of two to 500 in order to execute a more exhaustive search approaching the behavior of algorithms such as that implemented in PhyML.

As implemented here, the phylogenetic construction built using fragmentary sequences assumes the nucleotide distances of the hypervariable regions are positively correlated. To test this we isolated the V3, V4, and V9 hypervariable regions of the Cryptomycota reference sequences into separate alignments. Nucleotide distances between the sequences in each alignment were computed using Mega5 (167) and computed distances compared between the three regions by linear regression.

Detailed phylogenetic investigation of Iowa Aquifer sequences

The Iowa Aquifer is freshwater and sedimentary and is thus distinct from the sequence sets of the other studies (Table 3). To investigate the phylogenetic position of Cryptomycota sequences from the Iowa aquifer we constructed a FastTree maximum likelihood phylogeny by the same method as above using all candidate Cryptomycota sequences from the Iowa aquifer, from the freshwater Lakes Pavin and Aydat (122), and marine sources Mirs bay(39), Tolo Harbor(39), Wimereux coast(122) and La Rochelle coast(122). By utilizing all the sequences from only these sources we were able to represent each of the three types of environments but maintain a manageable total number of sequences. Phylogenies were constructed with sequences from all three studies collectively and individually

To compare the taxa represented in each of the specific environments sampled we used summary phylogenetic comparisons implemented in Mothur 1.13(153). From the Cryptomycota subtrees based on the three studies, nodes with likelihood lower than 0.75 were collapsed and the resultant phylogenies used as input to calculate the unweighted UniFrac metric for distance and probability of unique phylogenetic composition. Unifrac distances were used to produce principle coordinate and non-metric dimensionally scaled ordinations.

DNA sequences

Novel DNA sequences collected in this study have been deposited in Genbank (Accession Nos. JN612965-JN613014).

Results

Of 520,688 sequences from the Iowa aquifer there were 5,146 OTUs (computed at 97% threshold) of which 138 clustered with the Cryptomycota in a FastTree phylogeny (2.7% of OTUs, 23,633 total sequences) A RAxML phylogeny does not well resolve the positions of these sequences (low bootstrap values), but suggests Iowa aquifer sequences may be distributed throughout the Cryptomycota (Fig. 24).

Having found Cryptomycota sequences in pyrosequencing data from an Iowa aquifer we were inspired to interrogate previously collected 18S rRNA gene pyrosequencing sets for hidden diversity. Sequences clustering with the Cryptomycota were found in every dataset (marine and lacustrine) primarily at low sequences abundance (Table 3, <2% of sequences in 10 of 13 pyrosequencing sets). However, 2.6% of 18S rRNA sequences and 4.6% of OTUs from Tolo Harbor near Hong kong (39) Additionally, a pyrosequencing set from Lake Fuschl in Austria (129) was comprised of 30% cryptomycota sequences (27% of OTUs, 264,033 total sequences.)

The pyrosequencing sets targeted different regions of the 18S rRNA gene, so to determine comparability of DNA sequence fragments among hypervariable regions for

phylogenetic analysis we computed linear regressions between distances generated using V3, V4 or V9 regions. Distance computed with each of the regions are linearly related as observable in scatter plots (Fig 25), though somewhat low correlation coefficients (V3-V4: $R=0.68$, V3-V9: $R=0.69$, V4-V9: $R=0.72$, $N=378$, $p<0.0001$) indicate limited capacity for nucleotide distance based comparison of closely related sequences observed from different hypervariable region fragments.

To attempt a crude reconstruction of the Cryptomycota using sequences from all studies we built a maximum likelihood phylogeny based on previously validated reference sequences (88). The reference sequences formed a single clade with high probability (>0.96 using the Shimodaira-Hasegawa (SH) test) as seen in a condensed version of the entire phylogeny (Fig 26). Rooted to a non-fungal set of opisthokont sequences, the Cryptomycota appear basal to other fungi in this construction supporting the hypothesis the group is divergent from all other fungi and joined by a more recent common ancestor relative to the other eukarya.

Examination of the summary phylogeny containing sequences from all studies and the Iowa aquifer reveals a large number of sequences and clades from marine environments (Fig 27). Many of the clades are exclusively marine (at least 10 clades of 5 or more OTUs) but few are exclusively freshwater except one of the last diverging clades which is composed primarily of sequences from Lakes Pavin and Aydat (122) and the Iowa Aquifer. Finally, there are several large clades composed entirely of novel sequences collected from pyrosequencing data sets (at least 5 clades of 10 or more OTUs)

To determine the phylogenetic position and diversity of Cryptomycota OTUs derived from the Iowa aquifer we generated a phylogeny using all candidate sequences from the Iowa aquifer and two other studies (39, 122) representing both freshwater and marine environments. Examining the entire, uncollapsed phylogeny based on these sequences (Fig. 28A) reveals 6 highly supported lineages (likelihoods >0.8 using the SH test) roughly corresponding to the groups defined from the truncated phylogeny from all

studies. Separate phylogenies were constructed from each dataset in an attempt to detect variable influences of the datasets on observed relationships (Fig. 28C). When constructed with OTUs from the Iowa aquifer only, five of the six groups are distinct in the phylogeny except the third diverging group collapses into the fourth. In independent phylogenies built from OTUs retrieved from the other two datasets (39, 122) five of the six groups are again distinct, except that in both cases the fourth divergent group, which is distinct within the Iowa aquifer OTU phylogeny, disappears with reference sequences previously in the fourth diverging group collapsing into the sixth. Based on this observation, the fourth diverging group is defined by the presence of sequences from the Iowa aquifer with reference sequences from the Freshwater group 1 defined in the phylogeny built from all studies.

To perform holistic comparison of environments with adequate sequence representation in the full sequence limited study phylogeny (the Iowa aquifer (this study), Wimereux coast, La Rochelle Coast, Lake Pavin, Lake Aydat (122), Mirs Bay, Tolo Harbor (39), Banisveld aquifer (24)) irrespective of our group designations, we used ordinations based on the unweighted Unifrac distance (100). Displayed as simulated three dimensional graphs, ordinations reveal that the Iowa aquifer appears to group with the marine environments (Fig. 29) consistent with the fourth diverging group (Freshwater group 1) phylogenetically positioned between two groups of predominantly marine sequences.

Bootstrapped phylogenies were also constructed with reference sequences and a truncated set of candidate Cryptomycota sequences from each of the 13 pyrosequencing sets (Appendix C, Figs 40-50). Bootstrap support was low generally, consistent with the short sequence length of the alignments (100-300 nucleotides after masking)

Discussion

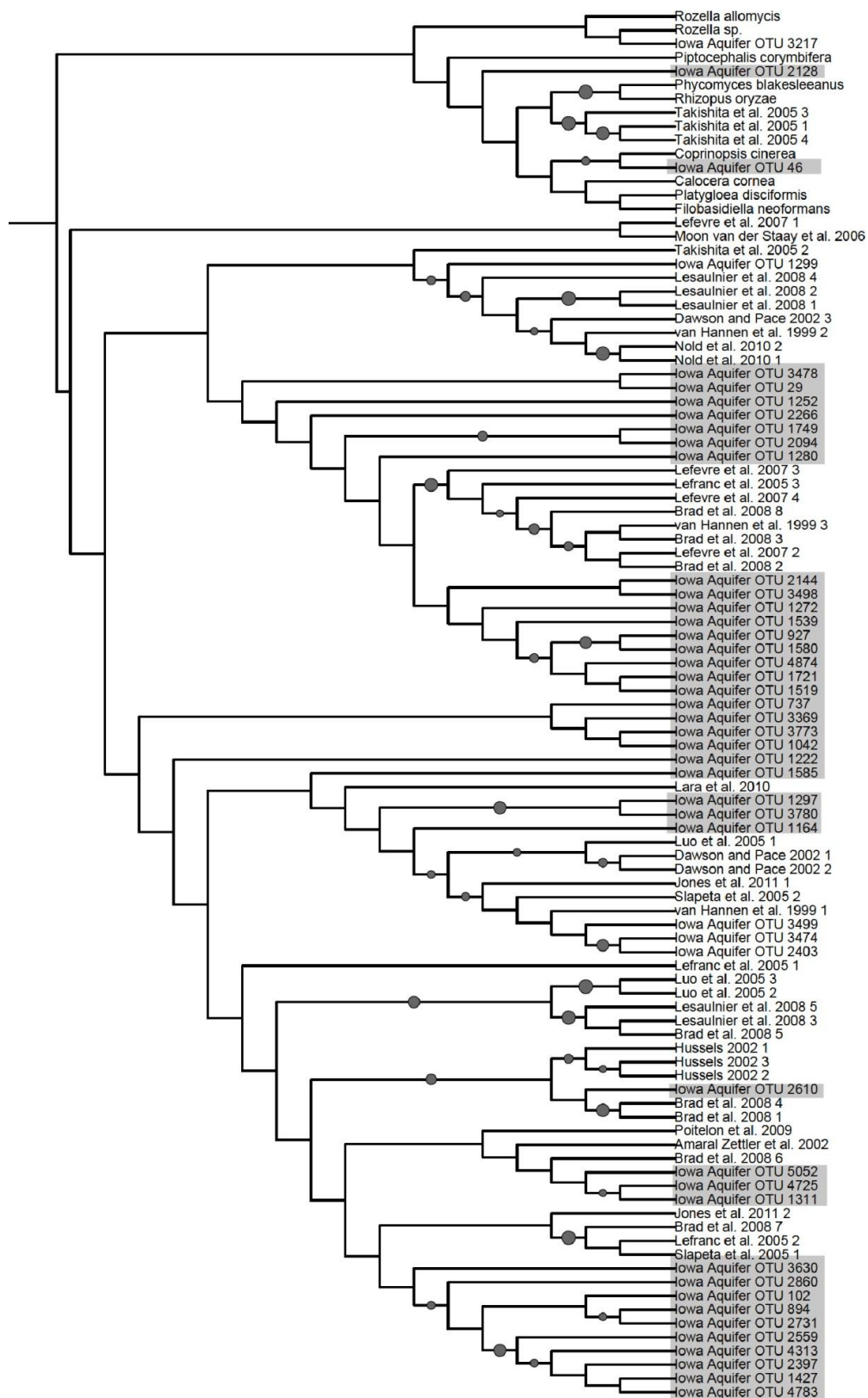
This work contributes substantially to known Cryptomycota diversity, especially from marine environments. This contradicts previous work in which Cryptomycota sequences were unamplifiable from marine environments and were under-represented in phylogenies (88). Additionally, this work adds sequences from a unique and previously unexplored groundwater environment. Observations of predominantly freshwater and marine clades in the Cryptomycota is consistent with observations of the same phenomena in multiple other eukaryotic groups (15, 17, 31, 33, 84, 177). The prominent endoparasitic *Rozella* genus appears in one of the first diverging groups indicating divergence from the marine Cryptomycota ancestors very early in the history of the Cryptomycota.

An additional observation regarding Cryptomycota groups is the presence of a potentially unique aquifer clade. A specific clade appears in phylogenies only when all the Iowa aquifer Cryptomycota sequences are included in the analysis indicating the group may be uniquely contributed from that environment. Significantly, when marine-derived pyrosequencing data is excluded from the analysis, members of marine-defined third diverging group collapse into the Iowa aquifer-associated clade, and in holistic comparisons, the Iowa aquifer environment is phylogenetically more similar to marine than freshwater environments. These observations that perhaps the Iowa aquifer was colonized by some Cryptomycota lineages that diverged from marine lineages. This potential colonization and subsequent allopatric species radiation is consistent with Iowa geologic history, which has experienced numerous marine inundations and exposures since the Paleozoic (14). It is possible that the aquifer or immediately underlying strata were deposited and colonized when the area was marine coastal during the Pennsylvanian period (14) consistent with the clustering of coastal sequences from Wimereux in Group 4 and close proximity of the Iowa Aquifer environment to Wimereaux in ordinations (Fig. 30).

In summary, the most clear revelation is the presence of a large diversity of marine Cryptomycota. Future work indicating the consequence of inclusion of a large number of fragmentary sequences will help to assess confidence in our phylogenetic placements. Finally, we have revealed sufficient sequences diversity so as to likely permit the design of Cryptomycota specific primers and probes necessary to selectively amplify Cryptomycota sequences from the environment or fluorescently illuminate novel members for single cell metagenomic strategies.

Figures

Figure 24: Subtree of RAxML Maximum Likelihood phylogeny of reference Cryptomycota sequences with query sequences from and Iowa Aquifer.

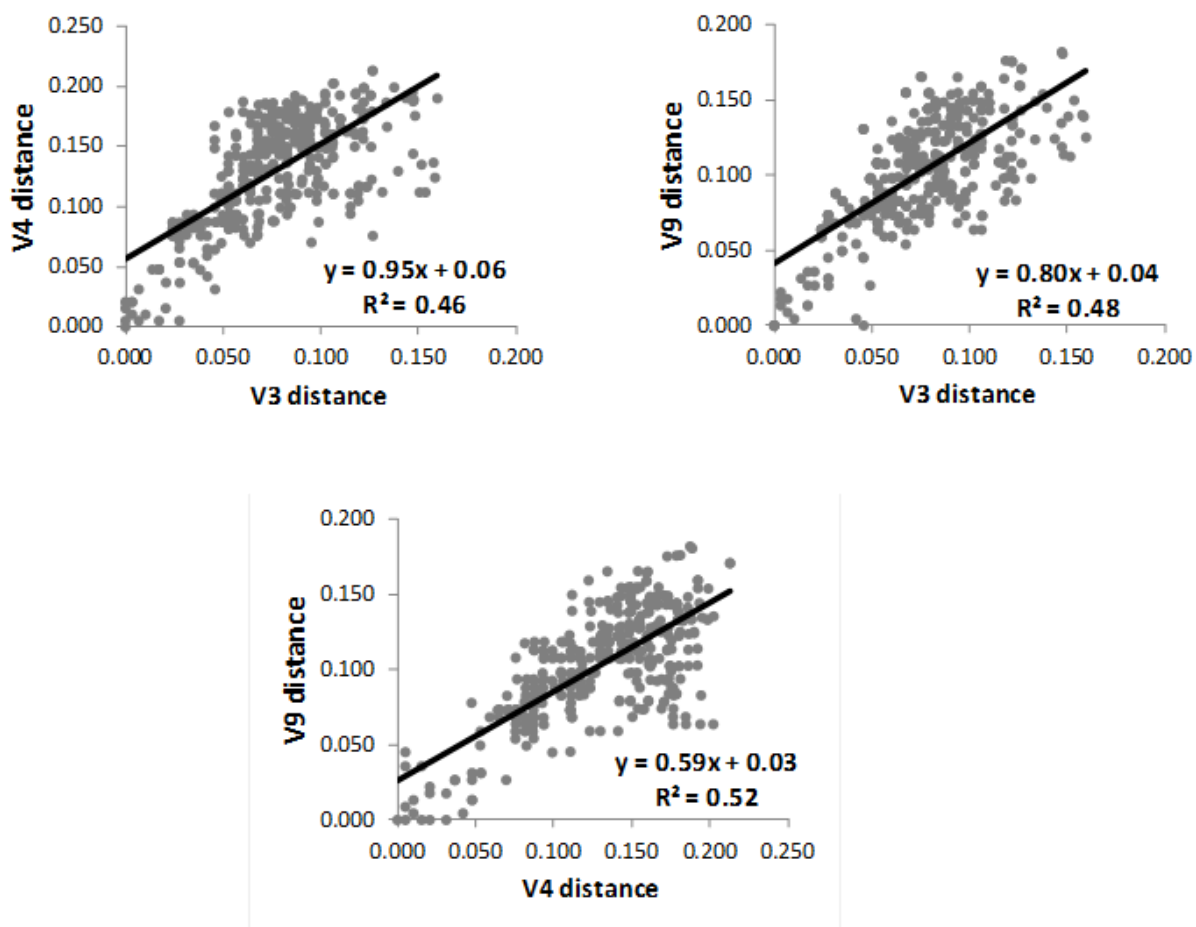


Notes- Highlighted sequences are from the Iowa Aquifer and dots on nodes indicate bootstrap values (500 replicates) >50% with larger circle denoting higher values.

Table 3: 18S rRNA gene pyrosequencing studies interrogated for potential Cryptomycota sequences

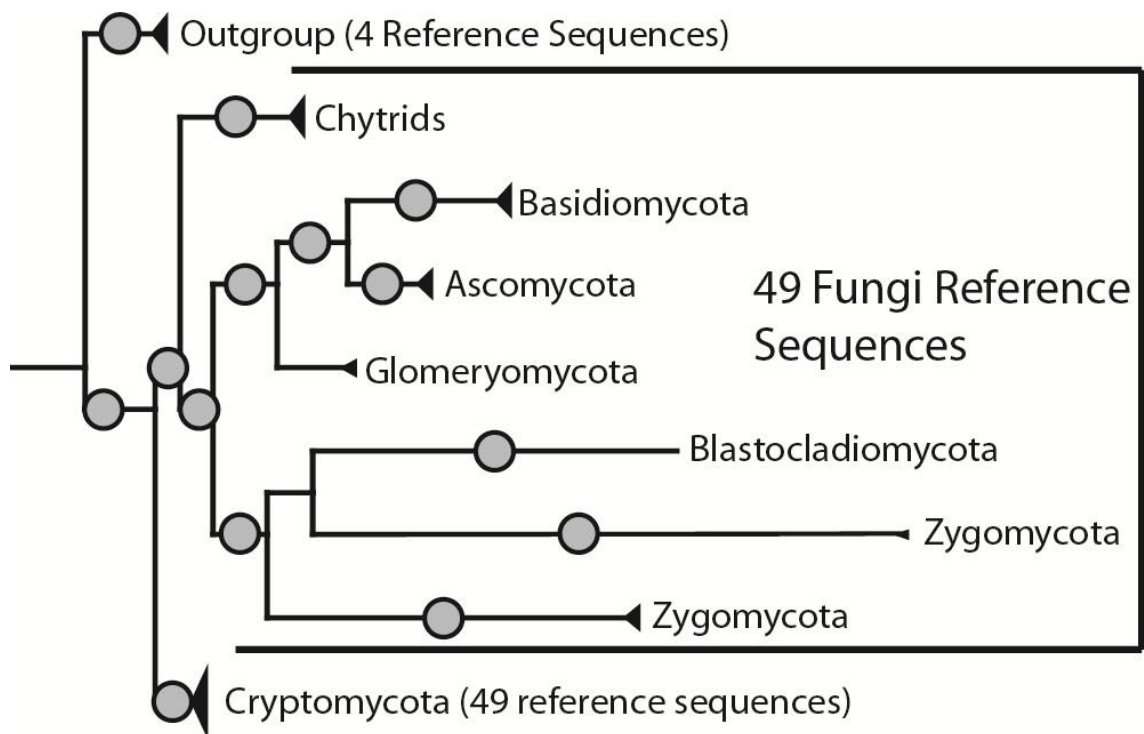
Study	Environment(s)	Hypervariable Region	Ref.	Total Seqs	Total 97% OTUs	% Crypto Seqs	% Crypto OTUs
Amaral-Zettler et al. 2009 MHB	Marine	V9	(11)	32655	1466	0.93%	5.3%
Amaral-Zettler et al. 2009 PAL	Marine	V9	(11)	12951	1023	1.1%	1.1%
Bik et al. 2011 F04	Marine	V4	(22)	316381	5833	0.93%	1.1%
Bik et al. 2011 NF1	Marine	V8-V9	(22)	186167	5418	1.8%	2.0%
Chariton et al. 2010	Marine	V8-V9	(37)	333462	5783	2.1%	4.4%
Cheung et al. Mirs 2010	Marine	V4	(39)	80751	1833	0.26%	1.5%
Cheung et al. Tolo 2010	Marine	V4	(39)	57582	1035	2.6%	4.6%
Edgcomb et al. 2011	Marine	V9	(56)	64649	3265	0.88%	1.8%
Monchy et al. lakes 2011	Freshwater	V3	(122)	21314	8726	0.49%	0.79%
Monchy et al. coastal 2011	Marine	V3	(122)	44033	14968	0.02%	0.06%
Nolte et al. 2010	Freshwater	V3	(129)	264033	1656	30%	27%
Pawlowski et al 2011	Marine	V9	(135)	221467	7497	0.37%	1.5%
Iowa Aquifer	Freshwater Aquifer	V4	This study	520688	5146	4.5%	2.7%

Notes- MHB is Mount Hope bay Estuary and PAL is the Palmer Station on The Antarctic Peninsula "% Crypto Seqs" is the proportion of total sequences clustering with the Cryptomycota and "% Crypto OTUs" is the proportion of all OTUs that are likely to be Cryptomycota.



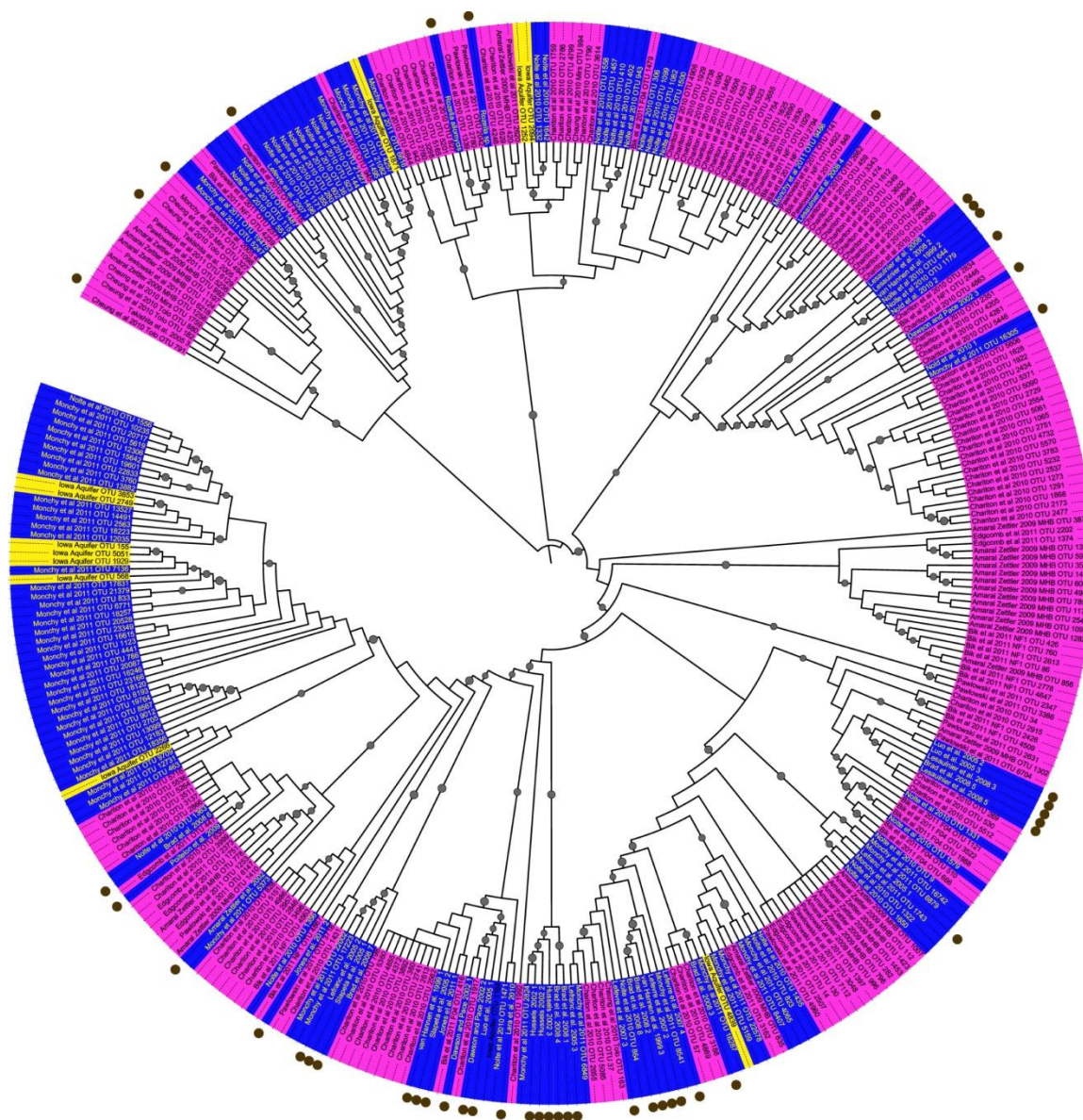
Notes- Top left: comparison of V4 and V3 distances per sequence, Top right: comparison of V9 and V3 distances, Bottom: comparison of V9 and V4 distances.

Figure 25: Linear regressions based on Tamura Nei 1993 distances between hypervariable regions of the same Cryptomycota sequence.



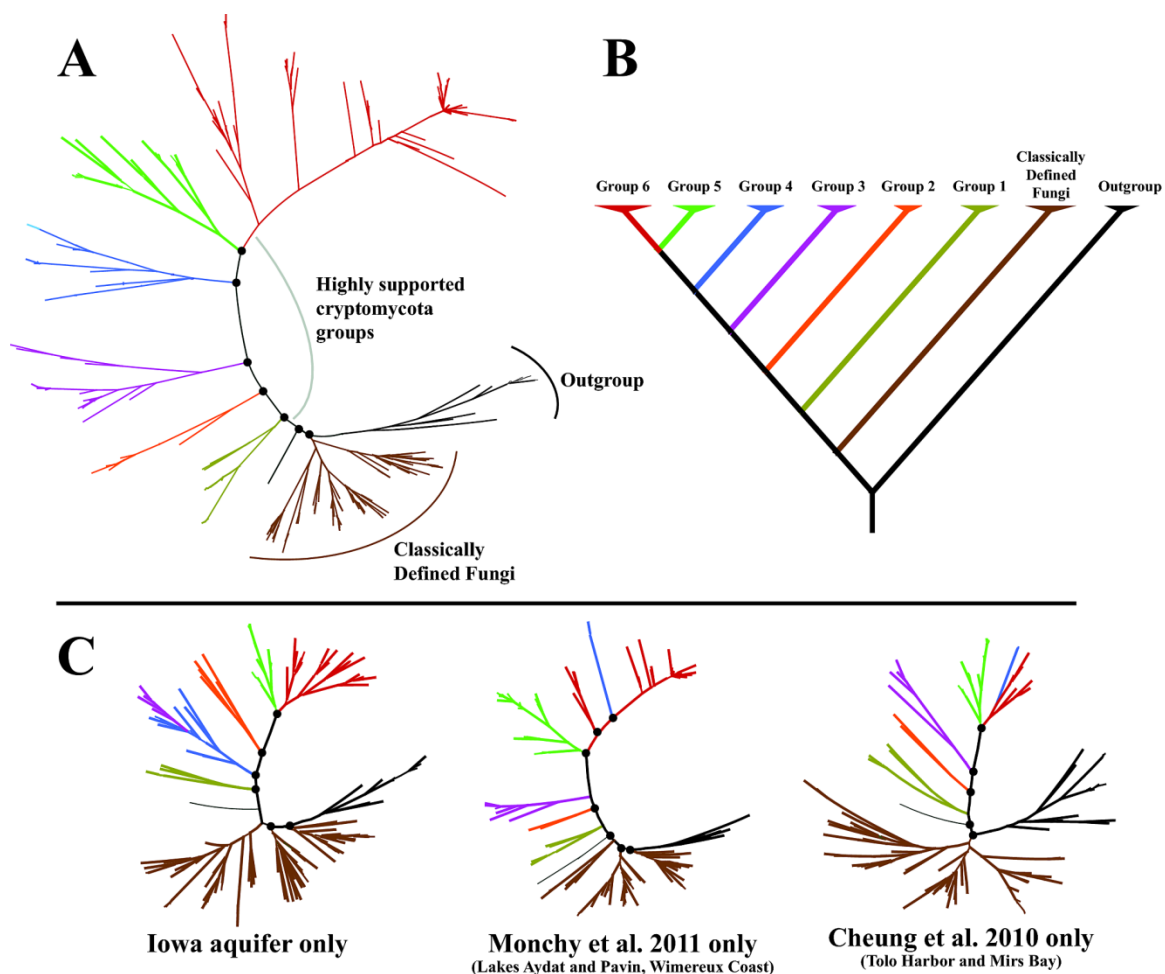
Notes- Branches are collapsed to phylum with highly supported clades (probability >0.80 using the SH test) annotated with a closed circle. The Cryptomycota was supported at >0.96 using the SH test.

Figure 26: Maximum likelihood phylogeny built from partial 18S rRNA genes of reference fungal lineages and sequences collected from 454 environmental pyrosequencing surveys



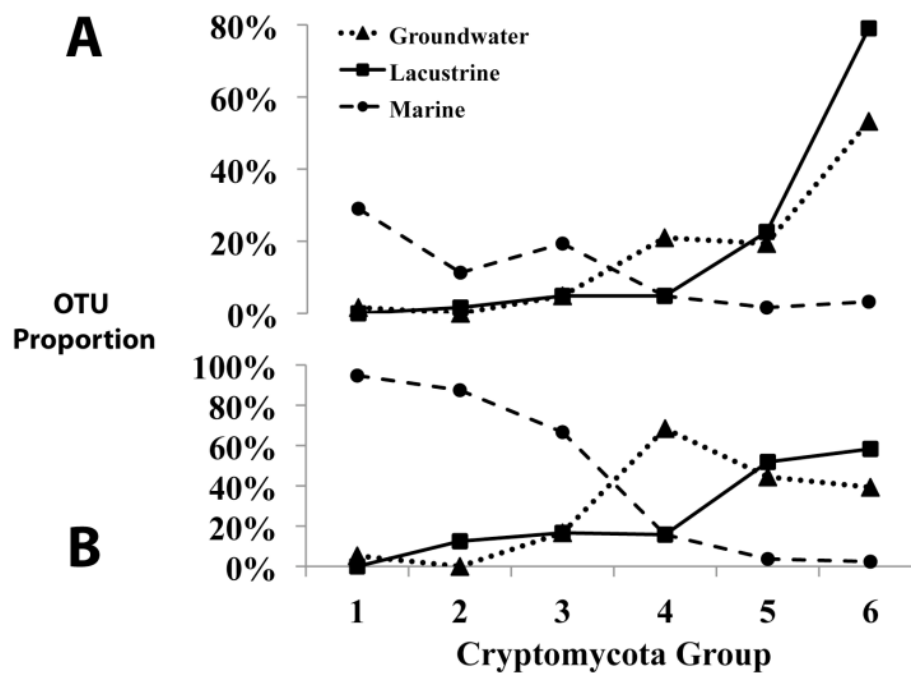
Notes- Pink names indicate marine sequences, blue names indicate freshwater sequences, and yellow names indicate locations of sequences from the Iowa Aquifer. Dots on a branch indicate SH test >0.7 , Brown dots on perimeter indicate reference sequences.

Figure 27: FastTree summary phylogeny of reference Cryptomycota sequences from a previous study and candidate sequences from 13 pyrosequencing sets.



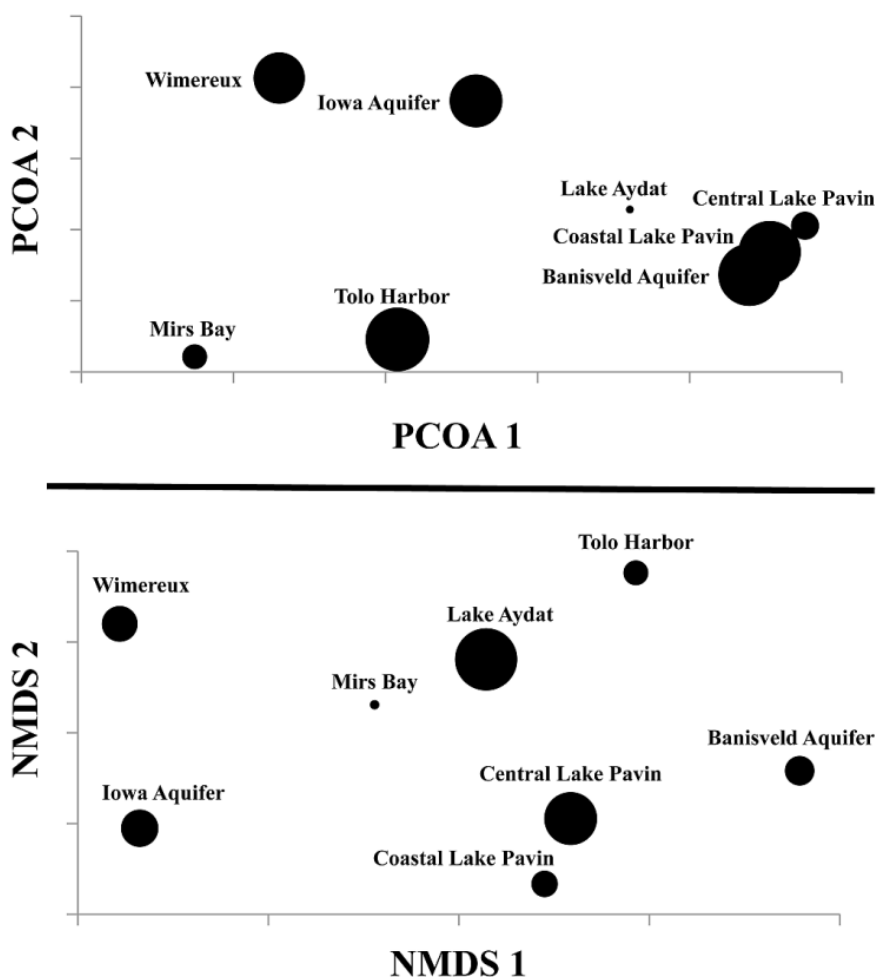
Notes- The outgroup are a set of non-fungal opisthokont sequences used in a previous study (88). A) Phylogeny built with sequences from all three environments. B) Key to groups. Highly supported C) Phylogenies constructed using pyrosequencing data from each of three studies (This study, (39, 122)) independently.

Figure 28: Maximum likelihood phylogenies of the Cryptomycota from 18S rRNA gene pyrosequencing libraries of aquifer, lacustrine, and marine environments with reference database sequences.



Notes- Group 1 is the earliest diverging and Groups 5 and 6 are the most recently diverged. A) Proportional of all OTUs from a specified environment in each group. B) Environmental distribution of OTUs in each group.

Figure 29: Proportional environmental representation of operational taxonomic units (OTUs) within defined groups of a Cryptomycota maximum likelihood phylogeny.



Notes- The third axis is represented by size of points. A) ordered on axes using principal coordinates, B) ordered using non-metric dimensional scaling. Input distances were the unweighted UniFrac distance calculated from a maximum likelihood phylogeny of Cryptomycota from pyrosequencing data along with database reference sequences.

Figure 30: Phylogenetic distances between several aquatic environments sampled for Cryptomycota diversity using 454 pyrosequencing

CHAPTER VI

ENGINEERING AND SCIENTIFIC SIGNIFICANCE

The primary goal of this work was to discover and functionally characterize cryptic biological components of a managed aquifer ecosystem. In accord with this purpose the preceding chapters included discussions of specific organisms participating in contaminant degradation, a survey of subsurface eukaryotic diversity, a method to extract and prepare aquifer organisms from sediments for imaging, and an in depth examination of the extent of diversity of Cryptomycota organisms in an aquifer compared to marine and surface freshwater ecosystems.

The first major innovation of this work was identifying a specific kind of microorganism affiliated with in situ aquifer RDX degradation during reductively enhanced bioremediation. This is a crucial advance in RDX bioremediation science and practice as a potential means of assessing and optimizing remediation performance. A body of knowledge has emerged regarding probable microorganisms responsible for natural RDX attenuation, but evidence that *Geobacter* may be the probable agent in natural systems is counter to results from laboratory studies aimed at identifying organisms that utilize the compound as a carbon or energy source (45, 148, 187). This was the first large scale study aimed at identifying possible degraders in situ thus augmenting the credibility of this result relative to those obtained from laboratory microcosms.

A number of possible research pathways exist to continue this work and investigate the hypothesis that *Geobacteraceae* like organisms are the probable causal biological agent of in situ RDX degradation. A number of studies have shown RDX transformation by biogenic reduced iron from *Geobacter metallireducens* (71, 183). Investigating in situ iron mineral transformation and capability to degrade RDX would provide another line of evidence of the complicity of *Geobacter spp.* Simulated aquifer

studies using previously collected sediments and fresh groundwater could similarly be used to the same end. Another possible direction is tracking the dynamics of *Geobacter spp.* activity during the remediation process in situ and in columns. This data could be collected using the quantitative polymerase chain reaction, fluorescence in situ hybridization, or 16S rRNA gene labeled microarrays (phylochip). A third set of investigations could include inhibition of *Geobacter spp.* viability or enzyme activity using targeted antibiotics or compounds that arrest Geobacteraceae specific enzymes. In columns, this type of experiment would help determine if other Iron reducers would fill the voided niche to the same effect (ie RDX transformation).

In addition to analyzing the eubacterial community of the Iowa Aquifer during the bioremediation process, this work also demonstrated the existence of a phylogenetically diverse community of eukaryotic organisms in the subsurface. This was one of the deepest subsurface environments (approximately 17 m) that eukaryotic organisms have ever been sampled. Current acknowledgements of subsurface eukaryotes are sparse thus ignoring a great potential source of ecosystem services and processes, as well as a community that could be very instructional in the study of basic ecosystem function and processes. The cursory examination of eukaryotic diversity in this Iowa aquifer showed great diversity in the fungi, platyhelminthes, and various "protist" lineages. Using in depth phylogenetic analysis a large number of Catenulidae clades emerged greatly enhancing the known diversity of this class of life during a single study. While this study examined in depth phylogenetic analysis of metazoans, this group holds a mere subset of the total eukaryotic diversity in this aquifer. The next phase in the analysis of this pyrosequencing data should be robust phylogenetic analysis of sequences in each of the different eukaryotic kingdoms. We expect to find novelty in each, though determining the most significant will require interaction with external expert collaborators.

There is vast potential societal significance to subsurface eukaryotic diversity. From an applied engineering standpoint we are interested in the potential of these

organisms to participate in subsurface pollutant attenuation, carbon and other nutrient cycling, predation effects, and regulation of ecosystem stability during and after management activities. For example, fungi are known to degrade RDX (156), and many other organisms throughout the eukaryotic tree of life possess cytochrome P450 like enzymes (182) which have RDX transformation potential (40). An organism need not assimilate RDX as an energy source, but simply degrade it cometabolically or as a means of intentionally affecting environmental suitability. Furthermore, RDX is merely one of the many contaminants found in groundwater. Eukaryotic organisms might be contributory to the natural attenuation of any number of other recalcitrant compounds in groundwater including chlorinated ethenes, methyl tert-butyl ether (MTBE), perchlorate, and pesticides to name a few. As ecosystem participants, groundwater eukaryotes may also be relevant during management activities through predation and limiting nutrient recycling. Already, we know that some predatory activity may prevent aquifer clogging during bioremediation (97) and predators might preferentially consume or avoid specific prokaryotic organisms we favor to enrich during aquifer substrate addition or bioaugmentation (96). Finally, microscopically observable eukaryotes may be useful as bioindicators of aquifer health, redox state, or bioremediation performance.

Aquifer eukaryotic organisms also hold great potential for study from a fundamental scientific standpoint. The aquifer environment is favorable for biogeographic studies as it is difficult to migrate into or out of (77). In this way, remote or deep aquifer regions may behave as "islands" in island biogeographical theory. In contrast to the predictions of island biogeography, however, the passage from biodiversity sources to sinks may involve graded series of adaptations to the subsurface environment providing the potential for new paradigms in dispersal ecology and allopatric evolution. Additionally, each time an aquifer is formed depositionally can be thought of as an allopatric event sequestering surface dwelling aquatic organisms in a subsurface environment to the eventual formation of species unlike any we have seen

before. Thereafter, these organisms would represent side branches on the tree of life affording the potential for observation of transitional states in the diversification of eukaryotic life.

The next phase of characterizing subsurface eukaryotes from this aquifer should involve culturing and imaging to describe the diversity morphologically and metabolically. To accommodate this goal, this dissertation describes a method to simultaneously preserve and extract organisms directly from collected sediments using a Nycodenz blanket to separate biological material from inorganics (Chapter 3). This is a major advance as it will permit imaging of native organisms independent of culturing. Sediment samples from this aquifer were preserved at -80°C and these may still hold some intact organisms which we could potentially image and collect DNA to forge the necessary links between morphotypes and DNA sequence.

The final major advance of this work was delineating diversity of Cryptomycota organisms in groundwater and other aquatic environment. Indeed, this was the first study to explicitly address Cryptomycota in groundwater and the marine upper water column. The observed apparent diversity will provide a baseline for studying Cryptomycota in all future environments given that this work depicted major differentiable groups within this new Phylum of eukaryotic multiplicity. Additionally, the appearance of this group in so many different environments opens the door for many functional relationships much like the discovery of the cryptic yet ubiquitous SAR11 revolutionized our understanding of global carbon cycle (125). While our data may not hold additional insights into the Cryptomycota, utilizing large numbers of sequences from many pyrosequencing datasets may prove a valuable method to compare and assess taxonomic diversity in a variety of other organisms relevant to aquifers.

Finally, and generally this work will change our perceptions and understandings of the function of subsurface ecosystems. The public and academia have only recently acknowledged the vital role prokaryotic organism play in the health of subsurface

environments. This acceptance was concurrent with increasing ability to cultivate and observe the organisms found therein. In the same way, the high-throughput molecular methods used in this study allowed the rapid and thorough characterization of the extent of eukaryotes in our one aquifer environment thus unveiling vast cryptic diversity with all its potential.

APPENDIX A: MULTIVARIATE RRNA GENE DATA AS
INDICATORS OF AQUIFER GEOCHEMICAL STATE DURING
CARBON AMENDMENT

Abstract

Bioindicators are a means of assessing the state of an ecosystem independent of chemical measurements, but bioindicators for groundwater aquifers remain in the early stages of development relative to those for surface waters. Ribosomal RNA (rRNA) gene data were tested as an aquifer bioindicator using samples from hexahydro-1,3,5-trinitro-1,3,5-triazine (RDX)-contaminated groundwater obtained near the Iowa Army Ammunition Plant (Middletown, IA, USA). Terminal restriction fragment length polymorphism was used to collect community phylogenetic data for eubacteria and denaturing gradient gel electrophoresis was used to collect micro-eukaryote data. The large data sets were reduced to a small number of independent variables using ordination and the new variables correlated to their associated geochemical factors. The results indicate that 16S rRNA gene data is useful as an indicator of aquifer geochemical state when compared to a reference state in an ordination. Similarly, 18S rRNA gene sequence diversity was positively correlated to dissolved oxygen concentration. Additionally, we identified members of the Clostridia, Platyhelminthes, and Tardigrada as individual candidate bioindicator organisms in this aquifer. Overall, our results indicate that multivariate rRNA gene data is useful for assessing aquifer geochemistry and identifying phylotypes as potential bioindicators.

Introduction

Clean and fresh water under the earth's surface is an important resource. Groundwater aquifers comprise 33% of municipal and 98% of private fresh water resources in the U.S. (94)Despite great public interest in aquifer protection, groundwater pollution has been reported in every U.S. state comprising an estimated minimum total of

one quadrillion gallons of contaminated water(142). Sources of some of this contamination are hundreds of military sites fouled with toxic munitions (102), many of which have been shown to migrate readily in aquifers (158, 174). Bioremediation is an attractive method of removing munitions contamination in aquifers because it can be performed in situ, it has the potential to be less costly, and engenders reduced worker exposure to toxic chemicals than techniques such as excavation or pump and treat(172).

Bioremediation is being used at the Iowa Army Ammunition Plant in Middletown, Iowa to remove one aquifer plume of the munitions constituent RDX (Hexahydro-1,3,5-trinitro-1,3,5-triazine). This proven bioremediation process consists of adding acetate to the groundwater as an electron donor to facilitate the transformation of the aquifer from an aerobic to anaerobic state permitting reductive transformation of RDX by a number of possible pathways(42, 180). While we understand that adding carbon to an aquifer will likely result in reductive RDX removal(180), we lack the tools to fully understand the geochemical and biological changes occurring during the bioremediation process. Additionally, due to aquifer heterogeneity it is difficult to predict if bioremediation in an aquifer will be successful and whether or not the remediation process will have long term consequences. Furthermore, we lack the ability to verify that bioremediation is proceeding by the desired path independent from measuring the contaminant and metabolites. A potential solution to these problems is to use bioindicators consisting of organisms or groups of organisms that reflect the physical and/or chemical state of an ecosystem. Similar bioindicators are used as a measure of environmental quality in surface freshwater systems (150), air pollution in terrestrial systems (114), and process control in wastewater treatment (152). One recent study examined a single organism as an indicator of migration barriers in shallow aquifers (165) demonstrating potential for their use in aquifers. In general, good bioindicators are easily measured, sensitive to stresses on the system, and respond to stresses in a predictable manner (46). Additionally, aquifer bioindicators should be independent from

geochemical measurements to provide self-reliant measures of remediation performance or physical-chemical state.

In this paper we examine multivariate data derived from the polymerase chain reaction (PCR) amplifications of whole community 16S eubacteria and 18S eukaryote rRNA genes as bioindicators in aquifers. Obtaining rRNA gene data from the environment is routine using a variety of high throughput techniques such as denaturing gradient gel electrophoresis (DGGE) and terminal restriction fragment length polymorphism (TRFLP) (128). Here we test the efficacy of 16S and 18S multivariate data to differentiate between samples in groundwater affected by acetate and those that are not. Additionally, we assess predictability associated with individual organisms represented in the data and diversity relationships along aquifer geochemical gradients.

Materials and Methods

Site Characterization and Geochemical Monitoring

The Iowa Army Ammunition Plant located near Burlington, IA (40° 48' N, 91° 15' W) is a source of RDX groundwater contamination. Located within the Mississippi River valley, the contaminated aquifer is of alluvial origin and composed of intermediate sands. Groundwater flow velocities range between 80 and 130 ft/yr (176). Our investigation focused on several wells in this aquifer within a one mile radius (Fig. 1). The well designated SMW-05 is an injection well while MW-309 and EMW-02 are monitoring wells located immediately down-gradient of the injection site and are thus subject to impact by acetate injections. MW-505 and MW-502 are background wells located up-gradient of the injection wells and provide a biological background community free of acetate influence.

At the time samples were taken we also measured pH, temperature, dissolved oxygen (DO), and turbidity in the groundwater using a multi-parameter field probe (YSI model 556, YSI Inc. Yellow Spring, OH, USA) while ferrous iron and sulfide

concentrations were measured with a field kit (Hach DR 2020, Hach Co. Loveland, CO, USA). Additionally, RDX, acetate, sulfate, nitrate, and total organic carbon concentrations were measured by a certified commercial laboratory (Accutest Laboratories, Dayton, NJ, USA) using established methods prescribed by the U.S. Environmental Protection Agency (specific methods available on the company website: www.accutest.com).

Collection, DNA extraction and PCR

RDX-contaminated groundwater was collected from wells MW-309, EMW-02, SMW-05, MW-502, and MW-505 using a low-flow purge method and filtered through Sterivex filters (Millipore, Billerica, MA, USA) at five time points between October 9, 2008 and June 20, 2009. Filters were overnight shipped on ice to the University of Iowa and frozen upon arrival at -20 °C until DNA extraction. We extracted microbial community DNA using the Mo Bio Ultraclean Soil DNA kit (MO BIO Laboratories, Carlsbad, CA, USA) according to the manufacturer's protocol except that bead beating was performed using a Biospec Mini Bead-Beater-8 for two minutes rather than vortexing the samples for ten minutes on a Mo Bio vortex tube adapter. We used PCR to amplify 16S rRNA and 18S rRNA genes from the community DNA by adding 2.0 µl of DNA extract (0.4 to 8 ng) to a 50 µl total reaction volume containing Qiagen Taq PCR Master Mix and 500 nanomoles of each primer. To amplify the 16S rRNA gene we selected primers 8F (with 5' attached 6-FAM) and 1492r (95). The thermo-cycling conditions were 2 minutes at 94° C, followed by 35 cycles of 30 seconds at 94° C, 45 seconds at 55° C, and 1 minute and 30 seconds at 72° C with a final extension of 2 minutes at 72° C. We selected primers Euk1A and Euk516r-gc (24) for amplifying eukaryotic 18S rRNA genes. The thermocycling conditions were 4 minutes at 94° C, followed by 40 cycles of 30 seconds at 94° C, 45 seconds at 56° C, and 2:10 at 72° C with a final extension of 7 minutes at 72° C.

TRFLP and DGGE

To resolve and visualize unique sequences from PCR mixtures we used TRFLP for 16S rRNA genes (95) and DGGE for 18S rRNA genes(51). We desalted PCR products using a Qiaquick PCR purification kit and determined DNA concentrations using the DS DNA broad range assay of the Qubit fluorometer (Invitrogen, Carlsbad, CA, USA). Purified 16S PCR products (~250 ng from each sample) were digested with 20 units MspI, RsaI, or AluI restriction enzyme (New England Biolabs, Ipswich, MA) in the recommended buffer at 37⁰ C for no more than 4 hours to minimize non-specific cleavage. Digests were desalted using ethanol precipitation with glycogen as a carrier (Fermentas, Burlington, Ontario) and electrophoresis used to separate 70 ng of digest at the University of Iowa DNA facility on an ABI 3730 DNA analyzer (Applied Biosystems, Carlsbad, CA, USA). To size the fragments we used Peak Scanner 1.0 with the ABI GeneScan™ 1200 LIZ® as an internal size standard. We performed DGGE for 18S PCR products using the Dcode Mutation Detection System (Bio-Rad Laboratories, Hercules, CA, USA) with an 8% polyacrylamide gel containing a 20-45% urea/formamide gradient. Undiluted (100%) denaturing reagents contained 7M urea and 40% v/v formamide. We placed 100 ng PCR product in each gel lane. Electrophoresis conditions were 60 V for 15.5 hours at 60⁰ C isothermal.

Immediately following electrophoresis, we stained gels with SYBR Gold (Invitrogen, Carlsbad, CA, USA) for exactly 40 minutes without agitation and then photographed them under UV light with the Kodak EDAS 290 Gel Documentation system (Carestream Health, Rochester, NY, USA). We digitized DGGE Bands from band intensities as described previously (186) except that the absolute position of DNA bands in the gel was measured rather than estimated with respect to denaturant concentration. Bands were identified and digitized using Carestream Health Molecular imaging software version 5.0.

We assembled TRFLP, DGGE, and Geochemical data into matrices with samples in rows and unique TRFLP peak heights, DGGE band relative intensities, or geochemical concentrations in columns. In subsequent analysis TRFLP peaks and DGGE bands were used as operational taxonomic units (OTU). For subsequent analysis we imported the data matrices into the R statistical system and multivariate analysis was performed using the “Vegan” supplemental package (132). Previously observed OTU distributions within this aquifer revealed that taxa fell within a narrow geochemical range rather than increasing or decreasing linearly over the entire range of geochemical measurements indicating our data is more appropriately addressed with correspondence analysis than the more popular principle component analysis (144). Therefore we used detrended correspondence analysis (DCA) with down-weighting of rare OTUs to determine sample similarities and level of specificity of OTUs to a given well. The detrended method is considered appropriate for our sample set because we are sampling across relatively large environmental gradients (e.g. aerobic to anaerobic conditions)(144). To determine which geochemical factors most closely relate to the underlying biological structure of our samples, we compared each geochemical factor to the first two dimensions of the detrended correspondence ordination, a non-metric dimensionally scaled ordination (NMDS), and a principle component analysis (PCA)(144). We determined significance by examination of R^2 values and subsequent examination of contour plots. Also, we reduced each samples collection of DGGE band intensities and TRFLP peak heights to Shannon diversity (155), Simpson diversity (159), and Berger-Parker diversity indices (19) using all three because each diversity estimate uses different parameters and calculations. We used regression analysis to examine the relationship between geochemical concentrations and each diversity index.

Organism identification

For TRFLP, we identified peaks of interest using an online TRFLP Phylogenetic Assignment Tool (95). DGGE bands were identified as described previously (51). We excised the bands and eluted them in 40 μ l TE buffer and used 2 μ l of the eluate as the template in a new PCR with conditions identical to those described above. The University of Iowa DNA facility sequenced the purified PCR product directly. The highest scoring NCBI nucleotide BLAST (9) hits were used to identify the most probable taxonomic source from 18S rRNA gene sequences.

Results

Geochemistry changes from acetate injections

Different portions of the aquifer responded variably to acetate injections on August 8, 2008 and April 15, 2009. Dissolved oxygen concentration in downstream well MW-309 was 5 mg/L on June 3, 2008 and slowly dropped to 1 mg/L by December 9, 2008. In contrast, dissolved oxygen in the other downstream well, EMW-02, remained above 4 mg/L throughout the study. Other markers of a changing terminal electron acceptor regime were consistent with changes in dissolved oxygen. The samples that had low dissolved oxygen also had higher than average (arithmetic mean) ferrous iron and sulfide and lower than average sulfate and ORP with the converse true for samples with high dissolved oxygen. Changes in inorganic speciation was consistent with a shift from aerobic to anaerobic conditions in MW-309 and lack thereof in EMW-02. It is also worth noting that RDX reduction to daughter products was observed in well MW-309.

Eubacteria response to acetate injections

We used two-dimensional plots of all combination from the four axes of a detrended correspondence analysis to visualize differences and groupings of groundwater samples (Fig. 31). Plotting the 2nd and 3rd ordination axes in two dimensions reveals an apparent split in the sample set as samples from downstream well MW-309 are on the left side of the Y axis and all other samples are on the right side including samples from downstream well EMW-02, upstream wells MW-502 and MW-505, and injection well SMW-05. We used regression to identify the relationship between ordinations of eubacteria OTUs and geochemical factors and the NMDS model correlated to total organic carbon concentrations ($R = 0.68$, $n = 13$, $p < 0.01$). Two TRFLP peaks affiliated with total organic carbon based on PCA values were identified as members of the Clostridia and Planctomyces. In many cases these two OTUs were either the most or second most abundant of all OTUs. No single geochemical variable significantly influenced the structure of the DCA and none of the diversity indices were correlated to geochemical factors (all R values < 0.43 ; all p values > 0.05).

Eukaryotes response to acetate injections

To examine the interaction between eukaryotic diversity and dissolved oxygen concentrations we used logistic regression and found the log of eukaryotic diversity in our groundwater samples was positively correlated to dissolved oxygen concentrations ($R = 0.85$, $n = 10$, $p < 0.001$) (Figure 32). Other diversity relationships include a positive relationship between Shannon diversity and nitrate concentration ($R = 0.71$, $n = 10$, $p < 0.05$), and negative relationships between the Berger-Parker index and Fe(II) and between the Berger-Parker index and sulfate (for both, $R > 0.7$, $n = 10$, $p < 0.05$).

Ordinations were used with eukaryote OTUs to differentiate acetate affected and unaffected sample and in the first two axes of the DCA (Fig 33) which illustrates sample

dispersion with no apparent explanation upon visual inspection. We identified interactions between ordinations and geochemical factors using regression and found correlation between sulfate concentration and the first two axes of the DCA , NMDS and the PCA (all $R > 0.66$; all $p < 0.05$) illustrated by sulfate iso-concentration lines and vector on the PCA plot (Fig. 34). Approximately five OTUs persist in regions of sulfate lower than 20 mg/L, two of which were identified as belonging to the phylum Platyhelminthes (Genbank accessions: HM484393, HM484394). Three organisms are found above 30 mg/L sulfate isoclines, one of which was from the phylum Tardigrada (Genbank accession: HM484391) and appeared with abundance correlated to sulfate concentration ($R^2 = 0.5$, $n=11$, $p < 0.01$). One organism was found near 50 mg/L (Genbank accession: HM484395) and was most closely related to *Catenula lemnae*, also of the Platyhelminthes. The remainder of the organisms sampled (about 50) fell between 20 and 30 mg/L sulfate.

Discussion

Our data indicates that multivariate rRNA gene data can be used as a bioindicator of aquifer geochemical state independent of geochemical measurements and without the need to culture any of the organisms. The 16S multivariate data subjected to ordination effectively separates wells based on classifiable characteristics (Fig 31), interpreted in the context of the “reference condition”(145) in which a set of samples with known or assumed characteristics are used as a baseline to assess unknown samples. In this fashion, the background wells (MW-502 and MW-505 up-gradient from the injection site) group to form the reference state on the right side of the y-axis and the samples that deviate from that reference are those expected to be under the influence of acetate. We expected that the injection well SMW-05 and down-gradient wells MW-309 and EMW-02 would diverge from the reference condition because of acetate injections. Indeed, the

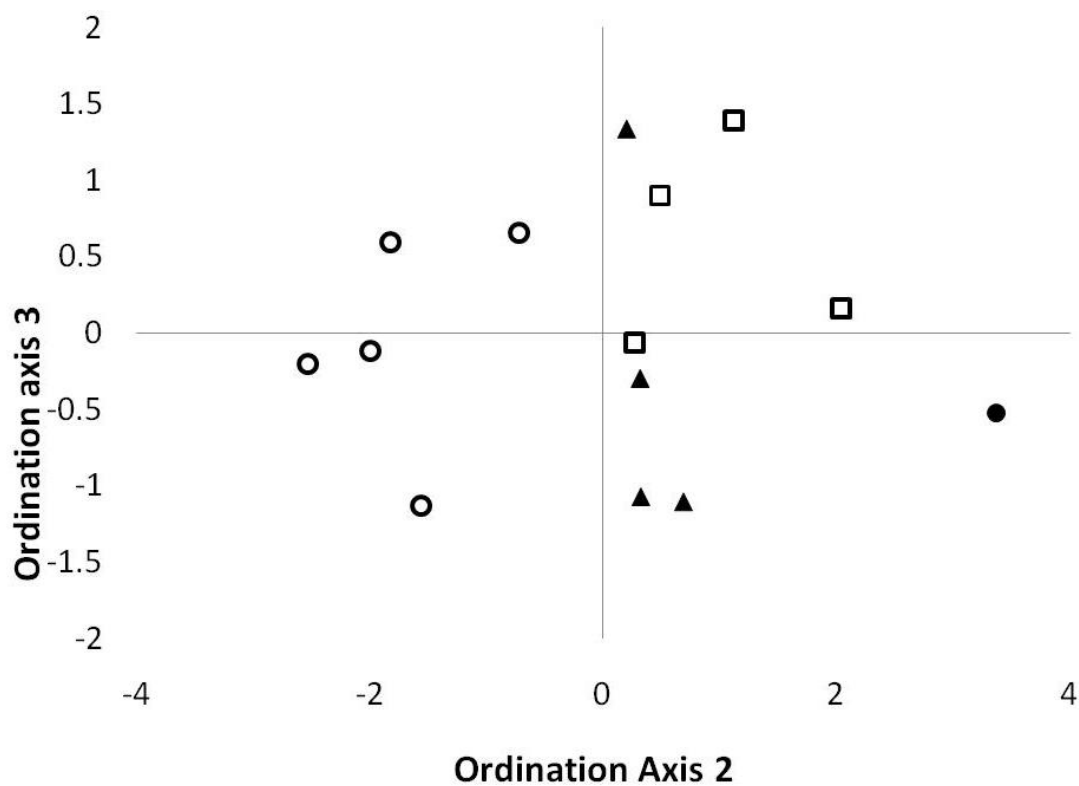
samples from MW-309 were separated from the reference condition and examination of geochemical measurements confirms the influence of acetate evidenced by depression of dissolved oxygen, and sulfate concentrations and increases in ferrous iron and sulfide concentrations. In contradiction, the EMW-02 samples group with the reference condition, but dissolved oxygen, sulfate, sulfide, and ferrous iron measurements reveal that EMW-02 remained aerobic thus refuting the influence of acetate in the region of EMW-02. As such, the state of EMW-02 was counter to our expectations, but the biological data was consistent with geochemical measurements and this consistency lends further credibility to the ordination result. Finally, SMW-05 was separated from all other samples in figure 33 but closer to the reference condition than samples from downstream well MW-309. While no dissolved oxygen measurements were taken for SMW-05, measurements from another injection well a few meters from SMW-05 revealed that at the time of our sample, dissolved oxygen concentrations likely ranged from 7 to 9 mg/L near SMW-05. Based on this observation, we speculate that the eubacteria community near SMW-05 recovered from acetate influence concurrent with oxygen saturation thus leading to close proximity to the reference condition in the ordination. We consider the ordination method on multivariate 16S data to be a good indicator of aquifer state because it is easy to measure, responds sensitively to changes, and is predictable based on the reference condition. It is also completely independent of geochemical evidence.

From the eukaryote data, the significant positive correlation of the Shannon diversity of eukaryotes from DGGE with dissolved oxygen concentration (Fig 32) is consistent with observations of eukaryote responses to nutrient addition in terrestrial aquatic environments (136). This diversity as a bioindicator is also easily measured, sensitive to change, predictable, independent of geochemical data, and has a sound theoretical basis. Furthermore, it is an optimum bioindicator to independently corroborate that the bioremediation process is proceeding as intended (i.e. induction of hypoxia).

Further comparison of 16S rRNA gene data and geochemical evidence reveals that an important underlying factor determining eubacterial community structure in the aquifer is total organic carbon as substantiated by correlation to the NMDS model. We expect this to be true because baseline measurements reveal this aquifer to be carbon poor, therefore influent organic carbon can be reasonably expected to perturb the biological communities much like an influx of nutrients leads to perturbation of surface waters as in eutrophication (75). We identified two organisms as closely corresponding to change in total organic carbon using constrained correspondence analysis (data not shown). One of these organisms belongs to the *Clostridia*, which are of particular interest because of known RDX degraders in this class (185, 188). Data on this organism was easily obtained, sensitive to change, and predictable. However, monitoring this organism using multivariate DNA data is hindered in utility as a bioindicator because identifying their putative role in the process depended on geochemical data as a constraint. We suggest our data justifies further exploration into the role of *Clostridia* in the process, and testing other methods of measuring their abundance as a possible indicator of aquifer state and/or process performance. Examination of the influence of geochemical indicators on eukaryote community structure revealed that the best predictor was sulfate in all three ordination methods. The PCA with sulfate isoconcentration lines allows us to identify candidate bioindicator organisms by examining those that fall at the extremes. As such we only sequenced organisms at the upper and lower ends of sulfate concentration. We identified Plathyhelminthes (flatworms) at both ends of the spectrum suggesting that we might be able to isolate a bioindicator analysis to this group and assess aquifer state depending on the specific flatworms we find. To this end we suggest further examination of the members of this group and their distributions in variant geochemical settings. The tardigrades are also intriguing as a potential aquifer bioindicator given their abundance correlation to sulfate and durability in extreme environments(90). Further support for their potential as a bioindicator comes from a high relative abundance in a

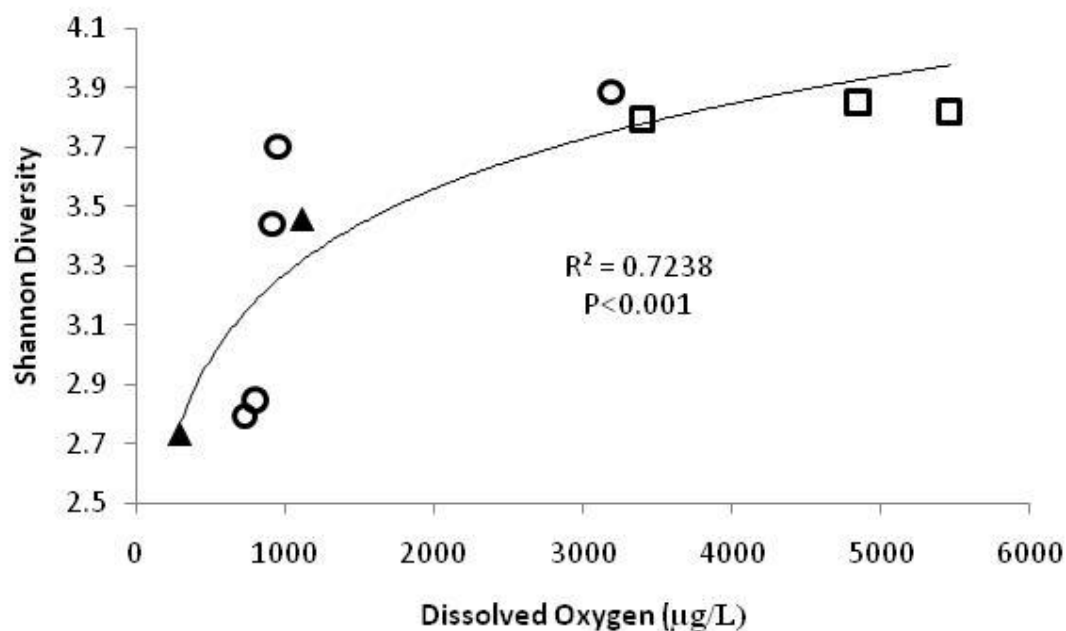
number of samples (maximum of 18%) The reason that either of these groups would be dependent on sulfate concentrations is unclear, but we would conjecture that the controlling factor is actually toxic hydrogen sulfide. Though we did not see any relationship between any ordination and sulfide, correlations could be hindered by chemical interactions between sulfide and iron minerals that do not occur between sulfate and iron(28).

Figures



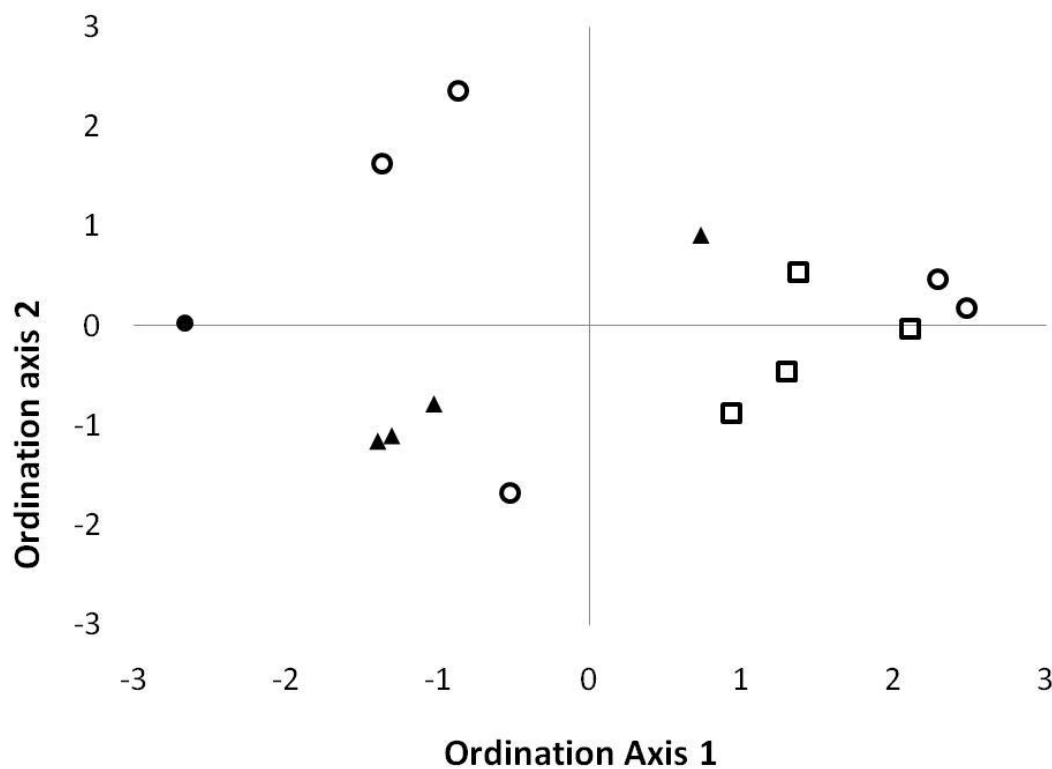
Notes- Open circles mark samples from MW-309, open squares from EMW-02, triangles from the background wells MW-505 and MW-502, and the closed circle is the sample from the injection well SMW-05.

Figure 31: Axes 2 and 3 of a detrended correspondence analysis for 16S TRFLP data from IAAAP wells.



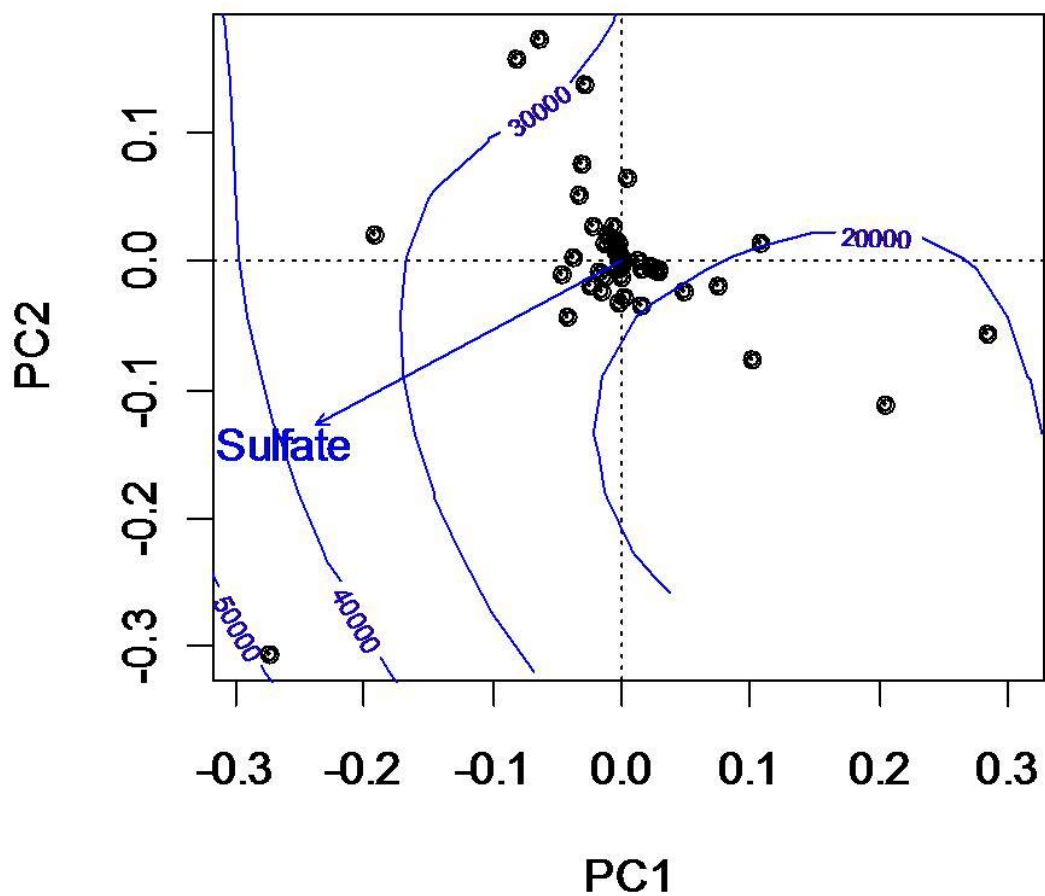
Notes- MW-309 (open circles), EMW-02 (open squares), and MW-502/MW-505 (closed triangles) plotted against dissolved oxygen concentration measurements taken at the time of sampling with logistic regression line (Shannon diversity = $0.4143 \cdot \ln(\text{Dissolved Oxygen}) + 0.4097$).

Figure 32: Shannon diversity (Log₂) for samples from well samples



Notes- Open circles mark samples from MW-309, open squares from EMW-02, triangles from the background wells MW-505 and MW-502, and the closed circle is the sample from the injection well SMW-05.

Figure 33: First two axes of a detrended correspondence analysis for eukaryote data from IAAAP wells.



Notes- Curved lines are sulfate iso-concentration lines in units of $\mu\text{g/L}$ and the vector is a simplified representation of the net direction of increasing sulfate.

Figure 34: OTUs from the Eukaryote DGGE data on the first two axes of a principle component analysis.

APPENDIX B:
SUPPLEMENTARY TABLES AND FIGURES FOR CHAPTER II

Table 4: Primer sequences used in Chapter II and the amplification conditions for primer pairs

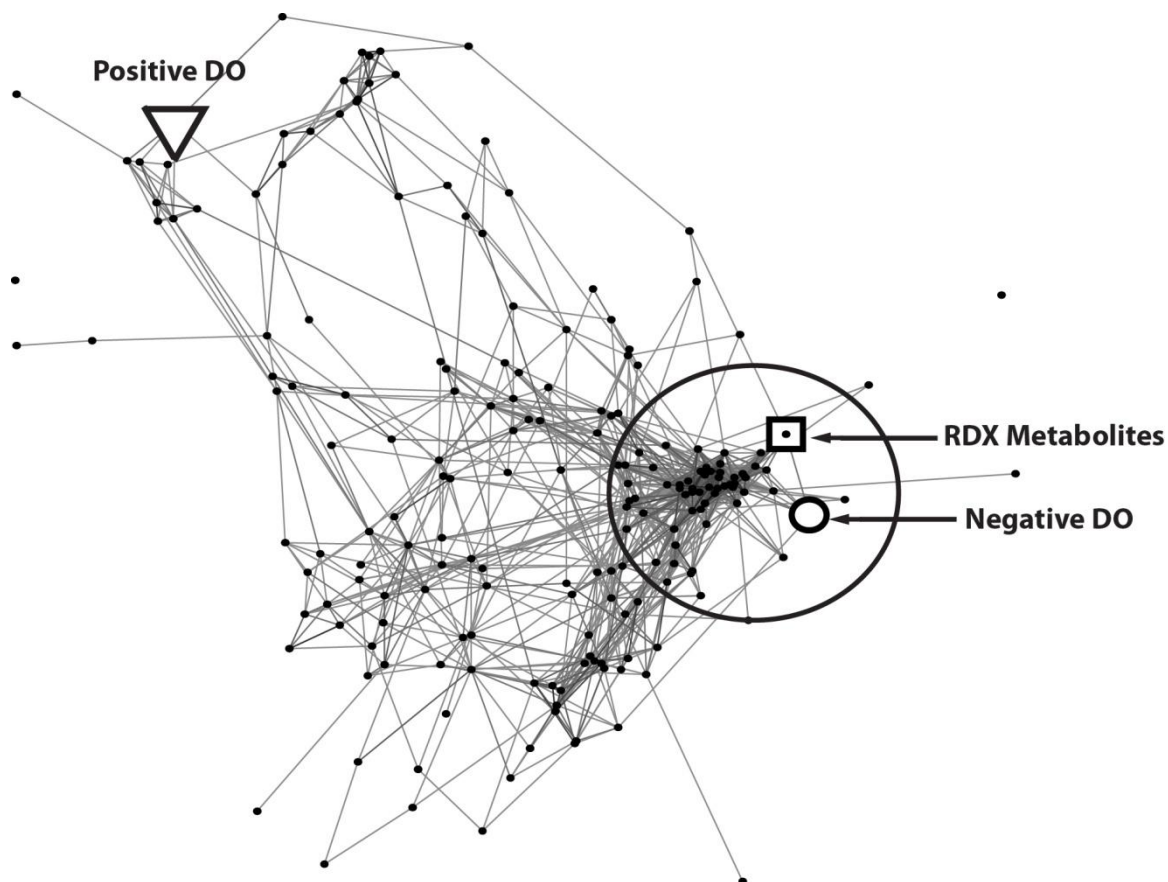
Primer name	Sequence
27f	5'-GAGAGTTTGATCCTGGCTCAG-3'
8fm	5'-AGAGTTTGATCMTGGCTCAG-3'
1492r	5'-GYTACCTTGTTACGACTT-3'
533r	5'-TTACCGCGGCTGCTGGCAC-3'
519r	5'-ATTACCGCGGCTGCTGG-3'
USR515	5'-CACCGCGGCKGCTGGCAC-3'
GC clamp	5'-CGCCCGCCGCGCGCGGCGGGCGGGGGCCCGGGG-3'
Lib-L adapter A	5'-CCATCTCATCCCTGCGTGTCTCCGACTCAG-MID-3'
Lib-L adapter B	5'-CCTATCCCCTGTGTGCCTTGGCAGTCTCAG-MID-3'

Primer Combination	Reaction Conditions	Usage
8fm-1492r	Qiagen Taq Master Mix 94°C-4:00, 35x-(94°C-1:00, 55°C-2:00, 72°C-1:00), 72°C-10:00	Cloning, 1st round PCR
8fm-533r	Qiagen Taq Master Mix 94°C-4:00, 35x-(94°C-0:30, 55°C-0:45, 72°C-1:30), 72°C-8:00	TRFLP
27f/gc- 519r	Qiagen Taq Master Mix 94°C-4:00, 35x-(94°C-1:00, 55°C-1:00, 72°C-1:00), 72°C-8:00	DGGE
8fm-USR515	Roche FastStart High Fidelity PCR system 94°C-10 min, 35x-(94°C-0:30, 55°C-0:45, 72°C-1:00), 72°C-5:00	Pyro-sequencing

Table 5: Wells samples from an aquifer near the Iowa Army Ammunition Plant

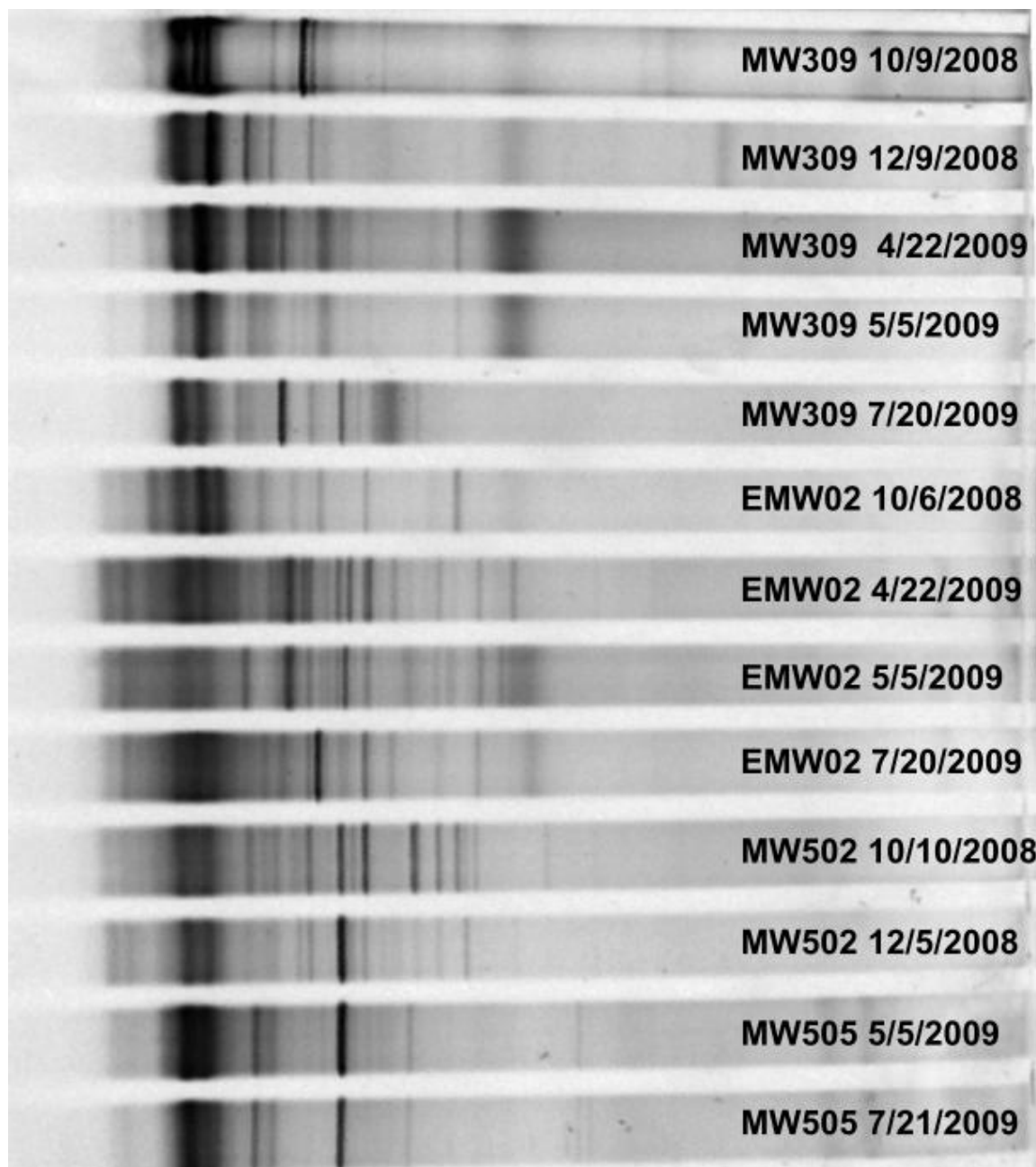
Well Name	Well type	Date	# TRFLP Replicates	RDX Classification	Metabolite Classification	Dissolved Oxygen mg/L
MW309	Monitoring	10/2/2007	1	Non-degrading	Non-producing	NA
		2/13/2008	3	Non-degrading	Non-producing	4.06
		3/14/2008	2	Non-degrading	Non-producing	3.93
		3/28/2008	4	Degrading	Non-producing	4.07
		6/3/2008	2	Non-degrading	Non-producing	5.29
		10/9/2008	1	Non-degrading	Producing	3.19
		12/9/2008	4	Degrading	Non-producing	0.95
		4/22/2009	5	Degrading	Producing	0.73
		5/5/2009	2	Degrading	Producing	0.80
		7/20/2009	1	Non-degrading	Non-Producing	0.91
EMW02	Monitoring	10/6/2008	3	Non-degrading	Producing	3.40
		4/11/2008	1	Non-degrading	Non-producing	5.93
		4/30/2008	3	Degrading	Non-producing	5.31
		6/3/2008	2	Non-degrading	Non-producing	7.05
		4/22/2009	1	Non-degrading	Non-producing	4.22
		5/5/2009	2	Non-degrading	Non-producing	4.85
		7/20/2009	1	Non-degrading	Non-producing	5.46
		12/17/2009	1	Non-degrading	Non-producing	7.44
EMW04	Monitoring	10/2/2007	1	Non-degrading	Non-producing	5.87
EMW05	Monitoring	10/1/2007	1	Non-degrading	Non-producing	4.72
EMW06	Monitoring	9/28/2007	2	Non-degrading	Non-producing	NA
EMW07	Monitoring	9/27/2007	1	Non-degrading	Non-producing	NA
SMW04	Injection	10/1/2007	1	Non-degrading	Non-producing	NA
SMW05	Injection	10/6/2008	2	Non-degrading	Non-producing	NA
SMW06	Injection	10/8/2008	2	Non-degrading	Non-producing	8.60
SMW07	Injection	10/8/2008	2	Non-degrading	Non-producing	7.72
		7/16/09	1	Non-degrading	Non-producing	8.03
		12/15/2009	1	Non-degrading	Non-producing	7.77
SMW08	Injection	12/15/2009	1	Non-degrading	Producing	2.12
SMW10	Injection	12/13/2009	1	Non-degrading	Non-producing	10.31
MW505	Background	5/5/2009	1	Non-degrading	Non-producing	0.47
		7/21/2009	1	Non-degrading	Non-producing	1.12
MW502	Background	10/10/2008	1	Non-degrading	Non-producing	0.30
		12/5/2008	2	Non-degrading	Non-producing	0.36

Notes- Classifications of RDX and metabolite status based on the change in concentration from most recent prior sample in the same well. Measured concentrations of dissolved oxygen are also shown where available or "NA" where unmeasured.



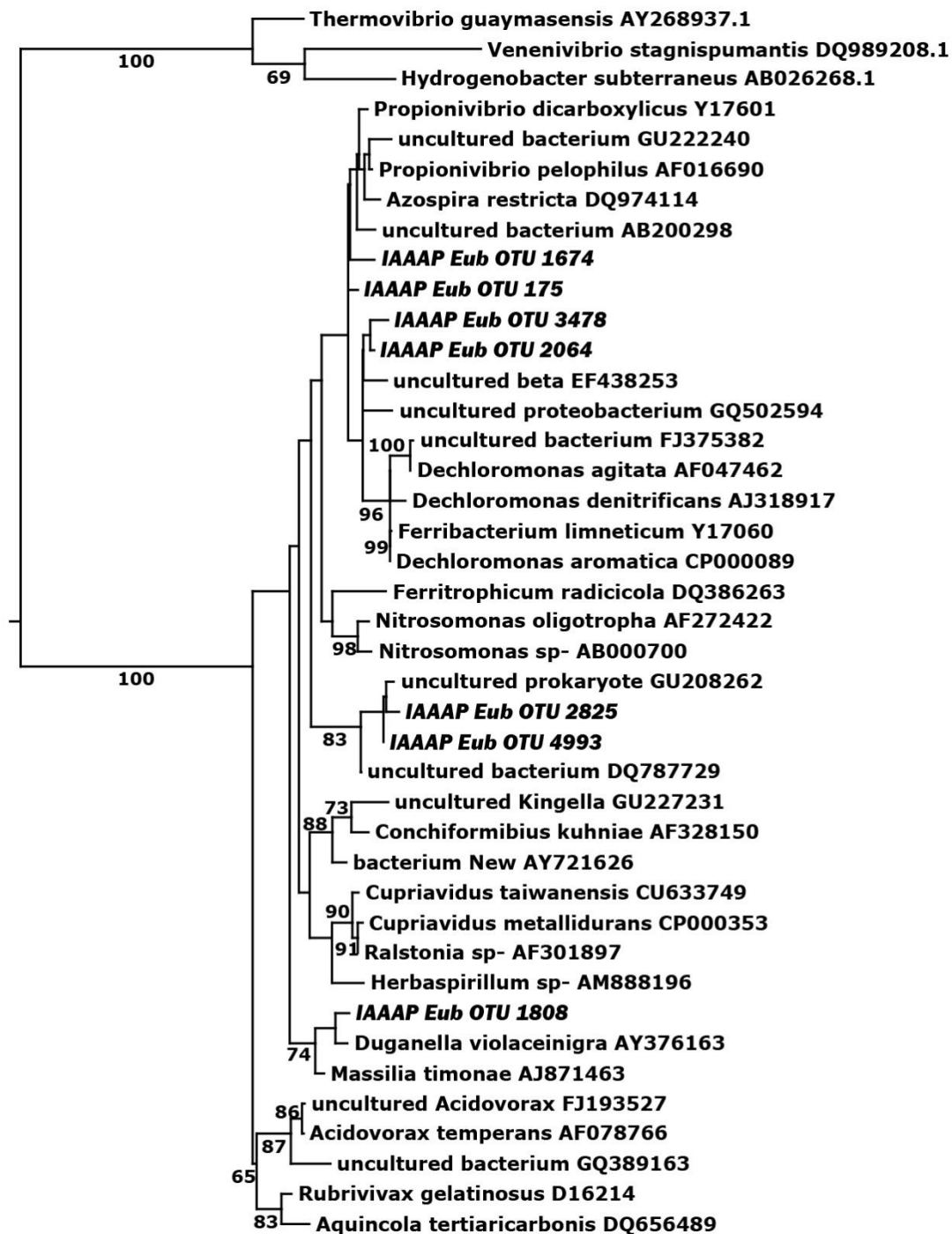
Notes- Dissolved oxygen, opposite of dissolved oxygen, and MNX concentration were also included in the analysis so the open triangle represents the point of highest positive correlation to Dissolved oxygen concentration, the open circle indicates highest negative correlation, and the open square highest correlation to MNX concentration. The cluster encompassing TRFs presumed affiliated with RDX degradation is circled. ∇ =point of maximum correlation to dissolved oxygen concentration, O = point of maximum negative correlation to dissolved oxygen, \square = point of maximum positive correlation to MNX concentration. The cluster encompassing TRFs presumed affiliated with RDX degradation is circled.

Figure 35: Two dimensional representation of a three dimensional CLANS map modeling clustering of terminal restriction fragments (vertices) by attraction values (lines) based on the Pearson correlation coefficient computed from absolute log transformed TRF intensity values



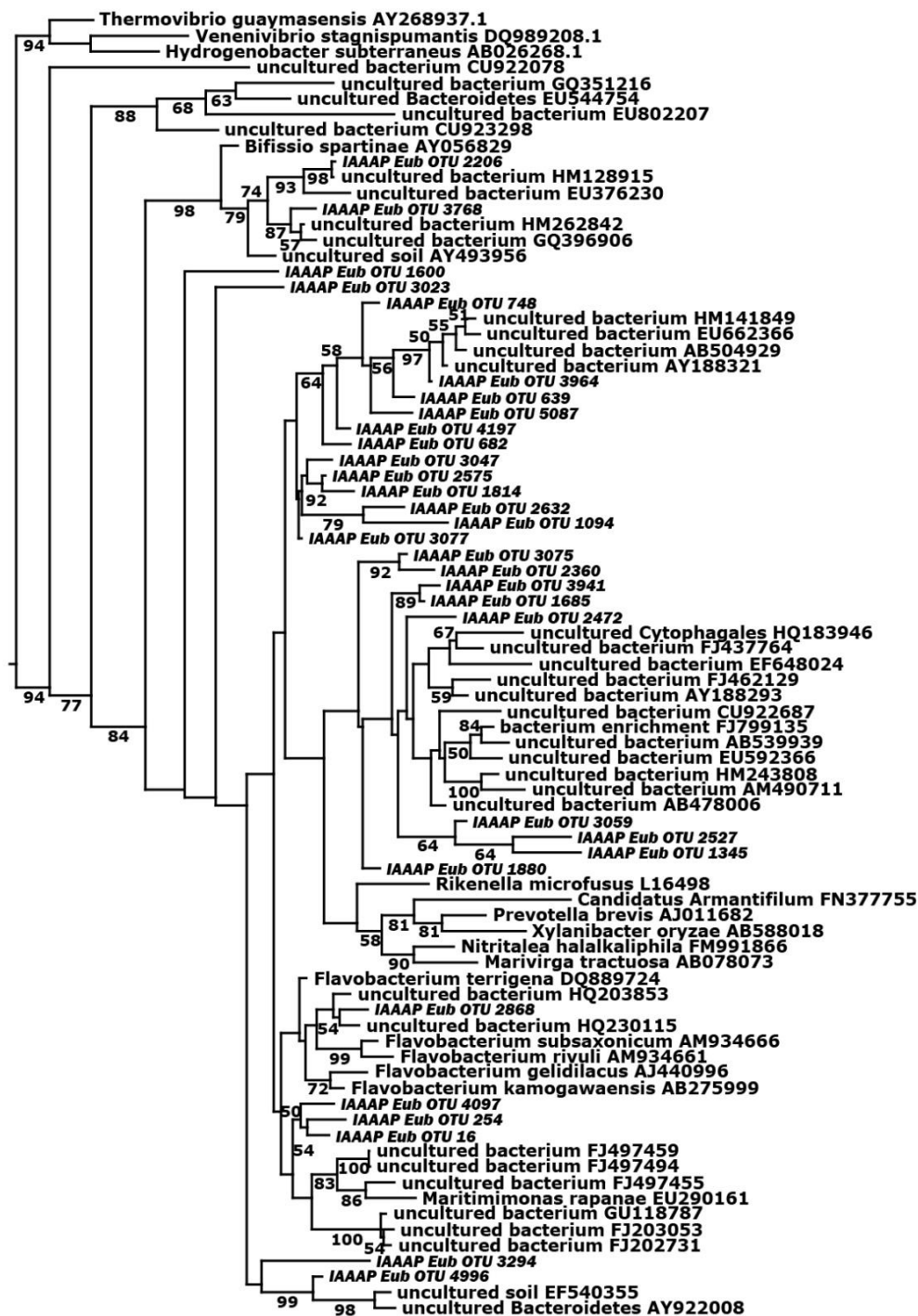
Notes- Labels indicate the well sampled and date of sampling.

Figure 36: Photograph of a denaturing gradient gel used to separate 16S rRNA gene PCR fragments in samples during RDX bioremediation.



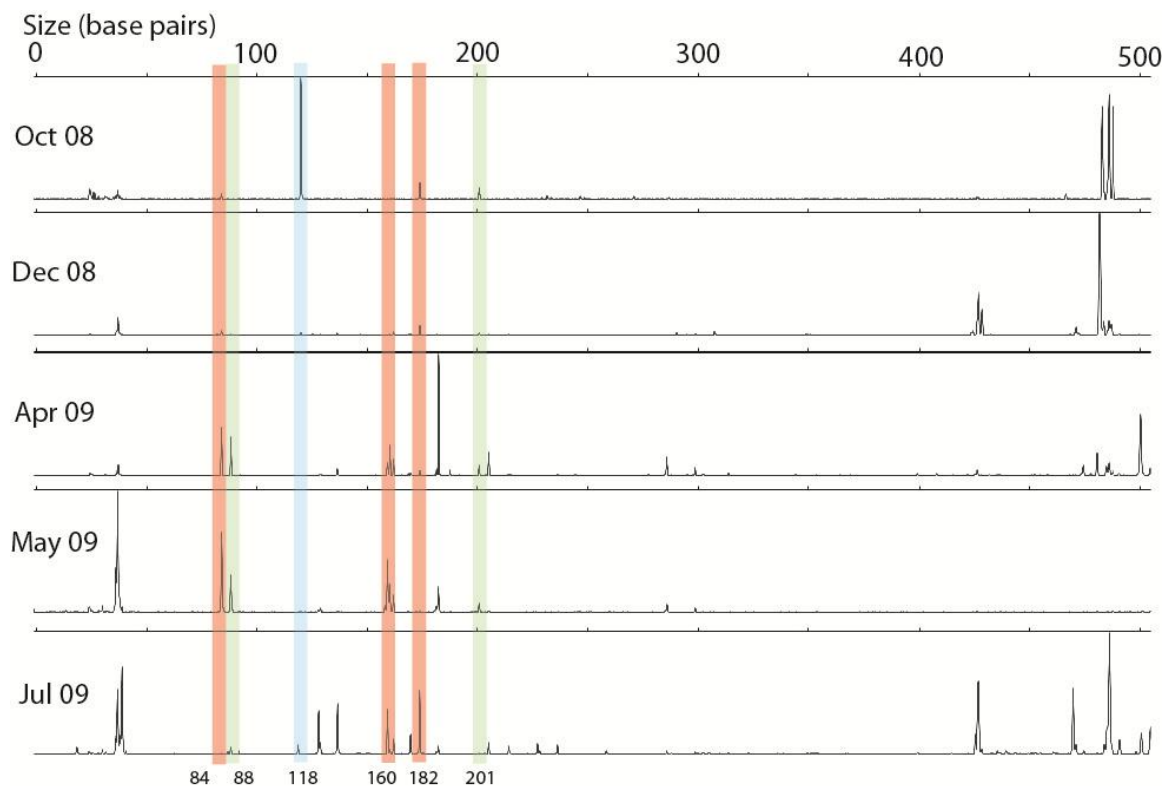
Notes- The alignment was 392 nt in length and optimal substitution model was HKY+G selected using ModelGenerator. Bootstrap values (100 replicates) greater than 50% are shown at the branch.

Figure 37: 16S rRNA gene maximum likelihood phylogeny of Betaproteobacteria pyrosequencing OTU representatives (labeled "IAAAP_Eub_OTU") and reference sequences with Aquificae outgroup.



Notes- The alignment was 622 nt in length and optimal substitution model was GTR+G+I selected using ModelGenerator. Bootstrap values (100 replicates) greater than 50% are shown at the branch.

Figure 38: 16S rRNA gene maximum likelihood phylogeny of Bacteroidetes pyrosequencing OTU representatives (labeled "IAAAP_Eub_OTU") and reference sequences with Aquificae outgroup.



Notes- Pink vertical bars highlight individual TRFs identified as Deltaproteobacteria based upon clone restrictions, the blue bar highlights a Betaproteobacteria TRF, and the green bars Bacteroidetes TRFs. Numbers below colored bars are the size of the corresponding TRF.

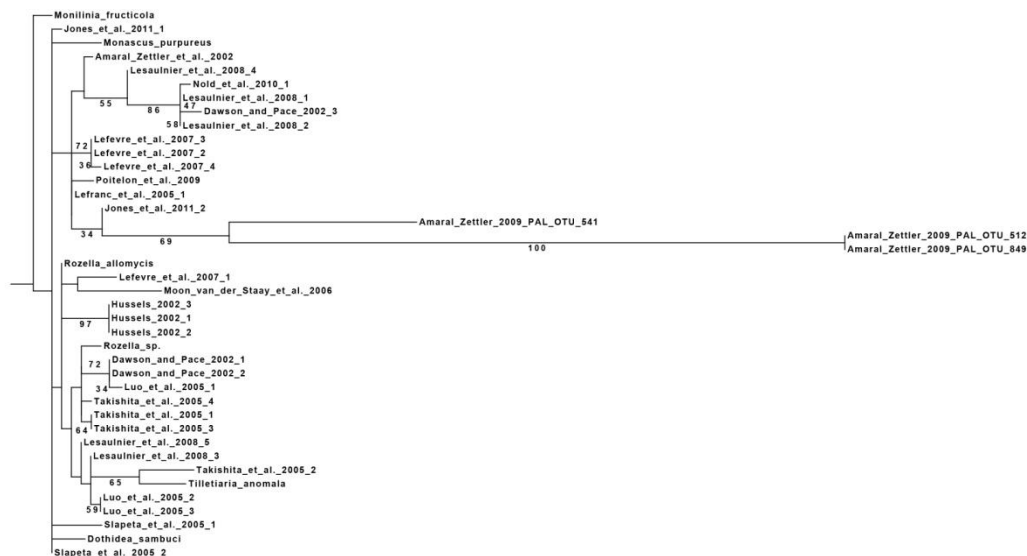
Figure 39: TRF profiles for five time points from well MW309 highlighting Deltaproteobacteria and Bacteroidetes TRFs enriched during RDX bioremediation.

APPENDIX C:
 SUPPLEMENTARY TABLES AND FIGURES FOR CHAPTER V



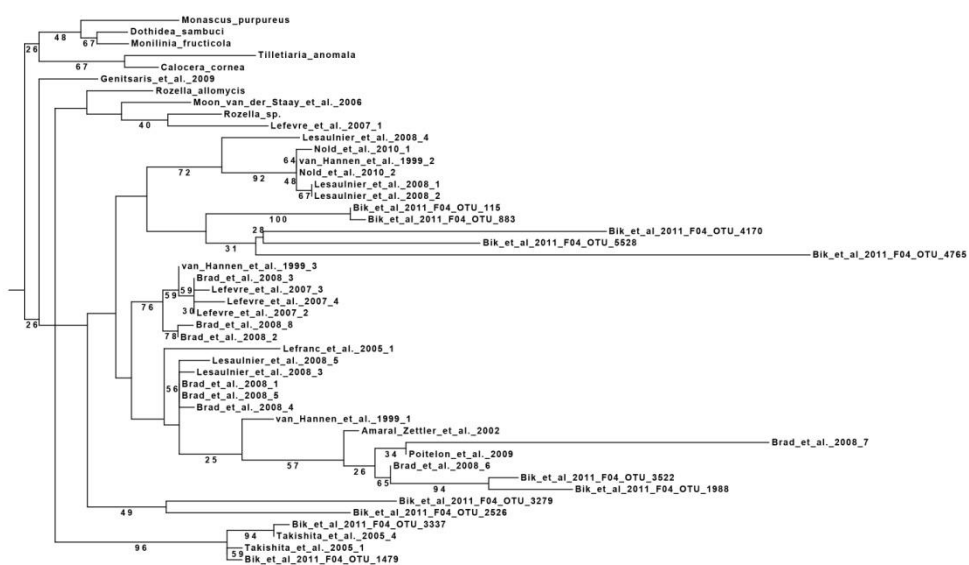
Notes: 109 nucleotide alignment, GTR+I model, 100 bootstraps with values greater than 25 shown at the branch. Tree was rendered in Archaeopteryx. Query sequences are marked "Amaral Zettler 2009 MHB" followed by the OTU number.

Figure 40: PhyML maximum likelihood phylogeny of Cryptomycota reference sequences and prosequencing derived OTUs collected from Mount Hope Bay (11).



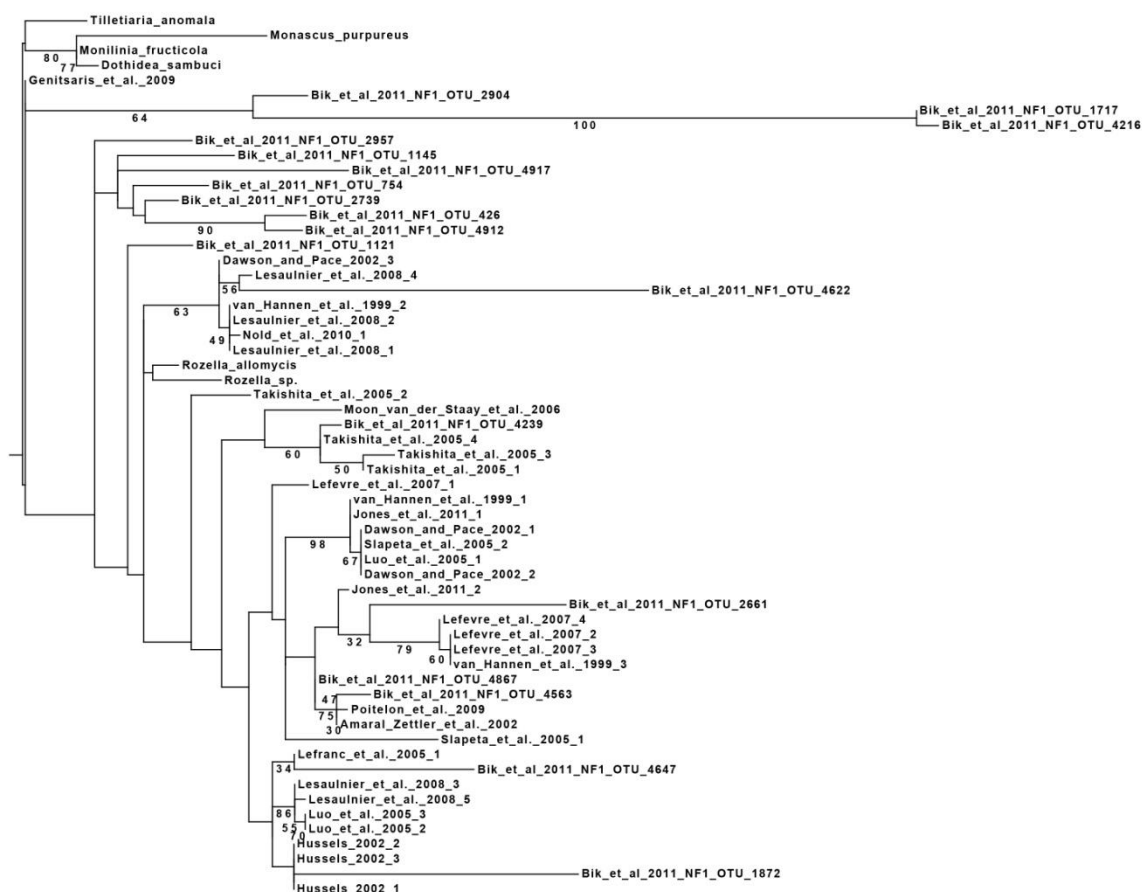
Notes: 119 nucleotide alignment, GTR+I model, 100 bootstraps with values greater than 25 shown at the branch. Tree was rendered in Archaeopteryx. Query sequences are marked "Amaral Zettler 2009 PAL" followed by the OTU number.

Figure 41: PhyML maximum likelihood phylogeny of Cryptomycota reference sequences and pyrosequencing derived OTUs collected from an Antarctic ocean research cruise (11).



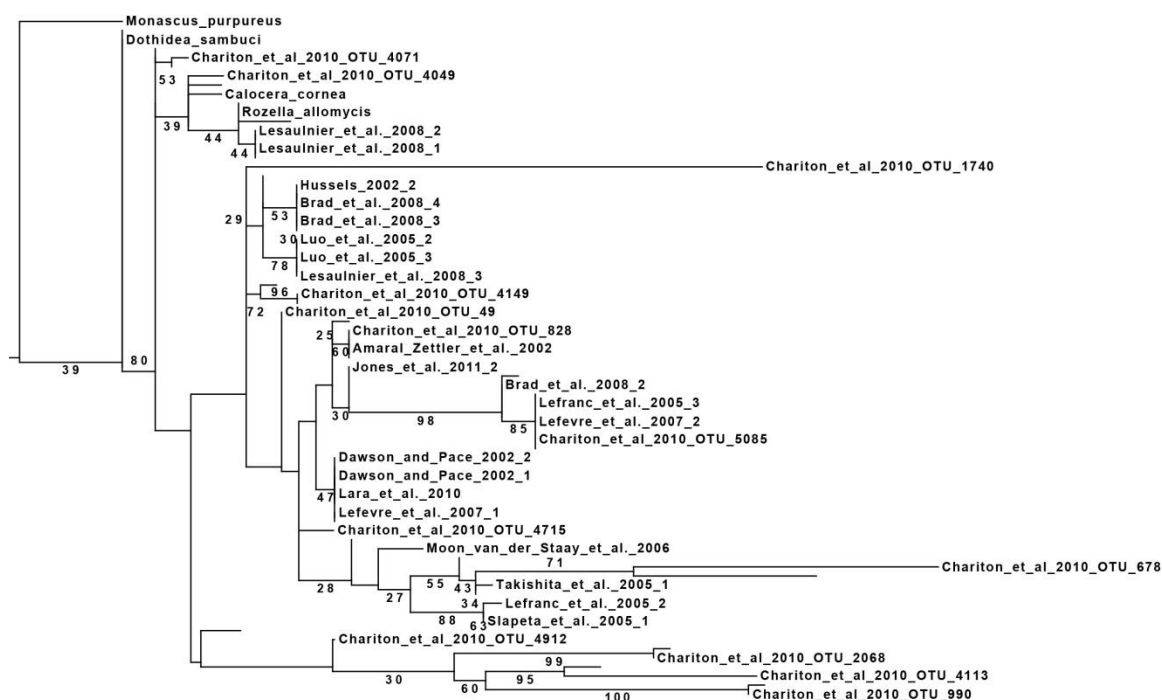
Notes: 273 nucleotide alignment, GTR+I model, 100 bootstraps with values greater than 25 shown at the branch. Tree was rendered in Archaeopteryx. Query sequences are marked "Bik et al 2011 F04" followed by the OTU number.

Figure 42: PhyML maximum likelihood phylogeny of Cryptomycota reference sequences and pyrosequencing derived OTUs collected from deep sea ocean samples (22).



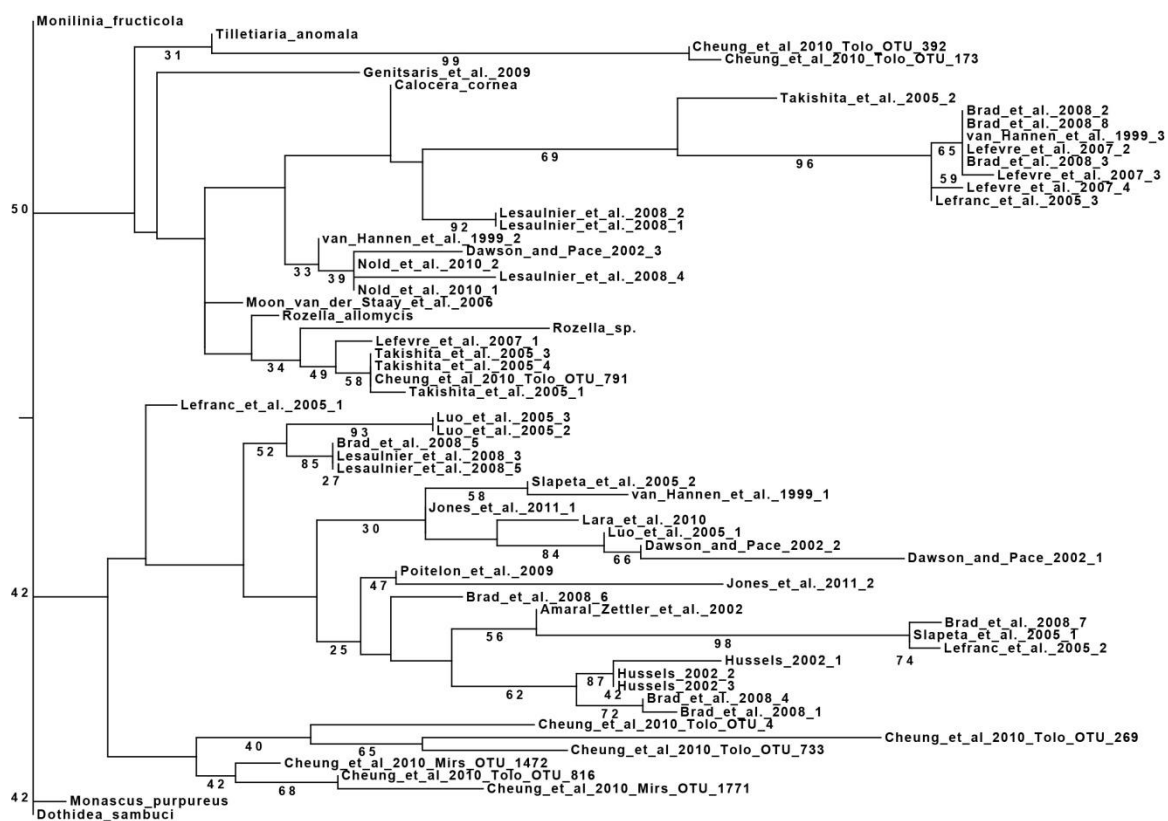
Notes: 222 nucleotide alignment, GTR+I model, 100 bootstrap with values greater than 25 shown at the branch. Tree was rendered in Archaeopteryx. Query sequences are marked "Bik et al 2011 NF1" followed by the OTU number.

Figure 43: PhyML maximum likelihood phylogeny of Cryptomycota reference sequences and pyrosequencing derived OTUs collected from deep sea ocean samples (22).



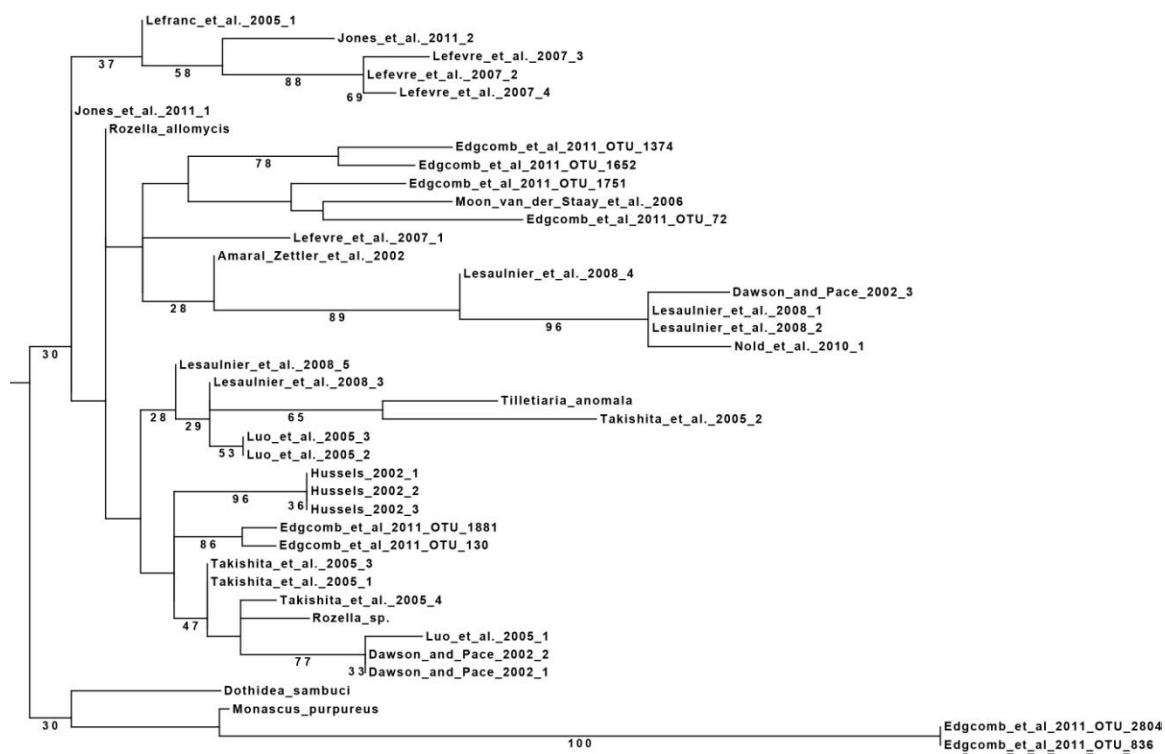
Notes: 123 nucleotide alignment, GTR+I model, 100 bootstrap with values greater than 25 shown at the branch. Tree was rendered in Archaeopteryx. Query sequences are marked "Chariton et al 2010 " followed by the OTU number.

Figure 44: PhyML maximum likelihood phylogeny of Cryptomycota reference sequences and pyrosequencing derived OTUs collected from Sydney Harbor (37).



Notes: 126 nucleotide alignment, GTR+I model, 100 bootstrap with values greater than 25 shown at the branch. Tree was rendered in Archaeopteryx. Query sequences are marked "Cheung et al 2010" followed by the OTU number.

Figure 45: PhyML maximum likelihood phylogeny of Cryptomycota reference sequences and pyrosequencing derived OTUs collected from Mirs Bay and Tolo harbor(39).



Notes: 108 nucleotide alignment, GTR+I model, 100 bootstrap with values greater than 25 shown at the branch. Tree was rendered in Archaeopteryx. Query sequences are marked "Edgcomb et al 2011" followed by the OTU number.

Figure 46: PhyML maximum likelihood phylogeny of Cryptomycota reference sequences and pyrosequencing derived OTUs collected from the Cariaco Basin near Venezuela (56).



Notes: 244 nucleotide alignment, GTR+I model, 100 bootstrap with values greater than 25 shown at the branch. Tree was rendered in Archaeopteryx. Query sequences are marked "Iowa Aquifer" followed by the OTU number.

Figure 47: PhyML maximum likelihood phylogeny of Cryptomycota reference sequences and pyrosequencing derived OTUs collected from an Iowa Aquifer.



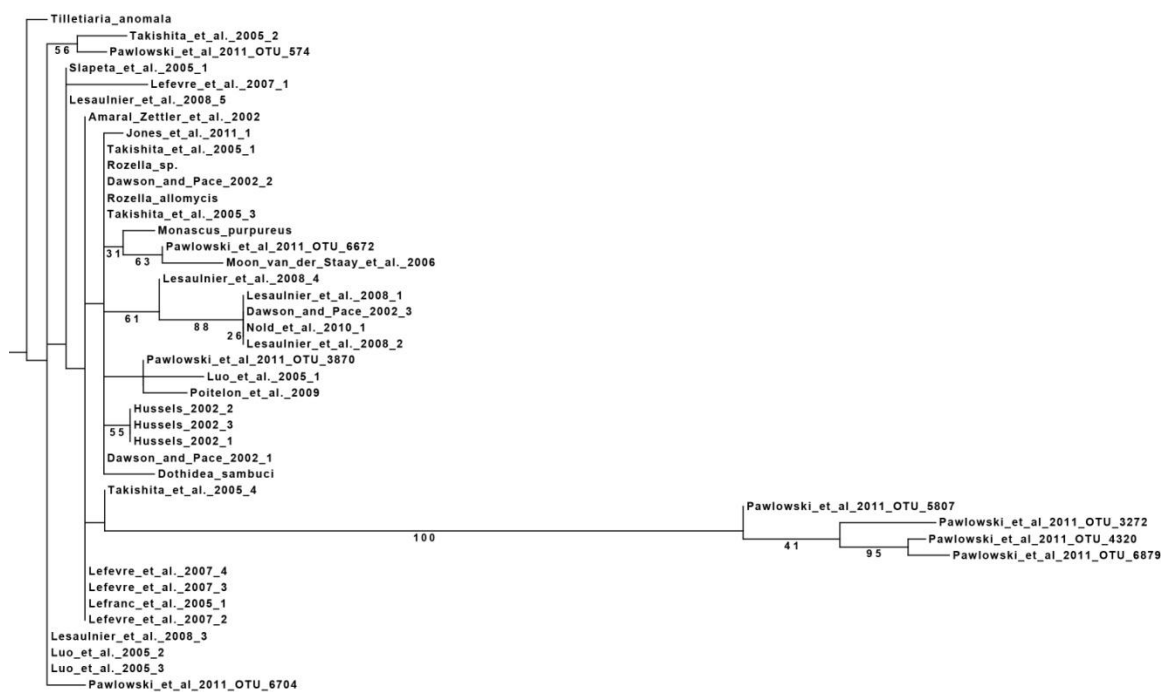
Notes: 244 nucleotide alignment, GTR+I model, 100 bootstrap with values greater than 25 shown at the branch. Tree was rendered in Archaeopteryx. Query sequences are marked "Monchy et al 2011" followed by the OTU number.

Figure 48: PhyML maximum likelihood phylogeny of Cryptomycota reference sequences and pyrosequencing derived OTUs collected from the Wimereux and La Rochelle Coast and Lakes Pavin and Aydat (122).



Notes: 168 nucleotide alignment, GTR+I model, 100 bootstrap with values greater than 25 shown at the branch. Tree was rendered in Archaeopteryx. Query sequences are marked "Nolte et al 2010" followed by the OTU number.

Figure 49: PhyML maximum likelihood phylogeny of Cryptomycota reference sequences and pyrosequencing derived OTUs collected from Lake Fuschlee in Austria (129).



Notes: 108 nucleotide alignment, GTR+I model, 100 bootstrap with values greater than 25 shown at the branch. Tree was rendered in Archaeopteryx. Query sequences are marked "Pawlowski et al 2011" followed by the OTU number.

Figure 50: PhyML maximum likelihood phylogeny of Cryptomycota reference sequences and pyrosequencing derived OTUs collected from the deep sea sediments(135).

APPENDIX D:
ENVIRONMENTAL HEALTH IMPLICATIONS OF WATER
CONTAMINATION WITH THE MUNITIONS CONSTITUENT RDX

Introduction

The U.S. military produces more toxic waste than any other segment of our economy (61). Inevitably, a subset of this waste contaminates soil, surface water, and ground water of military sites and adjacent lands (30). One contaminant of particular interest in Iowa is the munitions explosive hexahydro-1,3,5-trinitro-1,3,5-triazine (RDX). The Iowa Army Ammunition Plant in southwest Iowa is one of few places in the U.S. that the compound has been produced domestically and disposal practices have led to environmental contamination of the base and surrounding lands (2). Known toxicity and suspected carcinogenicity coupled with contamination at numerous U.S. sites has relegated RDX to a place on the priority pollutants list(93). Further exacerbating the RDX contamination problem is the compound's recalcitrance to degradation in natural systems(131). Efforts to eliminate contamination are great with cleanup spending at the Iowa Army Ammunition plant alone exceeding \$39 million (4). Despite the perceived threat to human health justifying extensive cleanup and research spending, little is understood about toxic effects of human exposure to environmentally relevant RDX concentrations. Even less is known about carcinogenic potential of the compound though it is currently treated as a carcinogen(59). This paper will review the public health implications of RDX pollution informed by the state of the knowledge in RDX toxicology and the exposure limits research has led to. I will also discuss extent of RDX contamination in the U.S. compared to recommended exposure limits.

RDX toxicity and recommended concentration limit

For the general U.S. public, the only available route of RDX exposure is by drinking contaminated water. Human oral exposure to RDX is rare, so insights into

human RDX toxicology are based upon a few accidental poisonings and effects on animal models. In one case, five men from Turkey accidentally ingested between 37 and 250 mg/kg RDX (102). As a toxin of the central nervous system (5), the RDX exposed five suffered from seizures accompanied by pain, confusion, headaches, and vomiting among other symptoms. RDX lethal dose to 50% of treatments (LD_{50}) in animals have been reported between 20 to 120 mg/kg in rats, 59 to 97 mg/kg in mice and 100 mg/kg in pigs(5). Comparatively, reports of LD_{50} s for capsaicin (the component of peppers that creates a burning sensation) are 98 to 120 mg/kg in mice (151), reports for arsenicals in mammals are 2.5 to 33 mg/kg(57), and one report for Benzene is 3000 mg/kg in mice(53). Apparently, acute RDX toxicity is comparatively potent indicated by a low LD_{50} and also is quite unpleasant as indicated by seizure induction.

LD_{50} values inform us of how acutely toxic a substance is, but these quantities may not be relevant at concentrations found in environmental media. Perhaps more applicable are studies examining low dose (i.e. chronic exposure). Chronic RDX studies were thoroughly reviewed in Etnier, 1989(58). One informative parameter of long term studies is the no observed adverse effect level (NOAEL) below which negative effects are absent. Levine et al. 1983 reported an NOAEL of 0.3 mg/kg-d in a two year exposure study on Fisher rats(112), and another study reported an NOAEL of 1.5 mg/kg-d in mice exposed for two years(115), while a third two year study indicated no toxicity to rats up to 10 mg/kg-d(76) (results compiled by Etnier, 1989(58)). Though sometimes contradictory, these collective results indicate RDX exhibits chronic mammalian toxicity at relatively low dosages. Additionally, these chronic results form the basis for drinking water standards to prevent human exposure to toxic concentrations.

There is no safe drinking water act mandated maximum contaminant limit (MCL) for RDX in drinking water. Rather, the EPA directs a lifetime health advisory concentration of 2 $\mu\text{g/L}$ (ppb) (59). In terms of scale, this amount would be roughly equivalent to a large drop of pure RDX in a volume of water the size of a gasoline tanker

truck. This is considered to be the concentration below which negative health effects will be unobservable. For public health protection, the advisory limit is extremely important in determining when an incidence of contamination is of concern and for establishing treatment goals. Because the single value of 2 µg/L is so important for decision making, it is critical we understand the kind of data and assumptions used for its derivation.

The process of establishing the RDX lifetime health advisory was summarized in Etnier and Hartley, 1990 (59). Underlying the process is extrapolation of human effects from above described animal toxicology studies while integrating conservative assumptions to account for uncertainty accumulated during transfer of relevance between the animal model and humans. The first step is establishing an NOAEL reference dose for humans. For RDX the EPA selected an NOAEL dose of **0.3 mg/kg-d** based on the chronic fisher rat exposure study in Levine et al. 1983 (112). Next, a conservative and error mitigating 100 fold safety factor was applied yielding a human reference dose of **0.003 mg/kg-d**(59). Assuming an average human size of 70 kg and water intake of 2 liters per day, a water concentration corresponding to this dose can be calculated as:

$$(0.003 \text{ mg/kg-d} \times 70 \text{ kg}) / (2 \text{ L/d}) = \mathbf{0.105 \text{ mg/L}} \text{ (59)}$$

Finally, the EPA determined there was evidence to indicate that RDX was a possible carcinogen(115) so another 10 fold safety factor was applied in addition to a relative source contribution factor (RSC) of 0.2. This relative source contribution implies and assumes that a given receptor receives only 20% of chemical exposure from drinking water with 80% additional exposure from unmeasured factors including food and air. The final calculation is as follows:

$$0.105 \text{ mg/L} \times 0.2 \text{ (RSC)} / 10 \text{ (Carcinogen SF)} = 0.002 \text{ mg/L} = \mathbf{2 \mu\text{g/L}} \text{ (59)}$$

This final recommendation serves as the guiding factor for regulation and action. Given the economic implications of regulation and action activities, the derived value of

2 µg/L deserves scrutiny. When compared to values pulled directly from animal toxicology studies, the 2 µg/L recommendation incorporates a **5000 fold** safety factor. Parts of the safety factor are unrealistic and removing them would provide a more accurate idea of a safe concentration for human exposure. First, the relative source contribution (RSC) factor is unnecessary because human exposure to RDX in the environment is almost exclusively from aquatic sources with only oral exposure significant(5) and RDX does not bioaccumulate in aquatically exposed food sources (i.e. fish) indicating that food probably is not a significant source(18). Second, classification of RDX as a carcinogen at relevant concentrations is dubious as most chronic studies indicated no evidence of increased tumors (1, 3, 76, 112), and the single study supporting carcinogen status(115) was criticized by Etnier 1989(58) as inadequate to substantiate carcinogenicity because of, “the absence of an adequate dose-response curve, the high mortality rate recorded at the highest concentration tested, and contamination with HMX, as well as the absence of any other supporting data.” Finally, the 100 fold safety factor seems excessive given that the chosen reference NOAEL of 0.3 mg/kg-d is the most conservative observed with all RDX NOAEL’s varying over three orders of magnitude (0.3 to 100 mg/kg-d (5)). A 50 fold safety factor is still very conservative and probably adequate. Applying all these adjustments would indicate that, realistically and conservatively, a water concentration of 100 µg/L is definitely safe for human consumption and a water concentration of 500 µg/L is probably safe for human consumption.

Typical U.S. contamination conditions and comparison to
recommended limits

Given that the most probable human exposure route to RDX is oral(5), the most relevant media are surface and ground waters that could be used as a drinking source. Also, the majority of RDX environmental contamination originates from military

installations such as packing plants, depots, and firing ranges (5). Based on these two facts, examination of contaminant concentration in discharges from these facilities and their surrounding water bodies will give an indication of theoretical maximum exposures. Approximately 18 U.S. military sites throughout the U.S. are suspected of having RDX contamination(30). Table 6 is a summary of some reported maximum concentrations in facility discharges, surrounding surface waters, and surrounding groundwater. These values represent what we expect to typically find near origination points.

Table 6: Reported Maximum RDX concentrations at some U.S. Military facilities

Site	Discharge Concentration	Groundwater Concentration	Surface water Concentration	Source
Cornhusker Army Ammunition Plant		340 µg/L		(124)
Iowa Army Ammunition Plant		30 µg/L	22 µg/L	(2)
Joilet Army Ammunition Plant	145 µg/L			(162)
Lonestar Army Ammunition Plant		4.5 µg/L		(173)
Louisiana Army Ammunition Plant	14 mg/L	13 mg/L		(5)
Milan Army Ammunition Plant	145 µg/L	30 µg/L		(8, 27)
Savanna Army Depot			37 mg/L	(5)

Every one of these sites exceeds recommended concentrations of 2 µg/L. Indeed, each one of these facilities has undergone some remedial action to remove contamination to concentrations to below acceptable levels [see table references]. The highest reported concentration was 37 mg/L (ppm) in a surface water body at the Savanna Army Depot near Savanna, Illinois. If the average human consumed this water, their dose would be 1.06 mg/kg-d. This is below the NOAEL in most test animals (5), but is too high by any measure when considering safety factors for the protection of the most sensitive

individuals in the human population. The lowest maximum concentration measured was 4.5 µg/L in groundwater at the Lonestar Ammunition plant in Texas.

While all of the measured values in table 6 are considered unacceptable for human consumption, the reality is that little to no human reception of this contamination occurs(5). The military is aware of the contamination, and any citizens that might be exposed are given alternative water sources. For example, citizens near the Iowa Army Ammunition plant were connected to a rural water system to dis-incentivize drilling unregulated shallow wells. Additionally, if we choose to believe my assertion that any exposure to concentrations below 100 µg/L is safe for human consumption, most of the observed contamination would be considered safe. Indeed, the reported concentrations range from 4.5 µg/L to 37,000 µg/L which straddles the discrepancy between what the EPA says is safe (2µg/L) and what I have argued is safe (100 µg/L). What we must recognize from this is that assumptions used to derive a regulatory limit will substantially affect the kind of action we take for a given instance of contamination. Had the EPA concluded that RDX is not a potential carcinogen, then it is likely that no remedial action would have been taken at three of the seven sites listed in table 6 (Three sites had concentrations below 100 µg/L).

Regardless of my argument, we probably should follow the 2 µg/L limit recommended by the EPA because the total weight of evidence is small. For example, there is no epidemiological data because of how few humans are exposed, and there are few chronic toxicology studies in larger mammals because these studies are expensive. Additionally, there are a large number of by-products produced from RDX degradation (42). The toxic and carcinogenic status of most of these is unknown. I argued that RDX (alone) is safe above 100 µg/L, but we have no idea of the safety of RDX degradation by-products or their safety in a mutual mixture. What is obvious, however, is that an easy way to limit the total concentration of by-products is to limit the concentration of RDX.

Ultimately, confidently determining the long term health effects of RDX and all degradation products as well as health interactions with other chemicals might prove more costly than simply removing the RDX. We know RDX is toxic at sufficient concentrations both acutely and chronically, and it seems reasonable to expunge toxic and artificial compounds from our natural resources. Additionally, it is clear that in the absence of sufficient data, a guiding number like the lifetime health advisory is rendered arbitrary through allowance of variation over orders of magnitude depending on application of assumptions. Perhaps rather than a limit or number it might be more useful simply to recommend, “Remove as much of this contaminant as possible,” rather than concerning ourselves with a variable number telling us how much is safe.

REFERENCES

1. 1975, posting date. The Acute and Chronic Biochemical and Behavioral Effects of Cyclotrimethylenetrinitramine. Ft. Belvoir Defense Technical Information Center. [Online.]
2. 1999. Public Health Assessment: Iowa Army Ammunition Plant. *In* ATSDR (ed.).
3. 1974, posting date. Subacute Toxicity of RDX and TNT in Monkeys. Ft. Belvoir Defense Technical Information Center. [Online.]
4. 2004. Tetra Tech Wins \$39 Million Iowa Army Ammunition Plant Environmental Program., Business Wire, vol. July 28, 2004. Berkshire-Hathaway.
5. 1995. Toxicological profile for RDX. U.S. Dept. of Health and Human Services, Public Health Service, Agency for Toxic Substances and Disease Registry, [Atlanta, Ga.].
6. 2009. Unidirectional Sequencing of Amplicon Libraries Using GS FLX Titanium emPCR Kits (Lib-L). *In* Roche (ed.). 454 Life Sciences Corp., a Roche Company, Branford, CT.
7. 2009. Using Multiplex Identifier (MID) Adaptors for the GS FLX Titanium Chemistry - Extended MID Set. 454 Life Sciences Corp., a Roche Company, Branford, CT.
8. 2002. Wildlife Toxicity Assessment for RDX. U.S Army Center for Health Promotion and Preventive Medicine.
9. **Altschul, S. F., W. Gish, W. Miller, E. W. Myers, and D. J. Lipman.** 1990. Basic Local Alignment Search Tool. *J Mol Biol* **215**:403-410.
10. **Altschul, S. F., T. L. Madden, A. A. Sch  ffer, J. Zhang, Z. Zhang, W. Miller, and D. J. Lipman.** 1997. Gapped BLAST and PSI-BLAST: a new generation of protein database search programs. *Nucleic Acids Research* **25**:3389-3402.
11. **Amaral-Zettler, L. A., E. A. McCliment, H. W. Ducklow, and S. M. Huse.** 2009. A Method for Studying Protistan Diversity Using Massively Parallel Sequencing of V9 Hypervariable Regions of Small-Subunit Ribosomal RNA Genes. *Plos One* **4**.
12. **Amaral Zettler, L. A., F. Gomez, E. Zettler, B. G. Keenan, R. Amils, and M. L. Sogin.** 2002. Microbiology: Eukaryotic diversity in Spain's River of Fire. *Nature* **417**:137-137.
13. **Anderson, R. T., H. A. Vrionis, I. Ortiz-Bernad, C. T. Resch, P. E. Long, R. Dayvault, K. Karp, S. Marutzky, D. R. Metzler, A. Peacock, D. C. White, M. Lowe, and D. R. Lovley.** 2003. Stimulating the in situ activity of geobacter species to remove uranium from the groundwater of a uranium-contaminated aquifer. *Appl. Environ. Microbiol.* **69**:5884-5891.

14. **Anderson, W. I.** 1998. Iowa's geological past : three billion years of earth history. University of Iowa Press, Iowa City.
15. **Arndt, H., F. Scheckenbach, C. Wylezich, A. P. Mylnikov, and M. Weitere.** 2006. Molecular comparisons of freshwater and marine isolates of the same morphospecies of heterotrophic flagellates. *Appl Environ Microbiol* **72**:6638-6643.
16. **Arnett, C. M., N. R. Adrian, D. B. Ringelberg, N. A. Wesslund, and K. N. Yenser.** 2009. Sulfate-Mediated Bacterial Population Shift in a Hexahydro-1,3,5-trinitro-1,3,5-triazine (RDX)-Degrading Anaerobic Enrichment Culture. *Bioremediation Journal* **13**:52-63.
17. **Baldauf, S. L., M. Carr, B. S. C. Leadbeater, R. Hassan, and M. Nelson.** 2008. Molecular phylogeny of choanoflagellates, the sister group to Metazoa. *Proc Natl Acad Sci USA* **105**:16641-16646.
18. **Belden, J. B., G. R. Lotufo, and M. J. Lydy.** 2005. Accumulation of hexahydro-1,3,5-trinitro-1,3,5-triazine in channel catfish (*Ictalurus punctatus*) and aquatic oligochaetes (*Lumbriculus variegatus*). *Environmental Toxicology and Chemistry* **24**:1962-1967.
19. **Berger, W. H., and F. L. Parker.** 1970. Diversity of Planktonic Foraminifera in Deep-Sea Sediments. *Science* **168**:1345-&.
20. **Bernardet, J. F., Y. Nakagawa, B. Holmes, and Subcommittee.** 2002. Proposed minimal standards for describing new taxa of the family Flavobacteriaceae and emended description of the family. *Int. J. Syst. Evol. Micr.* **52**:1049-1070.
21. **Bibby, K., E. Viau, and J. Peccia.** 2010. Pyrosequencing of the 16S rRNA gene to reveal bacterial pathogen diversity in biosolids. *Water Res.* **44**:4252-4260.
22. **Bik, H. M., W. A. Y. Sung, P. De Ley, J. G. Baldwin, J. Sharma, A. Rocha-Olivares, and W. K. Thomas.** 2011. Metagenetic community analysis of microbial eukaryotes illuminates biogeographic patterns in deep-sea and shallow water sediments. *Molecular Ecology*:no-no.
23. **Bouwer, E. J., and B. E. Rittmann.** 1992. Comment on: Use of Colloid Filtration Theory in Modeling Movement of Bacteria through a Contaminated Sandy Aquifer. *Environmental Science & Technology* **26**:400-401.
24. **Brad, T., M. Braster, B. M. van Breukelen, N. M. van Straalen, and W. F. M. Roling.** 2008. Eukaryotic diversity in an anaerobic aquifer polluted with landfill leachate. *Applied and Environmental Microbiology* **74**:3959-3968.
25. **Brate, J., R. Logares, C. Berney, D. K. Ree, D. Klaveness, K. S. Jakobsen, and K. Shalchian-Tabrizi.** 2010. Freshwater Perkinsea and marine-freshwater colonizations revealed by pyrosequencing and phylogeny of environmental rDNA. *ISME J* **4**:1144-1153.
26. **Breiman, L.** 2001. Random Forests. *Machine Learning* **45**:5-32.
27. **Bricka, M. R., and W. Sharp.** 1992. Presented at the Water Forum 1992, Baltimore, ME.

28. **Canfield, D. E., R. Raiswell, and S. H. Bottrell.** 1992. The reactivity of sedimentary iron minerals toward sulfide. *Am J Sci* **292**:659-683.
29. **Caporaso, G., J. Kuczynski, J. Stombaugh, K. Bittinger, F. Bushman, E. Costello, N. Fierer, A. Pena, J. Goodrich, J. Gordon, G. Huttley, S. Kelley, D. Knights, J. Koenig, R. Ley, C. Lozupone, D. McDonald, B. Muegge, M. Pirrung, J. Reeder, J. Sevinsky, P. Turnbaugh, W. Walters, J. Widmann, T. Yatsunenko, J. Zaneveld, and R. Knight.** 2010. QIIME allows analysis of high-throughput community sequencing data. *Nat Methods* **7**:335-336.
30. **Card, R. E., and R. Autenrieth** 1998, posting date. Treatment of HMX and RDX contamination. Amarillo, TX : Amarillo National Resource Center for Plutonium. [Online.]
31. **Cavalier-Smith, T.** 2009. Megaphylogeny, cell body plans, adaptive zones: causes and timing of eukaryote basal radiations. *J Eukaryot Microbiol* **56**:26-33.
32. **Cavalier-Smith, T., R. Lewis, E. E. Chao, B. Oates, and D. Bass.** 2009. *Helkesimastix marina* n. sp. (Cercozoa: Sainouroidea superfam. n.) a Gliding Zooflagellate of Novel Ultrastructure and Unusual Ciliary Behaviour. *Protist* **160**:452-479.
33. **Cavalier-Smith, T., and S. von der Heyden.** 2007. Molecular phylogeny, scale evolution and taxonomy of centrohelid heliozoa. *Mol Phylogenet Evol* **44**:1186-1203.
34. **Ceceres, C. E.** 1997. Dormancy in Invertebrates. *Invertebrate Biology* **116**:371-383.
35. **Chang, Y.-J., P. E. Long, R. Geyer, A. D. Peacock, C. T. Resch, K. Sublette, S. Pfiffner, A. Smithgall, R. T. Anderson, H. A. Vrionis, J. R. Stephen, R. Dayvault, I. Ortiz-Bernad, D. R. Lovley, and D. C. White.** 2005. Microbial incorporation of ¹³C-labeled acetate at the field Scale: detection of microbes responsible for reduction of U(VI). *Environ. Sci. Technol.* **39**:9039-9048.
36. **Charbeneau, R. J., P. B. Bedient, and R. C. Loehr.** 1992. Groundwater remediation. Technomic Pub. Co., Lancaster [Pa.].
37. **Chariton, A. A., L. N. Court, D. M. Hartley, M. J. Colloff, and C. M. Hardy.** 2010. Ecological assessment of estuarine sediments by pyrosequencing eukaryotic ribosomal DNA. *Frontiers in Ecology and the Environment* **8**:233-238.
38. **Chatelliers, M. C. D., J. Juget, M. Lafont, and P. Martin.** 2009. Subterranean aquatic Oligochaeta. *Freshwater Biology* **54**:678-690.
39. **Cheung, M. K., C. H. Au, K. H. Chu, H. S. Kwan, and C. K. Wong.** 2010. Composition and genetic diversity of picoeukaryotes in subtropical coastal waters as revealed by 454 pyrosequencing. *ISME J* **4**:1053-1059.
40. **Coleman, N. V., J. C. Spain, and T. Duxbury.** 2002. Evidence that RDX biodegradation by *Rhodococcus* strain DN22 is plasmid-borne and involves a cytochrome p-450. *Journal of Applied Microbiology* **93**:463-472.

41. **Crawford, R. L., and D. L. Crawford.** 1996. Bioremediation principles and applications. Cambridge University Press, Cambridge; New York.
42. **Crocker, F., K. Indest, and H. Fredrickson.** 2006. Biodegradation of the cyclic nitramine explosives RDX, HMX, and CL-20. *Appl Microbiol Biotechnol* **73**:274-290.
43. **Crosby, L. D., and C. S. Criddle.** 2003. Understanding bias in microbial community analysis techniques due to rrn operon copy number heterogeneity. *Biotechniques* **34**:790-+.
44. **Culman, S., R. Bukowski, H. Gauch, H. Cadillo-Quiroz, and D. Buckley.** 2009. T-REX: software for the processing and analysis of T-RFLP data. *BMC Bioinformatics* **10**:171.
45. **Cupples, A.** 2010. Final Report: Development of biomarkers for assessing in situ RDX biodegradation potential ER-1606. Strategic Environmental Research and Development Program.
46. **Dale, V. H., and S. C. Beyeler.** 2001. Challenges in the development and use of ecological indicators. *Ecol Indic* **1**:3-10.
47. **Dave, G., E. Nilsson, and A. Wernersson.** 2000. Sediment and water-phase toxicity and UV-activation of six chemicals used in military explosives. *Aquat Ecosys Health Manag* **3**:291-299.
48. **Davis, J. L., A. H. Wani, B. R. O'Neal, and L. D. Hansen.** 2004. RDX biodegradation column study: comparison of electron donors for biologically induced reductive transformation in groundwater. *J. Hazard. Mater.* **112**:45-54.
49. **Deharveng, L., F. Stoch, J. Gibert, A. Bedos, D. Galassi, M. Zgmajer, A. Brancelj, A. Camacho, F. Fiers, P. Martin, N. Giani, G. Magniez, and P. Marmonier.** 2009. Groundwater biodiversity in Europe. *Freshwater Biology* **54**:709-726.
50. **DeSantis, T. Z., P. Hugenholtz, N. Larsen, M. Rojas, E. L. Brodie, K. Keller, T. Huber, D. Dalevi, P. Hu, and G. L. Andersen.** 2006. Greengenes, a chimera-checked 16S rRNA gene database and workbench compatible with ARB. *Appl. Environ. Microbiol.* **72**:5069-5072.
51. **Diez, B., C. Pedros-Alio, T. L. Marsh, and R. Massana.** 2001. Application of Denaturing Gradient Gel Electrophoresis (DGGE) To Study the Diversity of Marine Picoeukaryotic Assemblages and Comparison of DGGE with Other Molecular Techniques. *Applied and Environmental Microbiology* **67**:2942-2951.
52. **Dole-Olivier, M. J., F. Castellarini, N. Coineau, D. M. P. Galassi, P. Martin, N. Mori, A. Valdecasas, and J. Gibert.** 2009. Towards an optimal sampling strategy to assess groundwater biodiversity: comparison across six European regions. *Freshwater Biology* **54**:777-796.
53. **Drew, R. T., and J. R. Fouts.** 1974. The lack of effects of pretreatment with phenobarbital and chlorpromazine on the acute toxicity of benzene in rats. *Toxicology and Applied Pharmacology* **27**:183-193.

54. **Eddy, S. R.** 1998. Profile hidden Markov models. *Bioinformatics* **14**:755-763.
55. **Edgar, R. C.** 2010. Search and clustering orders of magnitude faster than BLAST. *Bioinformatics* **26**:2460-2461.
56. **Edgcomb, V., W. Orsi, J. Bunge, S. Jeon, R. Christen, C. Leslin, M. Holder, G. T. Taylor, P. Suarez, R. Varela, and S. Epstein.** 2011. Protistan microbial observatory in the Cariaco Basin, Caribbean. I. Pyrosequencing vs Sanger insights into species richness. *Isme Journal* **5**:1344-1356.
57. **Eisler, R.** 2004. Arsenic Hazards to Humans, Plants, and Animals from Gold Mining, p. 133-165, *Reviews of Environmental Contamination and Toxicology*.
58. **Etnier, E. L.** 1989. Water quality criteria for hexahydro-1,3,5-trinitro-1,3,5-triazine (RDX). *Regulatory Toxicology and Pharmacology* **9**:147-157.
59. **Etnier, E. L., and W. R. Hartley.** 1990. Comparison of Water-Quality Criterion and Lifetime Health Advisory for Hexahydro-1,3,5-Trinitro-1,3,5-Triazine (Rdx). *Regulatory Toxicology and Pharmacology* **11**:118-122.
60. **Euringer, K., and T. Lueders.** 2008. An optimised PCR/T-RFLP fingerprinting approach for the investigation of protistan communities in groundwater environments. *Journal of Microbiological Methods* **75**:262-268.
61. **Feldman, B.** 2003. *War on The Earth, Dollars & Sense*.
62. **Fischer, S. G., and L. S. Lerman.** 1983. DNA Fragments Differing By Single Base-Pair Substitutions are Separated in Denaturing Gradient Gels- Correspondence with Melting Theory. *Proceedings of the National Academy of Sciences of the United States of America-Biological Sciences* **80**:1579-1583.
63. **Frickey, T., and A. Lupas.** 2004. CLANS: a Java application for visualizing protein families based on pairwise similarity. *Bioinformatics* **20**:3702-3704.
64. **Frickey, T., and G. Weiller.** 2007. Analyzing microarray data using CLANS. *Bioinformatics* **23**:1170-1171.
65. **Fuller, M. E., K. McClay, M. Higham, P. B. Hatzinger, and R. J. Steffan.** 2010. Hexahydro-1,3,5-trinitro-1,3,5-triazine (RDX) bioremediation in groundwater: Are known RDX-degrading bacteria the dominant players? *Bioremediation Journal* **14**:121-134.
66. **Galassi, D. M. P., R. Huys, and J. W. Reid.** 2009. Diversity, ecology and evolution of groundwater copepods. *Freshwater Biology* **54**:691-708.
67. **Galtier, N., M. Gouy, and C. Gautier.** 1996. SEAVIEW and PHYLO_WIN: two graphic tools for sequence alignment and molecular phylogeny. *Comput Appl Biosci* **12**:543-548.
68. **Gibert, J., and D. C. Culver.** 2009. Assessing and conserving groundwater biodiversity: an introduction. *Freshwater Biology* **54**:639-648.

69. **Gini, C.** 1912. Variability and mutability, contribution to the study of statistical distributions and relations. Studi Economico-Giuricici della R. Universita de Cagliari.
70. **Gouy, M., S. Guindon, and O. Gascuel.** 2010. SeaView version 4: A multiplatform graphical user interface for sequence alignment and phylogenetic tree building. *Mol. Biol. Evol.* **27**:221-224.
71. **Gregory, K. B., P. Larese-Casanova, G. F. Parkin, and M. M. Scherer.** 2004. Abiotic transformation of hexahydro-1,3,5-trinitro-1,3,5-triazine by ferric iron bound to magnetite. *Environmental Science & Technology* **38**:1408-1414.
72. **Griebler, C., and T. Lueders.** 2009. Microbial biodiversity in groundwater ecosystems. *Freshwater Biology* **54**:649-677.
73. **Guindon, S., F. Delsuc, J. F. Dufayard, and O. Gascuel.** 2009. Estimating maximum likelihood phylogenies with PhyML. *Methods mol bio* **537**:113-37.
74. **Haas, B. J., D. Gevers, A. M. Earl, M. Feldgarden, D. V. Ward, G. Giannoukos, D. Ciulla, D. Tabbaa, S. K. Highlander, E. Sodergren, B. Methe, T. Z. DeSantis, T. H. M. Consortium, J. F. Petrosino, R. Knight, and B. W. Birren.** 2011. Chimeric 16S rRNA sequence formation and detection in Sanger and 454-pyrosequenced PCR amplicons. *Genome Res.* **21**:494-504.
75. **Harper, D. M.** 1992. Eutrophication of freshwaters : principles, problems, and restoration, 1st ed. Chapman & Hall, London ; New York.
76. **Hart, E. R.** 1976. Two-year feeding study in rats. Litton Bionetics, Kensington, Md.
77. **Harvey, R. W., and S. Garabedian.** 1992. Use of Colloid Filtration Theory in Modeling Movement of Bacteria through a Contaminated Sandy Aquifer - Reply. *Environmental Science & Technology* **26**:401-402.
78. **Harvey, R. W., and S. P. Garabedian.** 1991. Use of Colloid Filtration Theory in Modeling Movement of Bacteria through a Contaminated Sandy Aquifer. *Environmental Science & Technology* **25**:178-185.
79. **Hawari, J., A. Halasz, T. Sheremata, S. Beaudet, C. Groom, L. Paquet, C. Rhofir, G. Ampleman, and S. Thiboutot.** 2000. Characterization of metabolites during biodegradation of hexahydro-1,3,5-trinitro-1,3,5-triazine (RDX) with municipal anaerobic sludge. *Applied and Environmental Microbiology* **66**:2652-2657.
80. **Heck, K. L., G. Vanbelle, and D. Simberloff.** 1975. Explicit calculation of rarefaction diversity measurement and determination of sufficient sample size. *Ecology* **56**:1459-1461.
81. **Hedrich, S., M. Schlomann, and D. B. Johnson.** 2011. The iron-oxidizing proteobacteria. *Microbiology-Sgm* **157**:1551-1564.

82. **Hibbett, D. S., M. Binder, J. F. Bischoff, M. Blackwell, P. F. Cannon, O. E. Eriksson, S. Huhndorf, T. James, P. M. Kirk, R. Lücking, H. Thorsten Lumbsch, F. Lutzoni, P. B. Matheny, D. J. McLaughlin, M. J. Powell, S. Redhead, C. L. Schoch, J. W. Spatafora, J. A. Stalpers, R. Vilgalys, M. C. Aime, A. Aptroot, R. Bauer, D. Begerow, G. L. Benny, L. A. Castlebury, P. W. Crous, Y.-C. Dai, W. Gams, D. M. Geiser, G. W. Griffith, C. Gueidan, D. L. Hawksworth, G. Hestmark, K. Hosaka, R. A. Humber, K. D. Hyde, J. E. Ironside, U. Kõljalg, C. P. Kurtzman, K.-H. Larsson, R. Lichtwardt, J. Longcore, J. Miadlikowska, A. Miller, J.-M. Moncalvo, S. Mozley-Standridge, F. Oberwinkler, E. Parmasto, V. Reeb, J. D. Rogers, C. Roux, L. Ryvarden, J. P. Sampaio, A. Schüßler, J. Sugiyama, R. G. Thorn, L. Tibell, W. A. Untereiner, C. Walker, Z. Wang, A. Weir, M. Weiss, M. M. White, K. Winka, Y.-J. Yao, and N. Zhang.** 2007. A higher-level phylogenetic classification of the Fungi. *Mycol Res* **111**:509-547.
83. **Holmes, D. E., R. A. O'Neil, H. A. Vronis, L. A. N'Guessan, I. Ortiz-Bernad, M. J. Larrahondo, L. A. Adams, J. A. Ward, J. S. Nicoll, K. P. Nevin, M. A. Chavan, J. P. Johnson, P. E. Long, and D. R. Lovley.** 2007. Subsurface clade of Geobacteraceae that predominates in a diversity of Fe(III)-reducing subsurface environments. *ISME J* **1**:663-677.
84. **Holzmann, M., A. Habura, H. Giles, S. S. Bowser, and J. Pawlowski.** 2003. Freshwater foraminiferans revealed by analysis of environmental DNA samples. *J Eukaryot Microbiol* **50**:135-139.
85. **Huelsenbeck, J. P.** 1995. Performance of phylogenetic methods in simulation. *Syst. Biol.* **44**:17-48.
86. **Istok, J. D., J. M. Senko, L. R. Krumholz, D. Watson, M. A. Bogle, A. Peacock, Y. J. Chang, and D. C. White.** 2003. In situ bioreduction of technetium and uranium in a nitrate-contaminated aquifer. *Environ. Sci. Technol.* **38**:468-475.
87. **James, T. Y., P. M. Letcher, J. E. Longcore, S. E. Mozley-Standridge, D. Porter, M. J. Powell, G. W. Griffith, and R. Vilgalys.** 2006. A molecular phylogeny of the flagellated fungi (Chytridiomycota) and description of a new phylum (Blastocladiomycota). *Mycologia* **98**:860-871.
88. **Jones, M. D. M., I. Forn, C. Gadelha, M. J. Egan, D. Bass, R. Massana, and T. A. Richards.** 2011. Discovery of novel intermediate forms redefines the fungal tree of life. *Nature* **474**:200-203.
89. **Jones, M. D. M., T. A. Richards, D. L. Hawksworth, and D. Bass.** 2011. Validation and justification of the phylum name Cryptomycota phyl. nov. *IMA Fungus* **2**:173-175.
90. **Jönsson, K. I., E. Rabbow, R. O. Schill, M. Harms-Ringdahl, and P. Rettberg.** 2008. Tardigrades survive exposure to space in low Earth orbit. *Curr Biol* **18**:R729-R731.
91. **Josefson, A. B., and B. Widbom.** 1988. Differential response of benthic macrofauna and meiofauna to hypoxia in the Gullmar Fjord basin. *Marine Biology* **100**:31-40.

92. **Junier, P., T. Junier, and K.-P. Witzel.** 2008. TRiFLe, a program for in silico terminal restriction fragment length polymorphism analysis with user-defined sequence sets. *Appl. Environ. Microbiol.* **74**:6452-6456.
93. **Keith, L., and W. Telliard.** 1979. Priority pollutants: I-a perspective view. *Environmental Science & Technology* **13**:416-423.
94. **Kenny, J. F., and Geological Survey (U.S.).** 2009. Estimated use of water in the United States in 2005, 1st ed. U.S. Geological Survey, Reston, Va.
95. **Kent, A. D., D. J. Smith, B. J. Benson, and E. W. Triplett.** 2003. Web-based phylogenetic assignment tool for analysis of terminal restriction fragment length polymorphism profiles of microbial communities. *Appl Environ Microbiol* **69**:6768-6776.
96. **Kinner, N. E., R. W. Harvey, K. Blakeslee, G. Novarino, and L. D. Meeker.** 1998. Size-selective predation on groundwater bacteria by nanoflagellates in an organic-contaminated aquifer. *Applied and Environmental Microbiology* **64**:618-625.
97. **Kinner, N. E., R. W. Harvey, and M. Kazmierkiewicz-Tabaka.** 1997. Effect of flagellates on free-living bacterial abundance in an organically contaminated aquifer. *Fems Microbiology Reviews* **20**:249-259.
98. **Kinner, N. E., R. W. Harvey, D. M. Shay, D. W. Metge, and A. Warren.** 2002. Field evidence for a protistan role in an organically-contaminated aquifer. *Environmental Science & Technology* **36**:4312-4318.
99. **Kirchman, D. L.** 2002. The ecology of Cytophaga–Flavobacteria in aquatic environments. *FEMS Microbiol. Ecol.* **39**:91-100.
100. **Knight, R., M. Hamady, and C. Lozupone.** 2010. Fast UniFrac: facilitating high-throughput phylogenetic analyses of microbial communities including analysis of pyrosequencing and PhyloChip data. *Isme Journal* **4**:17-27.
101. **Knights, D., E. K. Costello, and R. Knight.** 2011. Supervised classification of human microbiota. *FEMS Microbiol. Rev.* **35**:343-359.
102. **Kucukardall, Y., H. V. Acar, S. Ozkan, S. Nalbant, Y. Yazgan, E. M. Atasoyu, O. Keskin, A. Naz, N. Akyatan, M. Gokben, and M. Danaci.** 2003. Accidental Oral Poisoning Caused by Rdx (Cyclonite): A Report of 5 Cases. *J Intensive Care Med* **18**:42-46.
103. **Kwon, M. J., and K. T. Finneran.** 2010. Electron shuttle-stimulated RDX mineralization and biological production of 4-nitro-2,4-diazabutanol (NDAB) in RDX-contaminated aquifer material. *Biodegradation* **21**:923-937.
104. **Kwon, M. J., and K. T. Finneran.** 2008. Hexahydro-1,3,5-trinitro-1,3,5-triazine (RDX) and octahydro-1,3,5,7-tetranitro-1,3,5,7-tetrazocine (HMX) biodegradation kinetics amongst several Fe(III)-reducing genera. *Soil & Sediment Contamination* **17**:189-203.

105. **Kwon, M. J., and K. T. Finneran.** 2009. Hexahydro-1,3,5-trinitro-1,3,5-triazine (RDX) reduction is concurrently mediated by direct electron transfer from hydroquinones and resulting biogenic Fe(II) formed during electron shuttle-amended biodegradation. *Environ. Eng. Sci.* **26**:961-971.
106. **Kwon, M. J., and K. T. Finneran.** 2006. Microbially mediated biodegradation of hexahydro-1,3,5-trinitro-1,3,5-triazine by extracellular electron shuttling compounds. *Appl. Environ. Microbiol.* **72**:5933-5941.
107. **Kwon, M. J., E. J. O'Loughlin, D. A. Antonopoulos, and K. T. Finneran.** 2011. Geochemical and microbiological processes contributing to the transformation of hexahydro-1,3,5-trinitro-1,3,5-triazine (RDX) in contaminated aquifer material. *Chemosphere* **84**:1223-1230.
108. **Lara, E., D. Moreira, and P. López-García.** 2010. The Environmental Clade LKM11 and Rozella Form the Deepest Branching Clade of Fungi. *Protist* **161**:116-121.
109. **Lefèvre, E., C. Bardot, C. Noël, J.-F. Carrias, E. Viscogliosi, C. Amblard, and T. Sime-Ngando.** 2007. Unveiling fungal zooflagellates as members of freshwater picoeukaryotes: evidence from a molecular diversity study in a deep meromictic lake. *Environ Microbiol* **9**:61-71.
110. **Lefranc, M., A. Thenot, C. Lepere, and D. Debros.** 2005. Genetic Diversity of Small Eukaryotes in Lakes Differing by Their Trophic Status. *Appl Environ Microbiol* **71**:5935-5942.
111. **Lesaulnier, C., D. Papamichail, S. McCorkle, B. Ollivier, S. Skiena, S. Taghavi, D. Zak, and D. Van Der Lelie.** 2008. Elevated atmospheric CO₂ affects soil microbial diversity associated with trembling aspen. *Environ Microbiol* **10**:926-941.
112. **Levine, B. S., F. E. M., R. V. S., G. D. E., and L. P. M.** 1983, posting date. Determination of the Chronic Mammalian Toxicological Effects of RDX: (Twenty-Four Month Chronic Toxicity/Carcinogenicity Study of Hexahydro-1,3,5- Trinitro-1,3,5-Triazine (RDX) in the Fischer 344 Rat). Volume 1. Ft. Belvoir Defense Technical Information Center. [Online.]
113. **Lin, B., C. Hyacinthe, S. Bonneville, M. Braster, P. Van Cappellen, and W. F. M. Roling.** 2007. Phylogenetic and physiological diversity of dissimilatory ferric iron reducers in sediments of the polluted Scheldt estuary, Northwest Europe. *Environ. Microbiol.* **9**:1956-1968.
114. **Lippo, H., J. Poikolainen, and E. Kubin.** 1995. The use of moss, lichen and pine bark in the nationwide monitoring of atmospheric heavy metal deposition in Finland. *Water Air Soil Pollut* **85**:2241-2246.
115. **Lish, P. M.** 1984. Determination of the chronic mammalian toxicological effects of RDX : twenty-four month chronic toxicity/carcinogenicity study of hexahydro-1,3,5-trinitro-1,3,5-triazine (RDX) in the B6C3F1 hybrid mouse : final report phase VI, vol. 1. IIT Research Institute, Chicago, Ill.

116. **Liu, W. T., T. L. Marsh, H. Cheng, and L. J. Forney.** 1997. Characterization of microbial diversity by determining terminal restriction fragment length polymorphisms of genes encoding 16S rRNA. *Applied and Environmental Microbiology* **63**:4516-4522.
117. **Lotufo, G. R., J. D. Farrar, L. S. Inouye, T. S. Bridges, and D. B. Ringelberg.** 2001. Toxicity of sediment-associated nitroaromatic and cyclonitramine compounds to benthic invertebrates. *Environmental Toxicology and Chemistry* **20**:1762-1771.
118. **Ludwig, W., O. Strunk, R. Westram, L. Richter, H. Meier, Yadhukumar, A. Buchner, T. Lai, S. Steppi, G. Jobb, W. Forster, I. Brettske, S. Gerber, A. W. Ginhart, O. Gross, S. Grumann, S. Hermann, R. Jost, A. Konig, T. Liss, R. Lubmann, M. May, B. Nonhoff, B. Reichel, R. Strehlow, A. Stamatakis, N. Stuckmann, A. Vilbig, M. Lenke, T. Ludwig, A. Bode, and K. H. Schleifer.** 2004. ARB: a software environment for sequence data. *Nucleic Acids Research* **32**:1363-1371.
119. **Luo, Q., L. R. Krumholz, F. Z. Najar, A. D. Peacock, B. A. Roe, D. C. White, and M. S. Elshahed.** 2005. Diversity of the microeukaryotic community in sulfide-rich Zodleton Spring (Oklahoma). *Appl Environ Microbiol* **71**:6175-6184.
120. **Mccormick, N. G., J. H. Cornell, and A. M. Kaplan.** 1981. Biodegradation of Hexahydro-1,3,5-Trinitro-1,3,5-Triazine. *Appl. Environ. Microbiol.* **42**:817-823.
121. **Medlin, L., H. J. Elwood, S. Stickel, and M. L. Sogin.** 1988. The characterization of enzymatically amplified eukaryotic 16S-like rRNA-coding regions. *Gene* **71**:491-9.
122. **Monchy, S., G. Sancier, M. Jobard, S. Rasconi, M. Gerphagnon, M. Chabé, A. Cian, D. Meloni, N. Niquil, U. Christaki, E. Viscogliosi, and T. Sime-Ngando.** 2011. Exploring and quantifying fungal diversity in freshwater lake ecosystems using rDNA cloning/sequencing and SSU tag pyrosequencing. *Environ Microbiol* **13**:1433-1453.
123. **Moon-van der Staay, S. Y., V. A. Tzeneva, G. W. M. Van Der Staay, W. M. De Vos, H. Smidt, and J. H. P. Hackstein.** 2006. Eukaryotic diversity in historical soil samples. *FEMS Microbiol Ecol* **57**:420-428.
124. **Morley, M. C., and M. Fatemi.** 2010. Adsorption of RDX and its Nitroso Metabolites onto Activated Carbon. *Practice Periodical of Hazardous, Toxic, and Radioactive Waste Management* **14**:90-97.
125. **Morris, R. M., M. S. Rappe, S. A. Connon, K. L. Vergin, W. A. Siebold, C. A. Carlson, and S. J. Giovannoni.** 2002. SAR11 clade dominates ocean surface bacterioplankton communities. *Nature* **420**:806-810.
126. **Nawrocki, E. P., D. L. Kolbe, and S. R. Eddy.** 2009. Infernal 1.0: inference of RNA alignments. *Bioinformatics* **25**:1335-1337.
127. **Nipper, M., R. S. Carr, J. M. Biedenbach, R. L. Hooten, K. Miller, and S. Saepoff.** 2001. Development of marine toxicity data for ordnance compounds. *Archives of Environmental Contamination and Toxicology* **41**:308-318.

128. **Nocker, A., M. Burr, and A. K. Camper.** 2007. Genotypic microbial community profiling: A critical technical review. *Microbial Ecology* **54**:276-289.
129. **Nolte, V., R. V. Pandey, S. Jost, R. Medinger, B. OttenwÄlder, J. Boenigk, and C. SchlÖtterer.** 2010. Contrasting seasonal niche separation between rare and abundant taxa conceals the extent of protist diversity. *Molecular Ecology* **19**:2908-2915.
130. **Novarino, G., A. Warren, H. Butler, G. Lambourne, A. Boxshall, J. Bateman, N. E. Kinner, R. W. Harvey, R. A. Mosse, and B. Teltsch.** 1997. Protistan communities in aquifers: a review. *Fems Microbiology Reviews* **20**:261-275.
131. **Oh, S.-Y., P. C. Chiu, B. J. Kim, and D. K. Cha.** 2005. Zero-valent iron pretreatment for enhancing the biodegradability of RDX. *Water Research* **39**:5027-5032.
132. **Oksana, J., R. Kindt, P. Legendre, B. O'Hara, G. Simpson, P. Solymos, M. Henry, H. Stevens, and H. Wagner.** 2009. *Vegan: Community Ecology Package.*
133. **Park, S. C., K. S. Baik, D. Kim, and C. N. Seong.** 2009. *Maritimimonas rapanae* gen. nov., sp nov., isolated from gut microflora of the veined rapa whelk, *Rapana venosa*. *Int. J. Syst. Evol. Micr.* **59**:2824-2829.
134. **Parsons, D. J., and S. H. DeBenedetti.** 1979. Impact of fire suppression on a mixed-conifer forest. *Forest Ecology and Management* **2**:21-33.
135. **Pawlowski, J., R. Christen, B. Lecroq, D. Bachar, H. R. Shahbazkia, L. Amaral-Zettler, and L. Guillou.** 2011. Eukaryotic Richness in the Abyss: Insights from Pyrotag Sequencing. *Plos One* **6**.
136. **Pearson, E. A., and E. D. F. Frangipane.** 1975. *Marine pollution and marine waste disposal.* Pergamon, Oxford; New York.
137. **Peters, G. T., D. T. Burton, R. L. Paulson, and S. D. Turley.** 1991. The Acute and Chronic Toxicity of Hexahydro-1,3,5-Trinitro-1,3,5-Triazine (Rdx) to 3 Fresh-Water Invertebrates. *Environmental Toxicology and Chemistry* **10**:1073-1081.
138. **Poitelon, J. B., M. Joyeux, B. Welté, J. P. Duguet, J. Peplies, and M. S. DuBow.** 2009. Identification and phylogeny of eukaryotic 18S rDNA phylotypes detected in chlorinated finished drinking water samples from three Parisian surface water treatment plants. *Lett Appl Microbiol* **49**:589-595.
139. **Price, M. N., P. S. Dehal, and A. P. Arkin.** 2010. FastTree 2-Approximately Maximum-Likelihood Trees for Large Alignments. *Plos One* **5**.
140. **Pritchard, J. K., M. Stephens, and P. Donnelly.** 2000. Inference of population structure using multilocus genotype data. *Genetics* **155**:945-959.
141. **Pruesse, E., C. Quast, K. Knittel, B. M. Fuchs, W. Ludwig, J. Peplies, and F. O. Glockner.** 2007. SILVA: a comprehensive online resource for quality checked and aligned ribosomal RNA sequence data compatible with ARB. *Nucleic Acids Res.* **35**:7188-7196.

142. **Pye, V., and R. Patrick.** 1983. Ground water contamination in the United States. *Science* **221**:713-718.
143. **Ragni, E., A. Coluccio, E. Rolli, J. M. Rodriguez-Peña, G. Colasante, J. Arroyo, A. M. Neiman, and L. Popolo.** 2007. GAS2 and GAS4, a Pair of Developmentally Regulated Genes Required for Spore Wall Assembly in *Saccharomyces cerevisiae*. *Eukaryot Cell* **6**:302-316.
144. **Ramette, A.** 2007. Multivariate analyses in microbial ecology. *FEMS Microbiol Ecol* **62**:142-160.
145. **Reynoldson, T. B., R. H. Norris, V. H. Resh, K. E. Day, and D. M. Rosenberg.** 1997. The reference condition: a comparison of multimetric and multivariate approaches to assess water-quality impairment using benthic macroinvertebrates. *J N Am Benthol Soc* **16**:833-852.
146. **Risso, C., B. A. Methe, H. Elifantz, D. E. Holmes, and D. R. Lovley.** 2008. Highly conserved genes in *Geobacter* species with expression patterns indicative of acetate limitation. *Microbiology-Sgm* **154**:2589-2599.
147. **Roesch, L. F., R. R. Fulthorpe, A. Riva, G. Casella, A. K. M. Hadwin, A. D. Kent, S. H. Daroub, F. A. O. Camargo, W. G. Farmerie, and E. W. Triplett.** 2007. Pyrosequencing enumerates and contrasts soil microbial diversity. *Isme Journal* **1**:283-290.
148. **Roh, H., C. P. Yu, M. E. Fuller, and K. H. Chu.** 2009. Identification of Hexahydro-1,3,5-trinitro-1,3,5-triazine-Degrading Microorganisms via (15)N-Stable Isotope Probing. *Environmental Science & Technology* **43**:2505-2511.
149. **Rosen, G., and G. R. Lotufo.** 2005. Toxicity and fate of two munitions constituents in spiked sediment exposures with the marine amphipod *Eohaustorius estuarius*. *Environmental Toxicology and Chemistry* **24**:2887-2897.
150. **Rosenberg, D. M., and V. H. Resh.** 1993. *Freshwater biomonitoring and benthic macroinvertebrates*. Chapman & Hall, New York.
151. **Saito, A., and M. Yamamota.** 1996. Acute Oral Toxicity of Capsaicin in Mice and Rats. *J. Toxicol Sci*:195-200.
152. **Salvado, H., M. P. Gracia, and J. M. Amigó.** 1995. Capability of ciliated protozoa as indicators of effluent quality in activated sludge plants. *Water Res* **29**:1041-1050.
153. **Schloss, P. D., S. L. Westcott, T. Ryabin, J. R. Hall, M. Hartmann, E. B. Hollister, R. A. Lesniewski, B. B. Oakley, D. H. Parks, C. J. Robinson, J. W. Sahl, B. Stres, G. G. Thallinger, D. J. Van Horn, and C. F. Weber.** 2009. Introducing mothur: open-source, platform-independent, community-supported software for describing and comparing microbial communities. *Appl Environ Microbiol* **75**:7537-7541.

154. **Schockaert, E. R., M. Hooge, R. Sluys, S. Schilling, S. Tyler, T. Artois, E. V. Balian, C. Lévêque, H. Segers, and K. Martens.** 2008. Global diversity of free living flatworms (Platyhelminthes, "Turbellaria") in freshwater
Freshwater Animal Diversity Assessment, p. 41-48. *In* H. J. Dumont (ed.), vol. 198. Springer Netherlands.
155. **Shannon, C. E.** 1997. The mathematical theory of communication (Reprinted). *M D Computing* **14**:306-317.
156. **Sheremata, T. W., and J. Hawari.** 2000. Mineralization of RDX by the White Rot Fungus *Phanerochaete chrysosporium* to Carbon Dioxide and Nitrous Oxide. *Environmental Science & Technology* **34**:3384-3388.
157. **Shimodaira, H., and M. Hasegawa.** 1999. Multiple comparisons of log-likelihoods with applications to phylogenetic inference. *Mol Biol Evol* **16**:1114.
158. **Shulman, S.** 1992. The threat at home : confronting the toxic legacy of the U.S. military. Beacon Press, Boston.
159. **Simpson, E. H.** 1949. Measurement of Diversity. *Nature* **163**:688-688.
160. **Smits, T. H. M., C. Devenoges, K. Szynalski, J. Maillard, and C. Holliger.** 2004. Development of a real-time PCR method for quantification of the three genera *Dehalobacter*, *Dehalococcoides*, and *Desulfitobacterium* in microbial communities. *Journal of Microbiological Methods* **57**:369-378.
161. **Sogin, M. L., H. G. Morrison, J. A. Huber, D. M. Welch, S. M. Huse, P. R. Neal, J. M. Arrieta, and G. J. Herndl.** 2006. Microbial diversity in the deep sea and the underexplored rare biosphere. *Proc Natl Acad Sci USA* **103**:12115-12120.
162. **Spalding, R. F., and J. W. Fulton.** 1988. Groundwater munition residues and nitrate near Grand Island, Nebraska, U.S.A. *Journal of Contaminant Hydrology* **2**:139-153.
163. **Stamatakis, A.** 2006. RAxML-VI-HPC: Maximum likelihood-based phylogenetic analyses with thousands of taxa and mixed models. *Bioinformatics* **22**:2688-2690.
164. **Steevens, J. A., B. M. Duke, G. R. Lotufo, and T. S. Bridges.** 2002. Toxicity of the explosives 2,4,6-trinitrotoluene, hexahydro-1,3,5-trinitro-1,3,5-triazine, and octahydro-1,3,5,7-tetranitro-1,3,5,7-tetrazocine in sediments to *Chironomus tentans* and *Hyalella azteca*: Low-dose hormesis and high-dose mortality. *Environmental Toxicology and Chemistry* **21**:1475-1482.
165. **Sullivan, T. J., A. P. Dreyer, and J. W. Peterson.** 2009. Genetic variation in a subterranean arthropod (*Folsomia candida*) as a method to identify low-permeability barriers in an aquifer. *Pedobiologia* **53**:99-105.
166. **Takishita, K., H. Miyake, M. Kawato, and T. Maruyama.** 2005. Genetic diversity of microbial eukaryotes in anoxic sediment around fumaroles on a submarine caldera floor based on the small-subunit rDNA phylogeny. *Extremophiles* **9**:185-196.

167. **Tamura, K., D. Peterson, N. Peterson, G. Stecher, M. Nei, and S. Kumar.** 2011. MEGA5: Molecular Evolutionary Genetics Analysis Using Maximum Likelihood, Evolutionary Distance, and Maximum Parsimony Methods. *Molecular Biology and Evolution* **28**:2731-2739.
168. **Team, R. D. C.** 2008. R: A language and environment for statistical computing. *In* R. F. f. S. Computing (ed.), Vienna, Austria.
169. **Tetra_Tech_Inc.** 2004. Treatability Study Test Plan for In Situ Biodegradation of RDX in Off-Site Groundwater.
170. **Thompson, K. T., F. H. Crocker, and H. L. Fredrickson.** 2005. Mineralization of the cyclic nitramine explosive hexahydro-1,3,5-trinitro-1,3,5-triazine by *Gordonia* and *Williamsia* spp. *Appl. Environ. Microbiol.* **71**:8265-8272.
171. **Thompson, K. T., F. H. Crocker, and H. L. Fredrickson.** 2005. Mineralization of the cyclic nitramine explosive hexahydro-1,3,5-trinitro-1,3,5-triazine by *Gordonia* and *Williamsia* spp. *Applied and Environmental Microbiology* **71**:8265-8272.
172. **U.S. National Research Council, W. S. T. B.** 1993. *In situ bioremediation : when does it work?* National Academy Press, Washington, D.C.
173. **U.S.A.C.E.** 2006. Final Five Year Report: Unit 17, Old Demolition Area, Lonestar Army Ammunition Plant.
174. **U.S.D.O.D.** 2008. The Defense Environmental Programs annual report to Congress FY2008, Washington D.C.
175. **URS.** 2004. Groundwater Flow and Contaminant Fate and Transport Modeling. Technical Memorandum.
176. **URS.** 2005. Off-Site Groundwater Record of Decision: Iowa Army Ammunition Plant.
177. **Von der Heyden, S., E. E. Chao, and T. Cavalier-Smith.** 2004. Genetic diversity of goniomonads: an ancient divergence between marine and freshwater species. *Eur J Phycol* **39**:343-350.
178. **Wang, Q., G. M. Garrity, J. M. Tiedje, and J. R. Cole.** 2007. Naive Bayesian classifier for rapid assignment of rRNA sequences into the New Bacterial Taxonomy. *Appl. Environ. Microbiol.* **73**:5261-5267.
179. **Wang, X. J., J. Yang, X. P. Chen, G. X. Sun, and Y. G. Zhu.** 2009. Phylogenetic diversity of dissimilatory ferric iron reducers in paddy soil of Hunan, South China. *J. Soil Sediment* **9**:568-577.
180. **Wani, A. H., R. Wade, and J. L. Davis.** 2007. Field demonstration of biologically active zone enhancement using acetate as a sole carbon source for in situ reductive transformation of RDX in groundwater. *J Haz Tox Rad Waste* **11**:83-91.
181. **Weisburg, W. G., S. M. Barns, D. A. Pelletier, and D. J. Lane.** 1991. 16S ribosomal DNA amplification for phylogenetic study. *J. Bacteriol.* **173**:697-703.

182. **Werck-Reichhart, D. I., and R. Feyereisen.** 2000. Cytochromes P450: a success story. BioMed Central Ltd.
183. **Williams, A. G. B., K. B. Gregory, G. F. Parkin, and M. M. Scherer.** 2005. Hexahydro-1,3,5-trinitro-1,3,5-triazine transformation by biologically reduced ferrihydrite: Evolution of Fe mineralogy, surface area, and reaction rates. *Environmental Science & Technology* **39**:5183-5189.
184. **Yoon, H. S., J. Grant, Y. Tekle, M. Wu, B. Chaon, J. Cole, J. Logsdon, D. Patterson, D. Bhattacharya, and L. Katz.** 2008. Broadly sampled multigene trees of eukaryotes. *BMC Evolutionary Biology* **8**:14.
185. **Zhang, C. L., and J. B. Hughes.** 2003. Biodegradation pathways of hexahydro-1,3,5-trinitro-1,3,5-triazine (RDX) by *Clostridium acetobutylicum* cell-free extract. *Chemosphere* **50**:665-671.
186. **Zhang, T., and H. H. P. Fang.** 2000. Digitization of DGGE (denaturing gradient gel electrophoresis) profile and cluster analysis of microbial communities. *Biotechnology Letters* **22**:399-405.
187. **Zhao, J.-S., J. Spain, and J. Hawari.** 2003. Phylogenetic and metabolic diversity of hexahydro-1,3,5-trinitro-1,3,5-triazine (RDX)-transforming bacteria in strictly anaerobic mixed cultures enriched on RDX as nitrogen source. *FEMS Microbiology Ecology* **46**:189-196.
188. **Zhao, J. S., L. Paquet, A. Halasz, and J. Hawari.** 2003. Metabolism of hexahydro-1,3,5-trinitro-1,3,5-triazine through initial reduction to hexahydro-1-nitroso-3,5-dinitro-1,3,5-triazine followed by denitration in *Clostridium bifermentans* HAW-1. *Appl Microbiol Biotechnol* **63**:187-193.
189. **Zwickl, D. J., and D. M. Hillis.** 2002. Increased taxon sampling greatly reduces phylogenetic error. *Syst Biol* **51**:588-598.